GENERAL REPLY

The authors thank the two reviewers for their constructive comments and helpful suggestions that have improved the manuscript.

As mentioned by the both reviewers, the reconstruction method had some shortcomings, but the reviewers, especially reviewer #1, gave concrete and great suggestions to resolve them. The manuscript has been largely revised and improved along the suggestions. The authors describe first the revisions in the reconstruction method as a General Reply.

The suggestions are as follows:
(1) use of 10-year trajectory instead of 90-day, which can eliminate the remaining trajectories in the UTLS (k=5);
(2) reconstruction of chemical passive tracers with evaluation of transport timescale (as the first step); and
(3) reconstruction of chemical active tracers including chemical decay (as the second step).
The authors have made these procedures and some relating revisions as follows.

For point (1), as noted by the reviewers, the remaining trajectories in the UTLS (k=5) could be eliminated, i.e., it was confirmed that the all trajectories are categorized into any origins of k = 1, 2, 3, or 4 within 10 years (Note that the criteria have also been revised to avoid some shortcomings). In addition, the inversion method to estimate tracer mixing ratio for k=1 and 5 in the original manuscript could be also eliminated, i.e., the all tracers in the ExUTLS have been reconstructed only from their mixing ratios assumed in the high-latitude LT, mid-latitude LT, and tropical troposphere.

For point (2), using the 10-year trajectory, Age of Air (AoA) as well as SF6 and CO2 distributions have been reconstructed from the trajectories including the "Tail correction" (e.g., Diallo et al., 2012). The CH4, N2O, CO have been also reconstructed without any chemical decay in this step. AoA has been also estimated using observed SF6 mixing ratios obtained by CONTRAIL, and then the two AoAs have been compared to correct transport timescale expressed in the trajectories.

For point (3), the chemical active tracers, CH4, N2O, and CO, are finally reconstructed with simulating their chemical loss along an "average path" (Schoeberl et al., 2000). The use of the concept of average path was also suggested by the reviewer #1. Based on this concept, the authors believe that the active

tracers have been successfully reconstructed together with estimation of seasonally depending their chemical loss rate.

In relation to a suite of these revisions, the latter half of section 2.1 (Estimating the origin fraction and AoA), large part of section 2.2 (Air mass original composition and reconstruction) were significantly revised, especially section 2.2 was reorganized and a new subsections 2.2.1 and 2.2.2 were created for reconstructions of chemical passive and active tracers, respectively. The analyzing results, figures, and discussions were thus also changed in association with the revision of the reconstruction method, but the main thesis was essentially not changed.

References:

Diallo, M., Legras, B., and Chédin, A.: Age of stratospheric air in the ERA-Interim, Atmos. Chem. Phys., 12, 12133-12154, https://doi.org/10.5194/acp-12-12133-2012, 2012.

Schoeberl, M. R., Sparling, L. C., Jackman, C. H., and Fleming, E. L.: A Lagrangian view of stratospheric trace gas distributions, Journal of Geophysical Research: Atmospheres, 105(D1), 1537-1552, doi:10.1029/1999JD900787, 2000.

The authors believe that the revised manuscript has been improved by incorporating the more appropriate reconstruction method.

Point-by-point responses to the comments of individual reviewer are provided below.

REPLY TO COMMENTS BY REVIEWER #1

The authors are grateful for the thorough review and constructive comments on the manuscript. All of the points raised by the reviewer have been addressed. Regarding the reviewer's major comments, please also refer to the "General Reply" section. Point-by-point responses are detailed below, in red text.

Reviewer (Comments):
Review of "Seasonal characteristics of chemical and dynamical transports into the extratropical upper troposphere/lower stratosphere" (ExUTLS) by Yoichi Inai et al.

Recommendation: Publication after major revision
The paper is very well organised and written. The topic discussed in this paper, transport into the ExUTLS, is in general of high relevance. Our actual limitations in simulating water vapour transport in this complex region introduce large uncertainties in the Earth radiation budget (see Riese et al., 2012). Trajectory analysis in combination with observations could be and have been used in many cases to improve our knowledge on tracer transport and distribution in the UTLS, e.g. for H2O: Fueglistaler et al. (2004, 2005a, 2005b), e.g. for CO and H2O: Hoor et al. (2010), e.g. for STE (stratosphere-troposphere exchange) and O3: Skerlag et al. (2014), e.g. for CO2 and AoA: Diallo et al. (2012, 2017). This manuscript here falls a bit short of explaining what the novel aspect of the presented method really is and how the presented results augment our actual knowledge on the seasonal characteristics of transport in and into the ExUTLS, e.g. in comparison to the early studies by Appenzeller et al. (1996) and Ray et al. (1999) or to the many studies summarised in the ExUTLS review paper by Gettlemann et al. (2011).

The paper should be submitted after addressing the comments below.

General comments:
First of all, I don't fully understand the title (and/or the scope) of this paper. What is the meaning of chemical and dynamical transport? Is chemical transport a synonym for transport of chemical active tracers (N2O, CH4 and CO)? Should dynamical transport describe the transport of passive tracers (SF6, CO2 and AoA)? Pure Lagrangian transport (here backward

trajectories) differs from (both) tracer transports: There is no mixing and no chemistry included along the individual transport pathways.

What the authors meant to write by the phrase “chemical and dynamical transports” is 1) transport of chemical species and 2) transport of air mass which is expressed by the mixing fractions of air mass originating in the stratosphere, tropical troposphere, mid-latitude LT, and high-latitude LT. In order to make it clearer, the title has been changed to “Seasonal characteristics of trace gas transport into the ExUTLS.”

The latter is definitively a problem for CO, because the chemical decay along the 90-days backward trajectories cannot be neglected. For N2O and CH4 the chemical decay is not that significant, because only a few of the initialised trajectories will travel through the sink regions of both tracers higher up in the stratosphere during the 90-days. However, the unknown (non-observed) time series of the high-latitude stratospheric background (k=1) and the tropical and extratropical UTLS background (k=5) conditions for all tracers (not only for the chemical active tracers N2O and CH4) still remain the major problem for the reconstruction of the observed tracer distributions by CONTRAIL using only 90-days backward trajectories. The reconstruction in the chosen setup could not be used for quantitative studies of neither ERA-Interim (or other reanalysis data sets) nor the transport processes in the ExUTLS, because the trajectories itself are needed to define the boundary conditions for the original time series XS_ORG_k in the high-latitude stratosphere (k=1) and the UTLS (k=5) which are again the prerequisite to reconstruct the observed mixing ratios in the ExUTLS derived from CONTRAIL. This is a circular reference between the trajectory analysis and the CONTRAIL observations in the ExUTLS, whereby the non-observed (inverse reconstructed) original time series for k=1 and 5 could be seen as a kind of free parameters to tune the system or in other words to close the budget for the individual tracers.

The main problem, why this paper could, to my point of view, not add to the actual state of knowledge, although it has the potential, is the limitation of the backward trajectories to 90 days. The consequence of this limitation is the circular reference explained above (the authors call this an inversion technique) that has to be introduced to reconstruct the original time series of the tracer mixing ratios in the stratospheric overworld (k=1) and in the UTLS (k=5).

The authors claim that the mixing fractions derived from the coarser resolution ERA-Interim data (1.5x1.5, 37 levels) are the same as for the finer resolution ERA-Interim data (0.75x0.75, 60 levels). If this is the case, why not using the 10-year instead of the 90-days backward

trajectories? This would at least solve the problem to reconstruct the non-observed boundary conditions for the trajectories residing in the ExUTLS (k=5) during the 90 days and also partially for the trajectories originating from the stratospheric overworld (k=5). The latter is unfortunately only true for the passive tracers, SF6 and CO2 respectively. Both tracers could be reconstructed by combining their original tropospheric time series (k=2,3,4) and the 10-years trajectories all starting in the target region of this study – the ExUTLS – and ending in the troposphere (e.g. Diallo et al., 2017), beside a small residuum of trajectories that remains in the stratosphere and that has to be characterised (see e.g. Ploeger et al, 2016).

The strong point of this study here is to my opinion the combination of backward trajectories driven by a state-of-the-art reanalysis data set (ERA-Interim) with simultaneous measurements in the ExUTLS of five tracers with different characteristics in their lifetimes and tropospheric time series. My recommendation would be to separate the analysis on transport and chemical processes. In the first step, one could use the 10-years backward trajectories (if manageable, it would be better using the high resolution ERA-Interim data) together with the passive tracers CO2 and SF6 (the latter is literally the same as AoA in the UTLS) to evaluate the mixing fractions and transport timescales derived from the ERA-Interim driven backward trajectories by reconstructing the CONTRAIL observations of both passive tracers. This is already a valuable extension to the method shown by Diallo et al. (2017), because the additional simoultaneous SF6 observations are a second independent constraint for the evaluation due to the different (linearly independent) tropospheric time series compared to CO2.
In the next step, one could exploit the additional information from the simultaneously measured chemical active tracers. Given the transport properties (mixing fraction, air mass origin and timescale) that has been quantified and evaluated in the first step, the chemical decay along the transport pathways from the tropospheric origin into the ExUTLS could be analysed with the simultaneous measurements of the chemical active tracers CO, CH4 and N2O. The difference between the reconstructed passive CO, CH4 and N2O tracers without chemistry and observed values including chemical decay should allow to assign a photochemical loss for air parcels along an “average pathway” with the same AoA (see Schoeberl et al., 2000). This “average pathway” could be defined by a bulk of trajectories, e.g. by the trajectories in a given equivalent latitude-potential temperature bin. There might be many more and better approaches to derive quantitative information on the chemical decay along the transport pathways, but the huge advantage in general of using backward trajectories together with simoultaneous measured passive and chemical active tracers would be that one could disentangle dynamical and chemical effects on the observed tracer

distribution in a unique way. An urgent question that has to be answered to understand the processes driving and driven by climate change in this complex and important region of the atmosphere.

If the authors decide to stay with 90-days backward trajectory setup then the limitations of the 90-days backward trajectories and the sensitivity of the results due to these limitations have to be discussed in much more detail – see also the specific comments below.

Thank you for this great constructive suggestion on how to reconstruct both the chemically passive and active compositions. Following above suggestions, the reconstruction method has been revised, and the authors believe that it has been largely improved. Please see the General Reply.

Specific comments:
P.1, L.26: "*…, especially in the Arctic climate.*"
Please cite references for this statement or delete it.

The statement has been deleted.

P.1, L.27: "*… via stratospheric residual circulation (Brewer-Dobson circulation, BDC; Brewer, 1949; Dobson, 1956).*"
The stratospheric residual circulation describes the mean mass transport. The BDC includes mean mass transport and two-way mixing. The latter, by definition, does not lead to net mass exchange but may lead to net tracer exchange. Therefore, I would suggest to use stratospheric circulation instead of stratospheric residual circulation as a synonym for the BDC (see e.g. Shepard, 2002; Birner & Boenisch, 2011).

Thank you very much for informative comments. Following this comment, the statement "stratospheric circulation" has been used, instead of "stratospheric residual circulation."

P.2, L.28: In the text is written that the trajectories have been initialised between 0° E and 140° E longitude. In Fig. 1, the initialisation is all around the globe (0° E-360° E). What is actually the correct initialisation: figure or text?

Fig. 1 in the original manuscript was not correct. It has been corrected.

P.3, L.3-5: "*The distribution of some of the particles …*"
I can hardly see the described feature in Fig. 2. The data should be presented in a different way to illustrate this more clearly.

In association with the revision of the method using 10-year trajectory, the figure and descriptions for it have been changed.

P.3, L.6-9 & Table 1: The criteria for the classification of the air mass origins (k=1-5) seems to me somehow uncomplete or ambiguous:

1.) How trajectories are classified, if they satisfy the criteria < 350 K, < 4 km and 20° N < lat. < 30° N? Are they counted as tropical troposphere (k=2) or as mid-latitude LT (k=3)?

The trajectories had been categorized either compartment which was satisfied first. The authors confess that it was not appropriate, so the criteria have been revised to avoid such overlap as pointed out by this comment. The revised criteria have been shown in Table 1 in the revised manuscript.

2.) How trajectories are classified, if they satisfy the criteria > 380 K, lat. < 45° N and pot. vorticity > 6 PVU? Are the counted as UTLS (k=5)? This would mean that backward trajectories initialised e.g. at 15-16 km geopotential height and lat. = 45° N which has travelled upand equatorward would be counted as UTLS (see Fig. 2 right panel all points south of 45° N and above 15 km). To my feeling, some trajectories that should be assigned to the shallow branch (k=1b) of the BDC are classified here as UTLS (k=5).

Yes, they had been counted as k=5. Following this comment, the criteria for stratosphere (k=1) has been also revised as shown in Table 1 in the revised manuscript.

Another problem of this UTLS criteria (k=5) in combination with the 90-days backward trajectory limitation is that the mixing ratios of the tracers assigned to this category or region spanning from > 350 K in the tropics or > 4 km in the extratropics up to 25 km for lat. > 45° N are very different. For example CO, mixing ratios ranging from > 100 ppb (extratropical UT) to < 20 ppb (stratospheric values for lat. < 45° N) are condensed into the original UTLS time series needed to reconstruct the observations. The consequence is that

this original time series is mainly defined by the fact where in the UTLS the trajectory stemmed from.

As described in the General Reply, 10-year trajectory has been employed in addition to the revision of the classification of original regions. The authors believe that the problem pointed out here has been fixed.

P.3, L.22: The AoA definition in this paper is different to that of Hall&Plumb (1994). Here also for purely tropospheric transport AoA values are calculated, i.e. from the UT to the lower extratropical troposphere (< 4 km) or the tropical troposphere < 350 K potential temperature. Hall and Plumb defined an only stratospheric AoA using the tropopause as the reference surface. However, the AoA defined here is closer to the AoA derived from tracer measurements, e.g. SF6, for which the reference surface is in most cases and for practical reasons the tropical lower troposphere. This should be mentioned and clarified somehow, because tropospheric AoA are not really common.

To mention this point, the sentence "Thus, the AoA definition used here differs from that of Hall and Plumb (1994), who defined AoA as the elapsed time an air parcel spends in the stratosphere after across the tropopause" has been added in P3, L24ff in the revised manuscript.

P.3, L.26-30: It is not evident, if the underestimation of AoA found by Inai (2018) in the midlatitude stratosphere holds for the UTLS. This could be evaluated with AoA derived from the SF6 CONTRAIL observation in the ExUTLS. This issue is briefly discussed in section 4.3 and it is implicitly shown in Fig. 12f, but it would be much clearer, if the authors would show a figure with SF6-derived AoA vs. 10-years backward trajectories derived AoA. This issue is of high interest (too short transport timescales into the stratosphere for ERA-Interim driven trajectories) and it also would have implications for the interpretation of chemical active tracers, for which the exposure time to stratospheric photochemistry is of interest.

As described in the General Reply, the 10-year trajectory has been employed and the SF6-derived AoA is compared with traj-derived AoA to correct them.

P.4, L.10: No chemical decay during transport from the origin to the initial position during the 90 days of transport is included – this is definitely not true for CO (see also the general comments above).

Chemical decay of CO as well as the other species have been included as described in the General Reply.

P.4, L.19-27: Would it not be more consistent to use higher temporal resolved reference data from the NOAA/ESRL atmospheric baseline observatories for the definitions of the tropospheric time series? You already use the Barrow site (BRW) together with the Summit site (SUM, downgraded to a sampling site) to define high-latitude (lat. > 45° N) lower troposphere (k=4) time series. The airborne measurements at 11 km between 10° N and 30° N could be used to evaluate the differences between the remote tropical LT and the flight level.

The authors consider that there are two attitudes to incorporate such data into this analysis. The one is use of higher temporal resolved data as you pointed out, and another is use of larger special representative data. The authors have conducted such aircraft observations by ourselves and accumulate such data which have larger special representativeness. We choose own larger special representative data to use.

P.5, L.3: It is hard to believe that this equation system is not under-determined. At least there should be some auxiliary constraints, e.g. mixing ratio X for a tracer with stratospheric sink should be lower for high-latitude stratosphere (k=1) than for the UTLS (k=5), i.e. X(k=1) < X(k=5).
How the minimisation of the equation 4 has been technically performed? With a simple but robust parameter sweep or with a more sophisticated (but maybe numerical more instable) algorithm? This is to my opinion quite essential for the outcome of this paper. Therefore, this (inverse) procedure and the sensitivity of the results to the choice of parameters should be explained and shown in more details (see also general comments).

The inversion method has been eliminated in association with revision of the reconstruction method.

P.5, L.13-15: This means that you exclude most or at least a large part of the upper tropospheric CONTRAIL data, because CO > 80 ppb is not a spurious event in the extratropical UT of the northern hemisphere (e.g. Engel et al., 2006 and references within), especially during winter and spring. Sometimes, it would be better to use tropopause related coordinates (or filter) instead of exclusively using equivalent latitude-potential temperature

coordinates.

The number of such measurements that CO > 80 ppb and Theta > 340 K and Lat_eq > 60deg N is not large. Such measurements have been identified by cross-marks in Figs. 4, 5, and 8 of the revised manuscript.

P.6, L.1-2: This finding is different from the results of Hoor et al. (2005) and Boenisch et al. (2009). Are there any explanation for these differences? I would expect that there is a certain time lag between the time of maximal downwelling (winter) and the maximal stratospheric characteristic of the LMS (spring).

The result has been changed in association with the use of 10-year trajectory, and it has become consistent with the results of Hoor et al. (2005) and Boenisch et al. (2009). The statement has been changed (P7, L19-22).

P.7, L.1-2: The seasonality and the mixing ratios for CO in the high-latitude stratosphere (k=1) and UTLS (k=5) are unrealistic, especially for spring (see e.g. Tilmes et al., 2010 and references within). This is to my view the consequence that errors, e.g. missing chemistry, in the reconstruction of ExUTLS observations will be compensated by the reconstructed original time series of CO for the regions k=1 and 5.

The estimation method of compositions in the stratospheric air mass (k=1) has been revised as described in the first part of Sect. 3.2 (P8, L11ff), in association with revision of the reconstruction method.

P.7, L.5-10 & Figure 7: Why does the seasonality of AoA and SF6 differ, especially in the UTLS (see Fig. 7d vs. 7f)? During August, the phase of the oldest AoA in the UTLS, one would expect the lowest (detrended) SF6 mixing ratios. This seems here not to be the case, August corresponds to the season with the highest (detrended) SF6 mixing ratios, equivalent to the youngest AoA. What is the explanation for this contradiction?

The estimation method of traj-derived AoA has been revised. The revised results show in-phase seasonality of AoA and SF6, the description has been changed (P8, L25-29 in the revised manuscript).

P.7, L.19-21, & Figure 8-11: For me, it looks like April is simply the month with the most

stratospheric characteristic of the LMS – highest AoA and lowest mixing ratios of the chemical active tracers above the 4pvu-contour.

That is right. The following description has been made here (P9, L6-10): "The reconstructions and AoA for April (Fig. 16) show spatial distributions of all species that generally increase with decreasing potential temperature, equivalent latitude, or potential vorticity, as is the case for January. However, the gradients are larger, particularly for CH_4 and N_2O mixing ratios, such that in regions where the potential vorticity is >6 PVU the mixing ratios are much smaller than those in January, but in regions where the potential vorticity is <4 PVU the mixing ratios are almost the same as in January."

P.7, L.29 & Figure 10: Why does SF6, as a proxy for AoA, not show, in contrast to N2O and CH4, the minima at 370 K in the ExUTLS region (see Fig 10 a+b+d)?

Such "sandwich" structures have been commonly shown in Fig. 17 of the revised manuscript.

P.8, L.6-7 & Figure 10-11: "*The distribution of AoA during this season (autumn, comment by the reviewer) is similar to that during summer, with the AoA of nearly the entire region with potential vorticity of < 8 PVU being less than 1 year.*"
The seasonality of AoA here is different to that found by Boenisch et al. (2009). They found the minimum in AoA in October with AoA below 0.5 years for most of the LMS (< 8pvu). What is the explanation for the difference in the seasonality found in the study here?

The result has been changed in association with the use of 10-year trajectory, and it has become consistent with the results of Boenisch et al. (2009).

P.8, L.16-17: A direct comparison of AoA derived from SF6 and backward trajectories would be better (see comment: P.3, L.26-30). How does the contradiction of different seasonality of SF6 and AoA (derived from trajectories) in the UTLS fit to this result (see comment: P.7, L.5-10 & Figure 7)?

The comparison of traj-derived AoA and SF6-derived AoA has been made and the UTLS category has been removed.

P.8, L.29-30: How you confirm the impact of the Asian Monsoon (ASM) with your study? Do you use an algorithm marking and detecting ASM air, e.g. like Vogel et al. (2016)?

No, we simply confirm that the trajectories originating in Asian region increased in summer season. The statement has been corrected to "trajectories originating in the tropical troposphere over around Asia are strengthened." (P10, L10)

P.9, L.6 & Figure 13c: "*During winter, however, tropical tropospheric air masses dominate.*" This is true not only during winter, but also during spring (until the beginning of May).

Though the figure has been changed, but it remains true, so "and spring" has been added. (P10, L18)

P.9, L.10:"*In the high-latitude lower ExUTLS, mixing fractions of the mid- and high-latitude LT are enhanced but their fractions are lower than those of the mid-latitude lower ExUTLS.*" What is the reason? More of the trajectories started in the stratosphere in high- compared to mid-equivalent latitude lower ExUTLS (PV>2pvu at the initial starting point)?
A tropopause related analysis would help here to understand how much of the effect here is related to the starting location (UT or LMS) and how much is related to weaker uplift into the UT in mid- compared to high-equivalent latitudes.
Equivalent latitude might be not the optimal coordinate in the troposphere. In contrast to the stratosphere, where PV is dominated by the strong stratification (dTheta/dz), in the troposphere PV is dominated by relative vorticity. A consequence is that e.g. WCBs in the UT assigned with high tropospheric PV values (e.g. Madonna et al., 2014) would be classified as high-equivalent latitude air mass.

What the authors meant to here was "In the high-equivalent latitude lower (HL; such acronym has been used in the revised manuscript) ExUTLS, origin fractions of the mid- and high-latitude LT are enhanced during summer. Origin fractions of the high-latitude LT are comparable to those in the ML ExUTLS, but smaller than those of the mid-latitude LT in the HL ExUTLS."
Therefore, the literature has been revised (P10, L18-20), in addition, the following discussion has been added (P10, L20ff): "This can be explained by enhanced exchange at the bottom edge of the subtropical jet (i.e., along the 320–330 K surface for summer, e.g., Gettelman et al., 2011). As shown in Fig. 12d, enhanced origin fractions of the mid-latitude LT are distributed along such isentropes."

Relating this comment, the authors find that the phase "mid- latitude lower ExUTLS" should

be changed “mid-**equivalent** latitude lower ExUTLS,” this revision has been also done.

P.9, L.11-13 & Fig. 13+14: The seasonal pattern in Fig 13 and 14 has not the same pattern for species with strongly varying original time series in the different compartments (k=1-5), because the reconstructed time series shown in Fig 14 are a superposition of the mixing fractions shown in Fig. 13 with the original time series for k=1-5 of the individual tracers. The difference in the seasonal pattern between Fig 13 and Fig 14 is most obvious for CO2 which has a strong tropospheric seasonal cycle that is superimposed on the tropospheric mixing fractions.

The statement in the original manuscript was not correct. The statement has been revised to “Figure 20 reveals that seasonal variations in the reconstructions for each species and the trajectory-estimated AoA in each of the four locations have patterns that differ because they are based on a superposition of the origin fractions shown in Fig. 19 with the original time series for $k = 1–4$ of the individual tracers shown in Fig. 14.” (P10, L25-28)

P.9, L.33: Please add here the reference to Hoor et al. (2004)

It has been added (P11, L14).

P.10, L.20 & Fig. 15: The tracer-tracer relationships or “mixing lines” (AoA is a tracer like e.g. SF6) for sufficient long-lived tracers (chemical lifetime must be greater than at least the horizontal transport timescale) is in theory the consequence of sufficiently rapid mixing along isentropic surfaces. Please cite here the review by Plumb (2007) which includes many of the references to the pioneering works on this topic in the 80s and 90s.

Thank you very much for this informative comment. It has been cited and the following statement has been added (P12, L2-4): “Such linear “mixing lines” also suggest that the mixing took place rapidly (i.e., at a time-scale shorter than their chemical lifetimes) along an isentropic surface (Plumb, 2007 and references therein).”

P.10, L.21-23 & Fig. 15: CO2 mixing ratios and AoA does not correlate below a level of about 3 years AoA, because the propagated signal of the tropospheric seasonal cycle into the stratosphere is still detectable (not smeared out over a broad enough age spectra covering several seasonal cycles). This is the simple reason why CO2 mixing ratios in the LMS cannot be used to calculate AoA (see e.g. Engel et al., 2002; Boenisch et al., 2009).

Thank you for the instructive comment. CO2 is deleted in the sentence and the following statements has been added: "According to Engel et al. (2002) and Bönisch et al. (2009), the mixing ratios of CO_2 and AoA do not correlate below a level of ~3 years AoA because the propagated signal of the tropospheric seasonal cycle into the stratosphere is still detectable. In agreement with their results, the CONTRAIL CO_2 measurements also converge to the sign-reversed trend with increasing AoA." (P12, L5-8)

P.10, L.28-30 & Fig. 15f: "*Figure 15f shows seasonal variations in AoA and integrated PDF from 0 to 10 years for air masses originating in the high-latitude stratosphere*"
Fig. 15f only shows integrated PDFs for AoA from 0 to 6 years – please correct this.

The meaning of this sentence was that "The figure shows seasonal variations in AoA and the value that is calculated by integration of "age spectrum" (PDF) from 0 to *tf* for air masses originating in the stratosphere" The sentence has reworded (P12, L13-15).

P.12, L.3-4: The young-bias of AoA derived from backward trajectories in the LS should be verified (see my comment P.3, L.26-30 above)

It has been verified as described in the General Reply.

P.12, L.8-9: Please show this (see comment above).

It has been shown in Fig. 4 which has been newly made.

P.12, L.15-17: "*Moreover, these estimates are indirectly validated by the CONTRAIL observations, through the reconstruction of the chemical distributions (as evident in Figs 8–11).*"
This is only partially true, because you have a kind of free parameters, these are the original mixing ratio from the deep stratosphere (k=1) and the mixing ratios resided in the ExUTLS (k=5) during the 90 days of the backward trajectory simulation. Herewith, the interaction between CONTRAIL observed and trajectory-based mixing ratios can be adjusted. This is to my opinion most obvious for CO. The estimated CO for k=1 and 5 compensates other errors, e.g. chemical decay of CO during the transport from source region to the ExUTLS (see also other specific and general comments above).

In association with the change of the reconstruction method, the free parameters have been eliminated.

P.12, L.18-24: Both problems discussed here briefly, non-linear tropospheric trend and the lack of agreement in reconstruction of CONTRAIL observations during summer (Fig. 10e), concern mainly CO2, so please clarify and mention this here.

For the non-linear trend, the statement "In this study, linear trends for CH_4, N_2O, SF_6, and CO_2 are assumed for the reconstruction. Although this is a simplified treatment, given the length of the analysis period, these trends are roughly constant over this time period with the exception of CH_4, and the CH_4 reconstructions are more strongly affected by chemical loss, as is evident in a comparison of Figs 5a and 8a" has been added in P14, L33ff.
For the disagreement during summer, the statement "particularly for CO2 (Fig. 5e)" has been added in P14, L26.

P.12, L.24-26: It is true that the equivalent latitude-potential temperature (EqLat-Theta) coordinate system accounts for dynamical features in the stratosphere, because adiabatic motion is dominant in this strongly stably stratified region of the atmosphere. This is not true for the troposphere which is much more unstable (low static stability). Potential temperature (and PV) are not conserved or only for a much shorter timescale, because diabatic motion is much more prominent there. Therefore, potential temperature and equivalent latitude are not the coordinate system of choice in the troposphere. Also the problem of tracer uplift from the PBL into the UT during summer (most prominent for CO2, see above) is not minimised in an EqLat-Theta coordinate system.

Thank you for this instructive comment. The description "which are dynamically conserved quantities in the stratosphere. In the troposphere, which is more unstable, potential temperature and potential vorticity are not conserved, or are conserved only on much short timescales, because of diabatic motion. It should be noted that tracer uplift from the LT into the UT during summer (particularly for CO_2, as discussed above) cannot be reduced with the coordinate system employed here" has been added in P14, L27-30.

P.13, L.7: The mentioned role of Asian monsoon (ASM) is very likely, but it is speculation here, because it is not shown in this study, how much of the trajectories originated from the ASM (see also comment above).

The authors simply confirm that the trajectories originating in Asian region increased in summer season, so the statement "in association with the Asian summer monsoon" has been deleted.

P.13, L.15: "*The reconstructions agree well with CONTRAIL measurements in the ExUTLS.*"
If this is one key messages of the summary then the limitations of the 90-days backward trajectories and the sensitivity of the results due to this limitation have to be discussed in much more detail (see general and specific comments above).

The 10-years trajectory has been employed as described in the General Reply.

P.13, L.23-24:"*This method provides a means to understand both dynamical transport and chemical distribution from a new perspective.*"
There has been done a lot to understand dynamical, tracer transport and chemical processes in the UTLS. Some of these studies has been mentioned in this review and should be discussed in relation to the results in this manuscript. As outlined in my general comment, I am not convinced that the actual manuscript could contribute to the actual state of knowledge, but the results should be at least discussed in this framework. The uniqueness of this approach here, combination of different tracers and backward trajectories, could to my opinion be exploited much better, if one would use 10-years instead of 90-days backward trajectories.

The 10-years trajectory has been used, and the authors believe that this study has been significantly improved.

In addition to above revision following the reviewers' comments, the authors have added new Appendix (Appendix B and relating two figures) in the revised manuscript to visualize large perspective of seasonal variation in ExUTLS.

References:
Appenzeller, C., J. R. Holton, and K. H. Rosenlof (1996), Seasonal variation of mass transport across the tropopause, J. Geophys. Res., 101(D10), 15071-15078.
Birner, T., and H. Bönisch (2011), Residual circulation trajectories and transit times into the extratropical lowermost stratosphere, Atmos. Chem. Phys., 11(2), 817-827, doi:10.5194/acp-11-817-2011.

Bönisch, H., A. Engel, J. Curtius, T. Birner, and P. Hoor (2009), Quantifying transport into the lowermost stratosphere using simultaneous in-situ measurements of SF6 and CO2, Atmos. Chem. Phys., 9(16), 5905-5919, doi:10.5194/acp-9-5905-2009.

Diallo, M., Legras, B., and Chédin, A. (2012): Age of stratospheric air in the ERA-Interim, Atmos. Chem. Phys., 12, 12133-12154, https://doi.org/10.5194/acp-12-12133-2012, 2012.

Diallo, M., B. Legras, E. Ray, A. Engel, and J. A. Añel (2017), Global distribution of CO2 in the upper troposphere and stratosphere, Atmos. Chem. Phys., 17(6), 3861-3878, doi:10.5194/acp-17-3861-2017.

Engel, A., M. Strunk, M. Muller, H. P. Haase, C. Poss, I. Levin, and U. Schmidt (2002), Temporal development of total chlorine in the high-latitude stratosphere based on reference distributions of mean age derived from CO2 and SF6, J. Geophys. Res., 107(D12), doi:Artn 4136 Doi 10.1029/2001jd000584.

Engel, A., et al. (2006), Highly resolved observations of trace gases in the lowermost stratosphere and upper troposphere from the Spurt project: an overview, Atmos. Chem. Phys., 6, 283-301, doi:DOI 10.5194/acp-6-283-2006.

Fueglistaler, S., H. Wernli, and T. Peter (2004), Tropical troposphere-to-stratosphere transport inferred from trajectory calculations, Journal of Geophysical Research: Atmospheres, 109(D3), doi:10.1029/2003JD004069.

Fueglistaler, S., M. Bonazzola, P. H. Haynes, and T. Peter (2005), Stratospheric water vapor predicted from the Lagrangian temperature history of air entering the stratosphere in the tropics, Journal of Geophysical Research: Atmospheres, 110(D8), doi:10.1029/2004JD005516.

Fueglistaler, S., and P. H. Haynes (2005), Control of interannual and longer-term variability of stratospheric water vapor, Journal of Geophysical Research: Atmospheres, 110(D24), doi:10.1029/2005JD006019.

Gettelman, A., P. Hoor, L. L. Pan, W. J. Randel, M. I. Hegglin, and T. Birner (2011), The Extratropical Upper Troposphere and Lower Stratosphere, Rev. Geophys., 49, doi:Artn Rg3003, Doi 10.1029/2011rg000355.

Hall, T. M., and R. A. Plumb (1994), Age as a Diagnostic of Stratospheric Transport, J. Geophys. Res., 99(D1), 1059-1070.

Hoor, P., C. Gurk, D. Brunner, M. I. Hegglin, H. Wernli, and H. Fischer (2004), Seasonality and extent of extratropical TST derived from in-situ CO measurements during SPURT, Atmos. Chem. Phys., 4, 1427-1442.

Hoor, P., H. Fischer, and J. Lelieveld (2005), Tropical and extratropical tropospheric air in the lowermost stratosphere over Europe: A CO-based budget, Geophys. Res. Lett., 32(7), L07802, doi:10.1029/2004gl022018.

Hoor, P., H. Wernli, M. I. Hegglin, and H. Boenisch (2010), Transport timescales and tracer properties in the extratropical UTLS, Atmos. Chem. Phys., 10(16), 7929-7944, doi:10.5194/acp-10-7929-2010.

Madonna, E., H. Wernli, H. Joos, and O. Martius (2014), Warm Conveyor Belts in the ERA-Interim Dataset (1979–2010). Part I: Climatology and Potential Vorticity Evolution, Journal of Climate, 27(1), 3-26, doi:10.1175/jcli-d-12-00720.1.

Ploeger, F., and T. Birner (2016), Seasonal and inter-annual variability of lower stratospheric age of air spectra, Atmos. Chem. Phys., 16(15), 10195-10213, doi:10.5194/acp-16-10195-2016.

Plumb, R. A. (2007), Tracer interrelationships in the stratosphere, Rev. Geophys., 45(4), Artn Rg4005, doi:10.1029/2005rg000179.

Ray, E. A., F. L. Moore, J. W. Elkins, G. S. Dutton, D. W. Fahey, H. Vomel, S. J. Oltmans, and K. H. Rosenlof (1999), Transport into the Northern Hemisphere lowermost stratosphere revealed by in situ tracer measurements, J. Geophys. Res., 104(D21), 26565-26580.

Riese, M., F. Ploeger, A. Rap, B. Vogel, P. Konopka, M. Dameris, and P. Forster (2012), Impact of uncertainties in atmospheric mixing on simulated UTLS composition and related radiative effects, J. Geophys. Res., 117(D16), D16305, doi:10.1029/2012jd017751.

Schoeberl, M. R., L. C. Sparling, C. H. Jackman, and E. L. Fleming (2000), A Lagrangian view of stratospheric trace gas distributions, Journal of Geophysical Research: Atmospheres, 105(D1), 1537-1552, doi:10.1029/1999JD900787.

Shepherd, T. G. (2002), Issues in Stratosphere-troposphere Coupling, Journal of the Meteorological Society of Japan. Ser. II, 80(4B), 769-792, doi:10.2151/jmsj.80.769.

Škerlak, B., M. Sprenger, and H. Wernli (2014), A global climatology of stratosphere–troposphere exchange using the ERA-Interim data set from 1979 to 2011, Atmos. Chem. Phys., 14(2), 913-937, doi:10.5194/acp-14-913-2014.

Tilmes, S., et al. (2010), An aircraft-based upper troposphere lower stratosphere O3, CO, and H2O climatology for the Northern Hemisphere, Journal of Geophysical Research: Atmospheres, 115(D14), doi:10.1029/2009JD012731.

Vogel, B., et al. (2016), Long-range transport pathways of tropospheric source gases originating in Asia into the northern lower stratosphere during the Asian monsoon season 2012, Atmos. Chem. Phys., 16(23), 15301-15325, doi:10.5194/acp-16-15301-2016.

GENERAL REPLY

The authors thank the two reviewers for their constructive comments and helpful suggestions that have improved the manuscript.

As mentioned by the both reviewers, the reconstruction method had some shortcomings, but the reviewers, especially reviewer #1, gave concrete and great suggestions to resolve them. The manuscript has been largely revised and improved along the suggestions. The authors describe first the revisions in the reconstruction method as a General Reply.

The suggestions are as follows:
(1) use of 10-year trajectory instead of 90-day, which can eliminate the remaining trajectories in the UTLS (k=5);
(2) reconstruction of chemical passive tracers with evaluation of transport timescale (as the first step); and
(3) reconstruction of chemical active tracers including chemical decay (as the second step).
The authors have made these procedures and some relating revisions as follows.

For point (1), as noted by the reviewers, the remaining trajectories in the UTLS (k=5) could be eliminated, i.e., it was confirmed that the all trajectories are categorized into any origins of k = 1, 2, 3, or 4 within 10 years (Note that the criteria have also been revised to avoid some shortcomings). In addition, the inversion method to estimate tracer mixing ratio for k=1 and 5 in the original manuscript could be also eliminated, i.e., the all tracers in the ExUTLS have been reconstructed only from their mixing ratios assumed in the high-latitude LT, mid-latitude LT, and tropical troposphere.

For point (2), using the 10-year trajectory, Age of Air (AoA) as well as SF6 and CO2 distributions have been reconstructed from the trajectories including the "Tail correction" (e.g., Diallo et al., 2012). The CH4, N2O, CO have been also reconstructed without any chemical decay in this step. AoA has been also estimated using observed SF6 mixing ratios obtained by CONTRAIL, and then the two AoAs have been compared to correct transport timescale expressed in the trajectories.

For point (3), the chemical active tracers, CH4, N2O, and CO, are finally reconstructed with simulating their chemical loss along an "average path" (Schoeberl et al., 2000). The use of the concept of average path was also suggested by the reviewer #1. Based on this concept, the authors believe that the active

tracers have been successfully reconstructed together with estimation of seasonally depending their chemical loss rate.

In relation to a suite of these revisions, the latter half of section 2.1 (Estimating the origin fraction and AoA), large part of section 2.2 (Air mass original composition and reconstruction) were significantly revised, especially section 2.2 was reorganized and a new subsections 2.2.1 and 2.2.2 were created for reconstructions of chemical passive and active tracers, respectively. The analyzing results, figures, and discussions were thus also changed in association with the revision of the reconstruction method, but the main thesis was essentially not changed.

References:

Diallo, M., Legras, B., and Chédin, A.: Age of stratospheric air in the ERA-Interim, Atmos. Chem. Phys., 12, 12133-12154, https://doi.org/10.5194/acp-12-12133-2012, 2012.

Schoeberl, M. R., Sparling, L. C., Jackman, C. H., and Fleming, E. L.: A Lagrangian view of stratospheric trace gas distributions, Journal of Geophysical Research: Atmospheres, 105(D1), 1537-1552, doi:10.1029/1999JD900787, 2000.

The authors believe that the revised manuscript has been improved by incorporating the more appropriate reconstruction method.

Point-by-point responses to the comments of individual reviewer are provided below.

REPLY TO COMMENTS BY REVIEWER #2

The author is grateful for the thorough review and constructive comments on the manuscript. All of the points raised by the reviewer have been addressed. The major revision was made following the #1 reviewer's comments, please see first the "General Reply" section. Point-by-point responses are provided below, in red text.

Interactive comment on "Seasonal characteristics of chemical and dynamical transports into the extratropical upper troposphere/lower stratosphere" by Yoichi Inai et al.

Anonymous Referee #2

Received and published: 2 January 2019

The paper by Inai et al. investigates the air mass composition of the extratropical upper troposphere and lower stratosphere (exUTLS), and relates to CONTRAIL in-situ observations of several trace gas species (e.g., CH4, N2O, SF6, CO, CO2). The focus of the study lies on seasonal variations in air mass fractions and mixing ratios. In particular, it is found that seasonality in CH4, N2O and SF6 mixing ratios is controlled by transport from the deep stratosphere, due to the locations of the main chemical sink regions, whereas CO and CO2 are mainly controlled by transport from the tropical troposphere.

The air mass and tracer composition of the exUTLS is of particular relevance for global climate due to the radiative characteristics of this region. Hence, the present study fits well into the scope of ACP. The paper is well written and presented, and the current literature is appropriately discussed. I recommend publication after taking into account the several comments below, which I regard somewhere between major and minor.

Detailed comments:

1. Initialization: The trajectory initialization is somewhat unclear to me. In the respective text part it is said, that back trajectories are initialized between 0-140 deg E, but the corresponding Fig. 1 shows initialization locations for 0-360 deg E (P2/L27). How is the initialization done exactly?

Fig. 1 in the original manuscript was not correct. The figure has been corrected.

2. Model-measurement comparison: The CONTRAIL measurements are mainly from Siberia. How is the model-measurement comparison done, exactly at the measurement locations/times, or just averaged over specific regions? I would suggest to explain this clearly directly after the description of the trajectory initialization (P2).

Indeed, it could be designed to release trajectories exactly at the measurement location/time and it may make directly comparison with the CONTRAIL measurements; this study, however, attempts to reconstruct spatial-extending and uniform spatiotemporal tracer distributions as well as their transport, therefore, we choose to employ the grating initialization. Following the suggestion, the statement "Although trajectories could be released at the exact CONTRAIL measurement locations and times, the grating initialization is employed because this study attempt to obtain uniform spatiotemporal tracer distributions as well as their transports by capitalizing on the CONTRIAL measurements" has been added in P2, L31ff in the revised manuscript.

3. Reconstruction method: It would be good to mention (around P4/L10) that Eq. (2) holds only for species which are chemically inert along the trajectories. Can you give some quantitative information how well this assumption holds for the species and regions considered here? Perhaps some of the difference between reconstruction and measurements (e.g., Figs. 7-10) is related to neglecting chemistry effects?

As described in the General Reply, the reconstruction method has been revised. The chemically active species are reconstructed taking the chemical decay into account.

4. Origin mixing ratios (P4/L28): Why not using higher altitude in-situ measurements (e.g., from balloons, Geophysica/Halo/ER2/... aircrafts) or global satellite observations for the reference mixing ratios? At least the "inversion method" outlined below could be validated with such data.

As described in the General Reply, the reconstruction method has been revised. In association with the revision, the "inversion method" has been eliminated.

5. Minima in tracer distributions around 370K in spring/summer (P7/L21ff): I do not think these minima are just artifacts of the reconstruction. The fact that spring/summer transport of young tropical air strengthens first around 380-400K, leading to a "sandwich" structure with older air masses below is consistent with recent findings by Krause et al. (2018) (see e.g.

their Fig. 14) and Ploeger and Birner (2016) (e.g., their Fig. 7).
In agreement with these papers, Fig. 9/10 show evidence for strongest polward transport above about 380K, causing the mixing ratio minima below. I would suggest to discuss these distributions more appropriately.

Thank you for this informative comment and suggestion. Though the sandwich structures have changed their aspects due to the revision of reconstruction method, they have appeared at around 350 K as shown in Fig. 17. Following above suggestion, the following statements have been added (P9, L13-17): "In particular, all five chemical species show minima at ~350 K north of 60° N equivalent latitude. These minima might be formed by remainder of the deep stratospheric air masses which were transported during spring. The tracer minima near ~350 K at high equivalent latitudes begin forming in June. This "sandwich" structure in the ExUTLS has been reported by Ploeger and Biner (2016) for summer and by Krause et al. (2018) for spring. In agreement with their studies, the sandwich structures can show evidence for strong poleward transport above ~400 K, leading to mixing ratio minima at lower altitudes."

6. Trajectory method: Kinematic trajectories show stronger dispersion compared to diabatic trajectories (e.g., Schoeberl et al., 2003). Are the results presented here robust also for diabatic transport? At least include appropriate discussion in Sect. 4.3 ("Limitations of the current study").

The authors have not used diabatic trajectory, so we do not explicitly know how much the results change. Instead, statements "Trajectory results also generally depend on the vertical condition, i.e., kinematic (employed by the current study) or diabatic (employed by, for example, Diallo et al., 2017). Previous studies suggest that using kinematic trajectories leads to a stronger dispersion and somewhat young bias in AoA estimates compared with using diabatic trajectories (e.g., Schoeberl et al., 2003; Diallo et al., 2012). Therefore, using diabatic trajectories in this analysis might result in a correction factor (γTT) of <1.5." have been added in Sect. 4.3 (P14, L1-4).

Specific and technical comments:
P1/L29: maybe better "at/along the subtropical jet"?
Change made as suggested.

P3/L23: "...where IT satisfies..."?
Corrected.

P3/L28: What is the "actual value" what is referred to here? Observations? Which?
It is referred to observation. Statement “actual value” has been changed to “observed value.”

P7/L29: ware –> were
Corrected.

P9/L10ff: The sentence "In addition ..." sounds unclear to me - I suggest rewording.
The sentence has been reworded to “In addition to seasonal variations in origin fractions, seasonal variations in the tracer mixing ratios in origin regions (Fig. 14) also affect chemical distributions in the ExUTLS.” (P10, L24-25)

P9/L19: shown –> show
Corrected.

P10/L28ff: I don’t understand the description of Fig. 15f. What PDF is integrated here (transit time pdf?). What is the unit of the y-axis? Please clarify and improve the description.
The integration is done for age spectrum, so statement “the value that is calculated by integration of “age spectrum” (PDF)” was added in P12, L14.

P12/L7: The Ploeger and Birner reference cited here is not in the reference list.
The reference has been added.

P12/L20: non-linear
Corrected.

In addition to above revision following the reviewers’ comments, the authors have added new Appendix (Appendix B and relating two figures) in the revised manuscript to visualize large perspective of seasonal variation in ExUTLS.

References:
Krause et al. (2018), Atmos. Chem. Phys., 18, 6057-6073.
Schoeberl et al. (2003), J. Geophys. Res, 118, D3.

Seasonal characteristics of ~~chemical and dynamical transports~~trace gas transport into the extratropical upper troposphere/lower stratosphere

Yoichi Inai[1], Ryo ~~Fujita[1]~~Fujita[2,1], Toshinobu ~~Machida[2]~~Machida[3], Hidekazu ~~Matsueda[3]~~Matsueda[4], Yousuke ~~Sawa[3]~~Sawa[4], Kazuhiro ~~Tsuboi[3]~~Tsuboi[4], Keiichi ~~Katsumata[2]~~Katsumata[3,5], Shinji Morimoto[1], Shuji Aoki[1], Takakiyo Nakazawa[1]

[1]~~Center~~[1] Center for Atmospheric and Oceanic Studies, Graduate School of Science, Tohoku University, Sendai, 980-8578, Japan
[2]~~2~~ Department of Physics, Imperial College London, South Kensington Campus, London SW7 2AZ, United Kingdom
[3] National Institute for Environmental Studies, Tsukuba, 305-8506, Japan
[3]~~4~~ Meteorological Research Institute, Tsukuba, 305-0052, Japan
[5] Now at Takachiho Chemical Industrial Co., Ltd., Tokyo, 194-0004, Japan

Correspondence to: Yoichi Inai (yoichi_inai@tohoku.ac.jp)

Abstract. To investigate the seasonal characteristics of ~~chemical tracer~~trace gas distributions in the extratropical upper troposphere and lower stratosphere (ExUTLS) as well as stratosphere–troposphere exchange processes, ~~mixing~~origin fractions of air masses originating in the stratosphere, tropical troposphere, mid-latitude lower troposphere (LT), and high-latitude LT in the ExUTLS are estimated using ~~90-day~~10-year backward trajectories calculated with European Centre For Medium-Range Weather Forecasts (ECMWF) ERA-Interim data as the meteorological input. Time-series of ~~chemical tracers~~trace gases obtained from ground-based and airborne observations are incorporated into the ~~estimated mixing fractions~~trajectories, thus reconstructing spatiotemporal distributions of ~~chemical tracers~~trace gases in the ExUTLS. The reconstructed tracer distributions are analysed with the ~~mixing~~origin fractions and the stratospheric age of air (AoA) estimated using ~~a 10-year~~the backward ~~trajectory~~trajectories. The reconstructed distributions of CO and CO_2 in the ExUTLS are affected primarily by tropospheric air masses because of the short chemical lifetime of the former and large seasonal variations in the troposphere of the latter. Distributions of CH_4, N_2O, and SF_6 are controlled primarily by seasonally varying air masses transported from the stratosphere. For CH_4 and N_2O distributions, ~~air masses transported via~~chemical decay along the ~~deep branch of~~average path from the ~~Brewer–Dobson circulation are~~ source region is particularly important~~. This interpretation is qualitatively and quantitatively supported by the estimated spatiotemporal distributions of AoA~~.

1 Introduction

The extra-tropical upper troposphere and lower stratosphere (ExUTLS; e.g., Gettelman et al., 2011) accounts for about 40 % of the total stratospheric air mass (Appenzeller et al., 1996) and about 20 % of stratospheric aerosols (Andersson et al., 2015).

Trace gases and aerosols in the ExUTLS play an important role in atmospheric radiative processes~~, especially in the Arctic climate.~~. These species are transported to the ExUTLS from the deep stratosphere via stratospheric ~~residual~~ circulation (Brewer–Dobson circulation, BDC; Brewer, 1949; Dobson, 1956) and from the lower troposphere or the tropical troposphere via local convection, frontal cyclones, Rossby wave breaking ~~in~~at/along the subtropical jet, monsoon activity, and other systems (e.g., Holton et al., 1995; Wernli and Bourqui, 2002; Manney et al., 2011; Pan et al., 2016; Vogel et al., 2016; Boothe and Homeyer, 2017; Ploeger et al., 2017).

Air-mass transport processes into the ExUTLS are strongly dependent on the season. This leads to stratospheric and tropospheric mixing fractions that show clear seasonality. For example, Appenzeller et al. (1996) estimated the mass flux across the 380 K isentrope due to global-scale meridional circulation and found that the downwelling mass flux from the stratosphere varies from 8×10^9 kg s^{-1} in summer to 15×10^9 kg s^{-1} in winter, whereas the Asian summer monsoon and local convection, which supply tropospheric air to the ExUTLS, are active only during the summer and early autumn (e.g., Randel and Park, 2006; Randel et al., 2010). The composition of air masses transported from the deep stratosphere, lower troposphere, and tropical troposphere also shows seasonal variations (e.g., Boenisch et al., 2009). The seasonal variability in air-mass composition and mass-flux strength makes it difficult to essentially understand the distributions of trace gases in the ExUTLS and to describe their transport into the layer.

This study focuses on mixing fractions of air masses originating in the ~~high-latitude~~ stratosphere, tropical troposphere, mid-latitude lower troposphere (LT), and high-latitude LT (hereafter, referred to as "origin fractions") in the ExUTLS, based on the trajectory analysis of Inai (2018). Using estimated ~~mixing~~origin fractions, the transport of chemical species into the ExUTLS and the spatiotemporal distributions of methane (CH_4), nitrous oxide (N_2O), carbon monoxide (CO), sulphur hexafluoride (SF_6), and carbon dioxide (CO_2) in the layer are reconstructed with the aid of atmospheric trace- gas observations including aircraft measurements, such as those of the Comprehensive Observation Network for TRace gases by AIrLiner (CONTRAIL; Nakazawa et al., 1993; Matsueda and Inoue, 1996; Ishijima et al., 2001; Matsueda et al., 2002; Machida et al., 2008; Umezawa et al., 2014; Sawa et al., 2015). Reconstructed distributions for the five species are discussed in terms of dynamical transport as well as chemical loss, using the stratospheric age of air (AoA) as an indicator of air mass transport via the deep and shallow branches of the BDC.

2 Methods

2.1 Estimating the ~~mixing~~origin fraction and age of air

The CONTRAIL data were obtained by collecting air samples once a month from April 2012 to December 2016 at longitudinal intervals of 10° or 15° along individual flight tracks at around 11 km altitude between France/Russia and Japan. The period and longitudinal locations of this analysis were selected based on the CONTRAIL measurements, for which air sampling in the ExUTLS was usually made over Siberia. To identify the origins of ExUTLS air masses, kinematic backward trajectories are calculated for ~~90 days~~10 years following the method of Inai (2018). Trajectories are initialized at uniformly distributed

grid points (5.0° longitude × 2.5° latitude) within 45° N–80° N and 0° E–140° E at geopotential heights of 5, 6, 7, 8, 9, 10, 11, 12, 13, 14, 15, and 16 km (Fig. 1). Initializations are made at 00:00 UTC on the 5th, 15th, and 25th of every month from January 2012 to December 2016, and use meteorological conditions prescribed by the European Centre ~~For~~for Medium-Range Weather Forecasts (ECMWF) ERA-Interim dataset (~~0.75° × 0.75~~1.5° × 1.5° horizontal resolution, 6 hourly temporal resolution, and ~~60 model~~37 pressure levels; Dee et al., 2011). Although trajectories could be released at the exact CONTRAIL measurement locations and times, the grating initialization is employed because this study attempt to obtain uniform spatiotemporal tracer distributions as well as their transports by capitalizing on the CONTRIAL measurements. An example of the results is provided in Fig. 2, which shows where particles located as shown in Fig. 1 at 00Z on 15 January 2015 were located ~~90~~361 days prior (i.e., 00Z on ~~20 October~~19 January 2014). Many particles ending up at altitudes greater than 13 km (orange dots) travelled from the ~~mid- or high-latitude~~ stratosphere, above 18 km. However, many particles ending up at altitudes below 10 km (purple to blue-green dots) ~~originated near 10~~distribute below 15 km, typically in the troposphere. ~~The distribution~~Although the accuracy of ~~some~~individual trajectories is limited by the long-term nature of the ~~particles (green and yellow dots) in the troposphere near ~ 10° N (upper right panel~~calculations, statistical features of ~~Fig. 2) suggests significant vertical~~air-mass transport ~~from the LT to the UTLS in this latitudinal region~~can be investigated using a large number of trajectories.

Trajectories obtained from each run are categorized into several groups (trj_k; k = 1 to $kmax$) with criteria (hereafter denoted cri_k) of potential temperature, latitude, potential vorticity, and geopotential height along each trajectory. In this analysis, $kmax$ is set to ~~5~~4, with k = 1 for the ~~high-latitude~~ stratosphere, k = 2 for the tropical troposphere, k = 3 for the mid-latitude LT, and k = 4 for the high-latitude LT~~, and k = 5 for all other trajectories.~~. Criteria for each k are summarized in Table 1. ~~Note that mixing fractions in the high-latitude stratosphere (k = 1) that have~~The trajectories are also used to determine whether trajectories categorized as $trj_{k=1}$ passed through the deep ~~(k = 1a) and~~or shallow ~~(k = 1b) branches~~branch of the BDC ~~are evaluated separately using 10-year trajectory calculations with the coarse meteorological data described below. Air masses in the fifth group (k = 5) are considered to be of the tropical and extratropical UTLS, because for at least 90 days they~~ (k = 1d or 1s). These trajectories are classified ~~into neither the LT (all latitudes) nor the stratosphere (high latitudes) groups.~~as shallow-branch if they cross 400 K but do not reach 30 hPa within 4 years, and as deep-branch if they exceed 30 hPa within 4 years, following the method of Lin et al. (2015). Trajectories were categorized as trj_k, according to the first set of 3 continuous days along the trajectory that satisfied the cri_k~~, except for~~. This resulted in all trajectories being categorized as k~~= 5.~~ = 1, 2, 3, or 4 within 10 years. Trajectories trj_k are assumed to travel along ~~their own pass ways~~unique paths from origin k to the initial position of the backward trajectory. ~~Mixing~~Origin fractions of air parcels with origin k (hereafter denoted f_k) are calculated as a function of equivalent latitude ($\emptyset_{eq}$), potential temperature (θ), and month ($\mathcal{M}$) of their release. Denoting as N_k the number of trajectories, which are classified into trj_k groups with distinct $\emptyset_{eq}$, θ, and $\mathcal{M}$, the ~~mixing~~origin fraction for origin k is given by

$$f_k = \frac{\sum_{i=1}^{N_k} \rho_{trj_k ini}(i) * \cos \emptyset_{trj_k ini}(i)}{\sum_{k=1}^{kmax} (\sum_{i=1}^{N_k} \rho_{trj_k ini}(i) * \cos \emptyset_{trj_k ini}(i))}, \quad (1)$$

where $\emptyset_{trj_k ini}$ and $\rho_{trj_k ini}$ indicate the initial latitude and density of the individual backward trajectories, respectively. Note that $\rho_{trj_k ini}$ is calculated from the equation of state. Results of a sensitivity analysis indicate that the estimated origin fractions are independent of the resolution of the input meteorological data (see Appendix A).

Similar methods are used to estimate the AoA, which is calculated as the average elapsed time until a trajectory goes back to the troposphere where it satisfies whichever criteria k = 2, 3, or 4. ~~In this~~ Thus, the AoA definition used here differs from that of Hall and Plumb (1994), who defined AoA as the elapsed time an air parcel spends in the stratosphere after across the tropopause. In our estimates of AoA, however, a small fraction of trajectories are still in the stratosphere at the end of the 10-year calculation~~, the coarser ERA-Interim data (~~1. Figure 3 shows the percentage of such remaining trajectories estimated as a function of $\emptyset_{eq}$, θ, and $\mathcal{M}$ of their release. The percentages are almost zero in the region where potential vorticity is <4 PVU, whereas they are generally non-zero in the region where potential vorticity is >4 PVU. However, even in this region the values are <2.5~~° × 1.5° horizontal resolution, 6 hourly temporal resolution, and 37 pressure levels) are used to reduce the computational burden, as the~~ %. Here, we define ε as the percentage of trajectories that are still in the stratosphere after the 10-year backward calculation ~~period extends to~~ as a function of $\emptyset_{eq}$, θ, and $\mathcal{M}$ (Fig. 3). Then, the AoA (Γ_{Trj}) is obtained using the elapsed time since each trajectory $trj_k(i)$ left its origin k ($\equiv \tau_k(i)$) according to

$$\Gamma_{Trj} = \sum_{k=2}^{4} \frac{\sum_{i=1}^{N_k} \gamma TT * \tau_k(i) * \rho_{trj_k ini}(i) * \cos \emptyset_{trj_k ini}(i)}{\sum_{i=1}^{N_k} \rho_{trj_k ini}(i) * \cos \emptyset_{trj_k ini}(i)} * (1 - \varepsilon) + \overline{\Gamma_{\text{tail}}} * \varepsilon, \quad (2)$$

where $\overline{\Gamma_{\text{tail}}}$ is the average AoA for air parcels remaining in the stratosphere longer than the maximum length of the trajectory calculation tf (= 10 years~~. Results of a sensitivity~~), calculated as follows:

$$\overline{\Gamma_{\text{tail}}} = \frac{\int_{\gamma TT * tf}^{\infty} \tau' * PDF(\tau') * \exp\left(-b * (\tau' - \gamma TT * tf)\right) d\tau'}{\int_{\gamma TT * tf}^{\infty} PDF(\tau') * \exp(-b * (\tau' - \gamma TT * tf)) d\tau'}, \quad (3)$$

$$= (\gamma TT * tf + \frac{1}{b}), \quad (3')$$

where PDF is the age probability distribution function or "age spectrum," and b is the exponential decay parameter of the PDF, with its value (b = 0.2038 yr^{-1}) from Diallo et al. (2012). The decay parameter in the present analysis ~~indicate that estimated mixing fractions are independent of the resolution of the input data (see Appendix A). However,~~ may differ from that used by Diallo et al. (2012) because of differences in the vertical trajectory calculations (i.e., kinematic in the present study and diabatic in their work). However, this difference is expected to have little impact on the results because ε is small, as shown in Figure 3. The term γTT in Eqs (3 and 3') is a correction factor for τ_k and is required because previous studies (e.g., Inai~~(~~, 2018) have found that the AoA ~~evaluated from a~~estimated by trajectory analysis using ~~the same~~ ERA-Interim data ~~as used in~~is underestimated, particularly when using a kinematic treatment. Inai (2018) found that this ~~work is roughly~~underestimation corresponds to 70 % of the ~~actual~~observed value in the mid-latitude stratosphere. To address this underestimation, ~~AoA calculated here are multiplied by a correction factor of 1.43 (the reciprocal of 0.7).~~the AoA values calculated here are corrected

by comparing with AoA derived from SF_6 mixing ratios (Γ_{SF6}) assuming a linear trend relative to the time series at Mauna Loa (https://www.esrl.noaa.gov/gmd/obop/mlo/) of 0.33 ppt yr^{-1} (ppt: parts per trillion by mole, with similar definitions for ppm and ppb). When γTT is set at 1.5, Γ_{Trj} agrees well with Γ_{SF6} (Fig. 4). Thus, a value of 1.5 was used for γTT in this study. The AoA for air masses originating in the ~~high-latitude stratosphere and UTLS are also evaluated only using $trj_{k=1}$ for the former and $trj_{k=5}$ for the latter. The 10-year trajectories are also used to determine whether trajectories categorized as $trj_{k=1}$~~stratosphere and those that passed through the deep ~~or shallow branch of the BDC (k = 1a or 1b). These trajectories are classified as the shallow branch if they cross 380 K but do not reach 30 hPa within 4 years, and as the deep branch if they exceed 30 hPa within 4 years, following the method of Lin et al. (2015~~and shallow branches of the BDC were evaluated using $trj_{k=1}$, $trj_{k=1d}$, and $trj_{k=1s}$, respectively. Note that because this study performs a trajectory analysis using an objective reanalysis dataset, subgrid-scale processes, such as the sporadic injection of tropospheric air masses into the ExUTLS, cannot be explicitly reproduced. Thus, to remove the influence of such events, CONTRAIL data with CO mixing ratios higher than 80 ppb in the region above 340 K and north of 60° N equivalent latitude are not used in this comparison (the same criteria are applied to the comparison shown in Fig. 8 in Sect. 2.2.2).

2.2 Air-mass original composition and reconstruction

2.2.1 Reconstruction without chemical loss (step 1)

The relative abundance of chemical species in the ExUTLS is strongly affected by changes in the breakdown of transported air masses, reflecting the fact that air-mass chemical composition varies with origin. For example, low-latitude tropospheric air masses have relatively high N_2O mixing ratios, whereas high-latitude stratospheric air masses have low mixing ratios, because N_2O sources and sinks exist in the troposphere and the stratosphere, respectively. This study attempts to reconstruct the spatiotemporal distributions of the chemical species CH_4, N_2O, CO, SF_6, and CO_2, in the following two steps.

First, the chemically passive tracers (i.e., SF_6 and CO_2) are reconstructed. According to Inai (2018), if there is no chemical loss for S, the mixing ratio of chemical species S in the ExUTLS (~~X^S~~X^S_{NoChem}) can be reconstructed as a function of $\emptyset_{eq}$, θ, and $\mathcal{M}$ in combination with f_k and the chemical transport from origin k ($X^S{}_k$):

$$X^S_{NoChem} = \sum_{k=1}^{kmax} f_k * X^S{}_k. \quad (24)$$

As the time series $X^S{}_k$ should be treated climatologically for each k and S, as required for the origin fraction f_k, it is necessary to detrend their values. ~~By expressing the~~Therefore, the seasonality and trend of the mixing ratio of S are separately treated in this study. By expressing the detrended mixing ratio of S for an air mass originating in region k ($\equiv X^S{}_{ORG_k}$) as a function of month ~~$\mathcal{M}$ and the elapsed time of~~($\equiv \mathcal{M}_{ORG}(i)$) when trajectory $trj_k(i)$ ~~since leaving its~~goes back to origin k ~~($\equiv \tau_k(i)$), X^S~~after its advection during $\gamma TT * \tau_k(i)$ and assuming the tropospheric linear trend ($\equiv \lambda^S$), X^S_{NoChem} is calculated as a function of $\emptyset_{eq}$, θ, and $\mathcal{M}$ as follows:

~~$$X^S(\mathcal{M}) = \sum_{k=1}^{kmax} \frac{\sum_{i=1}^{N_k} X^S_{ORG_k}(\mathcal{M}-\tau_k(i))*\rho_{trj_k lnt}(i)*\cos\emptyset_{trj_k lnt}(i)}{\sum_{i=1}^{N_k}\rho_{trj_k lnt}(i)*\cos\emptyset_{trj_k lnt}(i)}. \quad (3)$$~~

~~As the time series $X^S_{ORG_k}$ should be treated climatologically for each k and S, as required for the mixing fraction f_k,~~

$$X^S_{NoChem} = \sum_{k=2}^{4} \frac{\sum_{i=1}^{N_k}\left(X^S{}_{ORG_k}(\mathcal{M}_{ORG}(i)) - \lambda^S * \gamma TT * \tau_k(i)\right) * \rho_{trj_k ini}(i) * \cos\emptyset_{trj_k ini}(i)}{\sum_{i=1}^{N_k} \rho_{trj_k ini}(i) * \cos\emptyset_{trj_k ini}(i)} * (1-\varepsilon) + \overline{X^S_{\text{tail}}} * \varepsilon, \quad (5)$$

where $\overline{X^S_{\text{tail}}}$ is average mixing ratio of S for air parcels remaining in the stratosphere more than tf and is calculated as follows:

$$\overline{X^S_{\text{tail}}} = \frac{\int_{\gamma TT * tf}^{\infty} (\chi_{2016} - \lambda^S * \tau\prime) * PDF(\tau') * \exp\left(-b * (\tau' - \gamma TT * tf)\right) d\tau\prime}{\int_{\gamma TT * tf}^{\infty} PDF(\tau\prime) * \exp(-b * (\tau' - \gamma TT * tf)) d\tau\prime}, \quad (6)$$

$$= \chi^S_{2016} - \lambda^S * (\gamma TT * tf + \frac{1}{b}). \quad (6')$$

For $X^S{}_{ORG_k}$ ~~it is necessary to detrend their values. In this study,~~ detrending is applied to the observed values for k = 2, 3, and 4 in which a linear trend is determined for each dataset for the period 2012–2016 and all the observed values are normalized to those on January 2016. ~~Data observed at around 11 km over 10° N–30° N using aircraft flying between Japan and Australia (Matsueda and Inoue, 1996; Matsueda et al., 2002) are used for k = 2, and monthly aircraft~~Monthly aircraft measurement data collected by Tohoku University (TU; Nakazawa et al., 1993; Ishijima et al., 2001; Umezawa et al., 2014) at around 2 km over the Pacific Ocean off the coast of Sendai, Japan are employed for k = 3 after taking a 3-month running average. For k = 2, an average of the data observed at ~11 km over 0° N–20° N using aircraft flying between Japan and Australia (Matsueda and Inoue, 1996; Matsueda et al., 2002) and the measurement data used for k = 3 are used. This averaging is required to account for underestimations of vertical transport from the LT in the trajectory analysis. This underestimation is discussed in more detail in Sect. 4.3. For k = 4, ground-based monthly mean data measured by NOAA/ESRL (National Oceanic and Atmospheric Administration/Earth System Research Laboratory) at Summit, Greenland (SUM) and Barrow, Alaska (BRW) are used after averaging the data from the two stations. N_2O and SF_6 data at ~~the~~ both sites, and CH_4 and CO_2 data at BRW were continuously measured in- situ, ~~while~~whereas other data were obtained using a flask sampling method- (Dutton et al., 2017;- Thoning et al., 2017; Dlugokencky et al., 2018a, 2018b, 2018c; Petron et al., 2018). These data are distributed by the World Meteorological Organization (WMO) World Data Centre for Greenhouse Gases (WDCGG; https://gaw.kishou.go.jp/). The χ^S_{2016} in Eqs (6 and 6') is assigned the mixing ratio of S for the mid-latitude LT (k = 3) after annual averaging for 2016. For the trend λ^S, 9.3 ppb yr^{-1} for CH_4, 1.0 ppb yr^{-1} for N_2O, 0.33 ppt yr^{-1} for SF_6, 2.3 ppm yr^{-1} for CO_2, and no trend for CO are assumed by reference to each time series from Mauna Loa (https://www.esrl.noaa.gov/gmd/obop/mlo/).

Figure 5 compares the reconstructions for CH_4, N_2O, CO, SF_6, and CO_2 and the CONTRAIL measurements after spatial interpolation to each measurement point for each month. The reconstructions for SF_6, and CO_2 generally agree with the measurements, with some outliers during the summer season. In particular, some observed CO_2 mixing ratios have much smaller values than the reconstructions during boreal summer (Fig. 5e). This might be caused by CO_2 absorption by the local Eurasian forest and enhanced subgrid-scale vertical transport (e.g., local convection) during summer. The reconstructions for other seasons, however, generally agree with the CONTRAIL measurements. In contrast to SF_6 and CO_2, reconstructions for chemically active species (i.e., CH_4, N_2O, and CO) overestimate the CONTRAIL measurements. Because this overestimation

is likely due to chemical loss along their path from the origin region to the ExUTLS, in the next step we perform a reconstruction while taking chemical loss into account.

2.2.2 Reconstruction with chemical loss (step 2)

The mixing ratios of chemically active species (CH_4, N_2O, and CO) are reconstructed using a simple model wherein each chemical loss is simulated along the path from its source region to the ExUTLS. Although each trajectory trj_k has a unique path and transit time from its origin k, an "average path" (AP; Schoeberl et al., 2000) can be defined by a cluster of such trajectories. In this study, APs are incorporated into the analysing framework using trajectories binned as a function of $\emptyset_{eq}$, θ, and $\mathcal{M}$. Because both the AP and AoA are defined using the same cluster of trajectories, the two values are considered to be consistent with each other. The relationship between AoA and the chemical loss rate is determined from observation results of Volk et al. (1997), who presented correlations between CH_4 and N_2O mixing ratios and AoA as well as the gradient of the mixing ratios with respect to AoA (figure 6a of their paper). Using their results, a relationship between the chemical decay and AoA is assumed, as shown in Fig. 6. The gradient of N_2O mixing ratio with respect to the AoA grows by −3 % yr^{-1} a year, whereas that for CH_4 is constant at −7 % yr^{-1} when the AoA is <2.5 years and becomes −11 % yr^{-1} when the AoA is >3.4 years. Using the assumed chemical decay, the relative abundances of CH_4 and N_2O are calculated (Fig. 6) and are found to agree well with the observed mixing ratios shown in figure 6a of Volk et al. (1997). The correlation between CO mixing ratio and AoA is not shown in their paper, so here it is assumed that the gradient of CO mixing ratio with respect to AoA is 20-times larger than that of CH_4. The expected relative abundance of CO with respect to AoA is also evaluated (Fig. 6).

To adapt the correlations between chemical decay and AoA (Fig. 6) to an AP, the chemical decay with respect to AoA is converted to an average loss rate with respect to transit time along an AP (TT_{AP}). Figure 7 shows the converted loss rates along an AP for the three tracers as well as the corresponding e-folding time. The converted loss rates produce the same relationships between the chemical decay and AoA shown in Fig. 6 if each species is reduced during TT_{AP} with the given e-folding time as a function of TT_{AP}. Using these e-folding times ($\equiv \tau_{AP}^{S}$), the mixing ratio of chemically active species S after travelling an AP ($\equiv X^S$) is calculated as follows:

$$X^S = X_{NoChem}^S * \exp\left(-\frac{\Gamma_{Trj}}{\gamma_{Loss}^S * \tau_{AP}^S}\right), \quad (7)$$

where γ_{Loss}^S is a correction factor for τ_{AP}^S and is determined as follows. Because chemical loss rates might change with the season, we determine a correction factor for each month, such that the reconstruction X^S agrees with CONTRAIL measurements. Scatter plots of CONTRAIL measurements versus reconstructions (Fig. 8) are linear with a slope of 1.0 for each month when the correction factors for CH_4 and N_2O are those shown in Fig. 9. Because the scatter plots have large dispersion for CO, instead of the slope, the difference between the CONTRAIL measurements and reconstructions is used for the determination of γ_{Loss}^S to minimize the difference. Thus, CH_4, N_2O, CO, SF_6, and CO_2 in the ExUTLS are reconstructed for a whole year ($X^S = X_{NoChem}^S$ for SF_6 and CO_2) and are summarised in Appendix B together with the origin fractions and AoA. The detailed descriptions about them are made in the next section. As in the estimation of Γ_{Trj} for stratospheric air

masses, the original mixing ratio S of air masses originating in the stratosphere $X^S{}_{ORG_{k=1}}$ is evaluated using only $trj_{k=1}$. The seasonal dependence of γ^S_{Loss} (i.e., ~~The time series $X^S_{ORG_k}$ cannot be directly obtained for k = 1 and 5; thus, their values are empirically estimated using a type of inversion technique based on Eq. (3) and CONTRAIL data for the ExUTLS (Sawa et al., 2015). If the i-th CONTRAIL datum is obtained at the spatiotemporal point $(\phi_{eqC(i)}, \theta_{C(i)}, \mathcal{M}_{C(i)})$, the mixing ratio for species S ($\equiv X^S_{C(i)}$) and the values reconstructed for S are interpolated to the same point ($=X^S(\phi_{eqC(i)}, \theta_{C(i)}, \mathcal{M}_{C(i)})$). The summation of square differences (SD_{sum}) between the two is calculated as~~

~~$$SD_{sum} = \sum_{i=1}^{N_{Cmax}} \{X^S_{C(i)}(\phi_{eqC(i)}, \theta_{C(i)}, \mathcal{M}_{C(i)}) - X^S(\phi_{eqC(i)}, \theta_{C(i)}, \mathcal{M}_{C(i)})\}^2, \quad (4)$$~~

~~where N_{Cmax} denotes the total number of CONTRAIL measurements used; $X^S_{ORG_1}$ and $X^S_{ORG_5}$ are obtained as values that minimize SD_{sum} for each target month ($\mathcal{M}_{target}$) by combining the variables for 4 months ($\mathcal{M}_{target} - 3$ to $\mathcal{M}_{target}$). In this estimation, X^S in Eq. (4) reconstructed for each combination is affected not only by the employed $X^S_{ORG_1}(\mathcal{M}_{target})$ and $X^S_{ORG_5}(\mathcal{M}_{target})$, but also by their values for specific months from $\mathcal{M}_{target} - 3$ to $\mathcal{M}_{target} - 1$, because trajectories extend to a maximum of 90 days in this study. Therefore, this procedure is repeated over a whole year by sequentially changing the target month until both $X^S_{ORG_1}$ and $X^S_{ORG_5}$ are unchanged and minimize SD_{sum} for all months.~~

~~Because this study performs a trajectory analysis using an objective reanalysis dataset, subgrid-scale processes, such as the sporadic injection of tropospheric air masses into the ExUTLS, cannot be explicitly reproduced. Thus, to remove the influence of such sporadic processes, CONTRAIL data with CO mixing ratios higher than 80 ppb, i.e., parts per billion by moles and hereafter the same goes ppm and ppt, in the region above 340 K and north of 60° N equivalent latitude are not used in this estimation. Thus, values obtained for $X^S_{ORG_1}$ and $X^S_{ORG_5}$ may show spurious fluctuations. To reduce these fluctuations, we take 3-month running averages of the values estimated for the two variables. The spatiotemporal distribution of S in the ExUTLS is reconstructed using Eq. (3) and $X^S_{ORG_k}$ (k = 1–5) values for a whole year.~~

the relative rate of chemical loss) estimated here is discussed in Sect. 4.2.

3 Results

3.1 ~~Mixing~~Origin fraction

~~Mixing~~Distributions of origin fractions ~~were estimated as a function of ϕ_{eq}, θ, and $\mathcal{M}$. Their distributions~~ in a ϕ_{eq}–θ cross-section are shown in Fig. ~~3~~10 for January together with the climatology of monthly ~~averaged~~average potential vorticity for the period ~~from~~ 2012 ~~to~~ –2016 obtained from ERA-Interim. In winter, ~~mixing~~origin fractions of the ~~high latitude~~ stratosphere dominate regions north of 40° N and higher than ~~350~~340 K in altitude. In particular, regions where the altitude and equivalent latitude are greater than 360 K and 50° N, respectively, are almost entirely occupied by stratospheric air masses, ~~of which roughly 30 % have originated in the deep stratosphere~~further, that via the deep branch of the BDC ~~in~~ shares roughly 30 % of the regions where the potential vorticity exceeds ~10 PVU (Fig. ~~3~~e10c). However, ~~mixing~~origin fractions of the tropical

troposphere dominate regions of lower latitude and ~~altitude~~altitudes where the potential vorticity is less than ~4 PVU. These ~~mixing~~origin fractions are ~~higher than~~ >50 %, except in regions lower than ~~310~~320 K in altitude. Air masses in regions lower than 310 K generally originate in the mid-latitude LT with mixing fractions up to ~~50~~70 %, with few air masses originating in the high-latitude LT~~. The remainder (i.e., UTLS air masses that are not categorized by their origins) are distributed between 4 and 8 PVU with a maximum at around 320 K at higher latitudes. The mixing fractions of the high-latitude LT are small during this season~~.

The ~~mixing~~origin fractions for April are shown in Fig. ~~4~~11. In spring, ~~mixing~~origin fractions of the ~~high-latitude~~ stratosphere ~~generally decrease from~~ are similar to their winter values~~. In particular, the region occupied by air masses originating in the shallow branch of the BDC becomes confined to above ~ 355 K in altitude. At the same time, mixing fractions of the UTLS increase. The region where UTLS mixing fractions are higher than 40 % spreads down to ~ 40° N equivalent latitude~~, and ~~up to 360 K in altitude. However, high latitude stratospheric air masses still~~ dominate regions north of ~~50~~40° N and higher than ~~370 K in altitude~~340 K in altitude. Origin fractions of the stratosphere via the shallow branch of the BDC become slightly smaller than during winter, and ~~tropical~~those of the deep stratosphere via the deep branch of the BDC increase instead. Tropical tropospheric air masses continue to dominate regions where the potential vorticity is less than ~4 PVU at equivalent latitudes below 50° N, except for regions below ~~310 K. Mixing~~320 K where mid-latitude air masses are present. Origin fractions of the high-latitude LT remain small during spring.

Estimated ~~mixing~~origin fractions for July are shown in Fig. ~~5~~12. In summer, ~~mixing~~origin fractions of the~~ high-latitude~~ stratosphere become less dominant. In particular, those originating in the deep branch of the BDC (Fig. ~~5c~~12c) are small over the whole ExUTLS. Stratospheric air masses, almost all of which originate in the shallow branch of the BDC, are generally distributed in a small region ~~above~~where the altitude and equivalent latitude are greater than ~370 K ~~at high latitudes.~~and 40° N exceeding 50% of the origin fraction. In contrast, there is expansion of the region in which the ~~mixing~~origin fractions of the tropical troposphere are dominant. In particular, nearly ~~100~~80 % of the air masses in the region above 340 K and south of 40° N originate in the tropical troposphere. ~~Mixing fractions of the UTLS are smaller than in spring but remain at values higher than 40 % in regions where the potential vorticity is greater than ~ 6 PVU and the potential temperature is less than 360 K, with a maximum at around 340 K.~~ Only during this season do ~~mixing~~origin fractions of air masses originating in the high-latitude LT reach up to ~~50~~70 %, but these are limited to a region below ~320 K. ~~Mixing~~Origin fractions of the mid-latitude LT become smaller~~,~~ than during spring, but the region where they are higher than ~~20 % becomes wider than during spring, expanding~~30 % expands up to 340 K at all equivalent latitudes.

~~Mixing~~Origin fractions for October are shown in Fig. ~~6~~13. During autumn, high ~~mixing~~origin fractions of the ~~high-latitude~~ stratosphere broaden again in the region above ~~350~~360 K. However, those originating in the deep branch of the BDC are small. ~~Mixing~~Origin fractions of the high-latitude LT are suppressed, and ~~those of the UTLS decrease to below 40 %, except for a small region around 330 K between 70° N and 90° N. At the same time,~~ the region where ~~mixing~~origin fractions of the tropical troposphere are higher than ~~40~~50 % becomes larger than during summer and extends up to 80° N along ~~~ 4–6 PVU~~330–340 K potential ~~vorticity~~temperature surfaces. In the region below ~~320~~325 K, mid-latitude LT air masses dominate. These seasonal

results are compared with previous studies in Sect. 4.1. The robustness and limitations of our estimates are discussed in Sect. 4.3.

3.2 Original composition and AoA

As described in Sect. 2.2, detrended mixing ratios of CH_4, N_2O, CO, SF_6, and CO_2 observed in the tropical troposphere, mid-latitude LT, and high-latitude LT are assigned to their original mixing ratios for k = 2, 3, and 4, respectively. For k = 1 ~~and 5~~, the original mixing ratios are estimated ~~from mixing fractions (e.g., Figs 3~~ by Eqs (5 and 6) ~~and CONTRAIL measurements in the ExUTLS~~using trajectories $trj_{k=1}$ for ~~each month~~passive tracers and APs, and Eq. (7) for chemically active species. Figure ~~7~~14 shows the original mixing ratios of each species assigned to an individual trajectory according to Eq. (~~3~~5). Whereas CH_4 and SF_6 show ~~some~~ seasonal variations and latitudinal gradients in the troposphere, N_2O does not. In contrast to the troposphere, CH_4~~, N_2O,~~ and ~~SF_6,~~N_2O in ~~high latitude~~ stratospheric ~~and UTLS~~ air masses show distinct seasonal variations ~~of similar~~but somewhat different phase, with ~~minima~~a minimum in boreal summer and maximum in winter for CH_4, and a minimum in boreal spring/summer and ~~maxima~~maximum in ~~summer~~/autumn/winter for N_2O. SF_6 mixing ratios are significantly smaller in stratospheric air masses than in the troposphere throughout the year, and show seasonal variations with a maximum in September and minimum in March. Note that these values for stratospheric air masses are estimated based on their final state, unlike the case for regions k = 2, 3, and 4, for which the values correspond to their original state. For CO, there are large seasonal variations in high- and mid-latitude tropospheric air masses, but tropical tropospheric values show ~~little~~smaller seasonal ~~variation~~variations. The CO mixing ratios for the ~~high latitude~~ stratosphere ~~and UTLS~~ show a slight seasonal variability ~~(they may be analytical artefacts),~~ but are less than ~~50 and 70~~~30 ppb throughout the year~~, respectively.~~. For CO_2, seasonal variations are largest in the high-latitude troposphere; mixing ratios in the ~~tropical troposphere, high-latitude~~ stratosphere~~, and UTLS~~ show small seasonal variations, but with ~~differing phases~~a phase that differs from that in the troposphere.

The estimated AoA of ~~the~~ stratospheric ~~and UTLS~~ air masses ~~estimated from 10-year trajectories are~~is shown in Fig. ~~7~~f14f. Stratospheric air masses transported via the deep branch of the BDC have AoA exceeding 5~~.5~~ years, whereas those transported via the shallow branch have AoA of ~~~~1 ~~year~~ ~1.5 years. The average AoA among air masses originating in both branches shows a seasonal variation, with maximum values of ~2.~~5~~7 years in March and minimum values of ~1.4~~9~~ years in ~~August. The AoA~~September, of ~~UTLS air masses also shows a seasonal variation, with a maximum in boreal summer and minimum in winter~~almost opposite phase to that of SF_6 mixing ratios. The relationship between the original composition of stratospheric air masses and their AoA is discussed in Sect. 4.2.

3.3 Reconstructions

Chemical distributions reconstructed ~~from~~in the ~~mixing fractions of air masses (~~manner described in Sect. ~~3.1) and their original compositions (Sect. 3.~~2~~)~~.2 are shown for January (Fig. ~~8~~15) together with observation results obtained from CONTRAIL measurements over Siberia and monthly ~~averaged~~average potential vorticity obtained from the ERA-Interim

dataset during the period from 2012 to 2016. Spatial distributions of all chemical species generally show higher mixing ratios with decreasing potential temperature, equivalent latitude, or potential vorticity. Conversely, the distribution of AoA generally shows a higher age with increasing potential temperature, equivalent latitude, or potential vorticity. In particular, an AoA of greater than 3 years is estimated in the deep ExUTLS for regions higher than ~~390~~380 K and north of ~~75~~70° N.

The reconstructions and AoA for April (Fig. ~~9~~16) show spatial distributions of ~~CH_4, N_2O, and SF_6 mixing ratios~~all species that generally increase with decreasing potential temperature, equivalent latitude, or potential vorticity, ~~whereas those of CO and CO_2 have minima near 370 K north of 50° N equivalent latitude. Although the minimum for CO may be an artefact of the reconstruction procedure, its magnitude is less than 10 ppb, which is significantly smaller than the seasonal variation. Thus, it is not expected to have an influence on the seasonal characteristic results. The minimum for CO_2 may be considered part of the "tape recorder" of CO_2 mixing ratios in the UTLS (Andrews et al., 1999).~~as is the case for January. However, the gradients are larger, particularly for CH_4 and N_2O mixing ratios, such that in regions where the potential vorticity is >6 PVU the mixing ratios are much smaller than those in January, but in regions where the potential vorticity is <4 PVU the mixing ratios are almost the same as in January. The AoA distribution has a structure similar to that shown for January; i.e., age that increases with potential temperature, equivalent latitude, or potential vorticity.

The spatial distributions of the chemical species and AoA change more during summer than during winter and spring (Fig. ~~10~~17). In particular, ~~those of CH_4 and N_2O~~all five chemical species show minima at ~~around 370~~~350 K ~~at high~~north of 60° N equivalent ~~latitudes, similar to those of CO_2 during April (Fig. 9e). They may~~latitude. These minima might be formed by remainder of the ~~high latitude~~deep stratospheric air masses which were transported during spring ~~when CH_4 and N_2O mixing ratios ware small. However, those of SF_6 do not show such minima~~. The tracer minima near ~350 K at high equivalent latitudes begin forming in June. This "sandwich" structure in the ExUTLS ~~region.~~has been reported by Ploeger and Biner (2016) for summer and by Krause et al. (2018) for spring. In agreement with their studies, the sandwich structures can show evidence for strong poleward transport above ~400 K, leading to mixing ratio minima at lower altitudes. For CO_2, ~~the minimum descends to around 345 K potential temperature, and~~ some CONTRAIL measurements show significantly lower mixing ratios than the reconstructed values. The difference between the CONTRAIL measurements and the reconstructions ~~will be~~are discussed in ~~the last part of this section~~Sect. 4.3. The AoA becomes significantly smaller during this season compared with winter and spring. In particular, the AoA of nearly the entire region ~~with potential vorticity of <8 PVU is less than 1 year~~is <1.6 year with the exception of the region where the tracer minima are formed.

In autumn, the chemical gradients for CH_4, N_2O, SF_6, and CO_2 in the ExUTLS are reduced (Fig. ~~11~~18), in large part because CH_4 and N_2O mixing ratios in the deeper ExUTLS increase up to 1750 ppb for CH_4 and 315 ppb for N_2O. The reconstructed CO_2 mixing ratios show a nearly homogeneous distribution in the ExUTLS~~.~~, leading to a distribution of higher CO_2 air masses along the 6–8 PVU potential vorticity surface. The spatial distribution of CO, however, retains a steep gradient, because its chemical lifetime is small (~~a few~~several months). The distribution of AoA during ~~this season~~autumn is similar to that during summer, with the AoA of nearly the entire region with potential vorticity of <8 PVU being less than 1 year.

~~Reconstructions for CH_4, N_2O, CO, SF_6, and CO_2 are compared with CONTRAIL measurements after spatial interpolation to each measurement point for each month (Fig. 12). The reconstructions generally agree with the measurements, with some outliers during the summer season. In particular, some observed CO_2 mixing ratios have much smaller values than the reconstructions during boreal summer (Fig. 12e). This may be caused by CO_2 absorption by the local Eurasian forest and enhanced subgrid-scale vertical transport by local convection during the summer season. Figure 12f shows the relationship between AoA estimated from the 10-year trajectory analysis and SF_6 observed by CONTRAIL. Results of the analysis show a negative correlation with a fit-line of slope −0.33 ppt/year, which is the inverse of the increasing trend of SF_6 measured at Mauna Loa. This means that our AoA estimates agree well with other AoA estimates based on SF_6 mixing ratios and their trend in the troposphere (e.g., Sawa et al., 2015). Thus, SF_6 decreases with increasing AoA at a rate equal to the sign-reversed increasing trend of background SF_6, thereby supporting the robustness of our AoA estimates.~~

4 Discussion

One goal of the current study is to visualize how seasonal variations in ~~dynamical and chemical~~air masses as well as trace gas transport affect the spatiotemporal distributions of chemical species in the ExUTLS. This is accomplished by determining the seasonal characteristics of ~~mixing~~origin fractions of ExUTLS air masses originating in each region *k* at fixed points with those of the reconstructions for each species, and comparing the distribution of each species in the ExUTLS with the original mixing fraction in each origin region. We next discuss the results of this analysis and some implications revealed through the reconstructing procedures, together with the limitations of the current study.

4.1 Seasonal ~~characteristics of dynamical and chemical transport~~variations in origin fractions and reconstructions at fixed locations

To identify the characteristics of seasonal variations in ~~mixing~~origin fractions and reconstructions at fixed locations, four regions are selected: mid-equivalent latitude upper (MU) ExUTLS (45° N, 370 K), high-equivalent latitude upper (HU) ExUTLS (75° N, 370 K), mid-equivalent latitude lower (ML) ExUTLS (45° N, 320 K), and high-equivalent latitude lower (HL) ExUTLS (75° N, 320 K). Figure ~~13~~19 shows seasonal variations in the ~~mixing~~origin fractions of each origin evaluated at the four locations. In the ~~mid-latitude upper~~MU ExUTLS, ~~mixing~~origin fractions of the tropical troposphere become high, exceeding ~~40~~50 % during summer and autumn. ~~This~~Accompanying this increase ~~may be related to the Asian summer monsoon according to confirmation of the~~, trajectories~~.~~ originating in the tropical troposphere over around Asia are strengthened. In the other seasons, ~~mixing~~origin fractions of the ~~high latitude~~ stratosphere dominate. In particular, those that travelled via the shallow branch of the BDC exceed 50 %. The ~~mixing~~origin fractions of the mid- and high-latitude LT are nearly zero throughout the year~~. In the high~~, with the exception of that for the mid-latitude ~~upper~~LT in autumn. In the HU ExUTLS, ~~mixing~~origin fractions of the ~~high latitude~~ stratosphere dominate and exceed 60 % throughout the year. Furthermore,

~~mixing~~origin fractions of air masses that travelled via the deep branch of the BDC exceed 20 % during the period from January to April, whereas tropical tropospheric air masses generally fail to reach this region during this period. In the ~~mid-latitude lower~~ML ExUTLS, tropospheric ~~mixing~~origin fractions are dominant. In particular, those of the mid-latitude troposphere exceed ~~40~~50 % during summer and those of the high-latitude troposphere exceed 20 % during July and August. During winter and spring, however, tropical tropospheric air masses dominate. In the ~~high-latitude lower~~HL ExUTLS, ~~mixing~~origin fractions of the mid- and high-latitude LT are enhanced ~~but their~~during summer. Origin fractions ~~are lower~~of the high-latitude LT are comparable to those in the ML ExUTLS, but smaller than those of the mid-latitude ~~lower ExUTLS.~~LT in the HL ExUTLS. This can be explained by enhanced exchange at the bottom edge of the subtropical jet (i.e., along the 320–330 K surface for summer, e.g., Gettelman et al., 2011). As shown in Fig. 12d, enhanced origin fractions of the mid-latitude LT are distributed along such isentropes. In winter, ~~mixing~~origin fractions of the tropical troposphere and ~~high-latitude~~ stratosphere are roughly ~~20 %, whereas those of the UTLS achieve the highest value, with a maximum exceeding 60 % in March~~50 % and 40 %, respectively.

In addition to seasonal ~~variation~~variations in ~~the mixing~~origin fractions, ~~that in the composition of the original air masses (Fig. 7) also contribute to~~ seasonal variations in the tracer mixing ratios in origin regions (Fig. 14) also affect chemical distributions in the ExUTLS. Figure ~~14~~20 reveals that seasonal variations in the reconstructions for each species and the trajectory-estimated AoA in each of the four locations ~~follow the same patterns as shown in Fig. 13.~~have patterns that differ because they are based on a superposition of the origin fractions shown in Fig. 19 with the original time series for k = 1–4 of the individual tracers shown in Fig. 14. Note that the CONTRAIL data are plotted if the measurement was conducted within ±5° in equivalent latitude and within ±5 K in potential temperature of one of the four locations. This results in few plotted CONTRAIL observations in mid- and ~~high-latitude lower~~HL ExUTLS regions during summer, and no observations in ~~mid-~~MU and ~~high-latitude upper~~HU ExUTLS regions from June to January. This is caused by the seasonality of the thermal and dynamical structures of the ExUTLS and fixed flight altitudes. Despite the sparse and non-uniform observational field, the spatiotemporal distributions of chemical species, together with the ~~mixing~~origin fractions of the original air masses, can be resolved. This ability is one of the important advantages of the current analysis. The mixing ratios of CH_4 and N_2O ~~shown~~show modest seasonal variations in the lower ExUTLS, whereas they show large seasonal variations in the upper ExUTLS, with minima in spring and maxima in autumn. The minima in spring are due to the transport of stratospheric air masses via the deep branch of the BDC, which have low CH_4 and N_2O mixing ratios ~~during this season (Fig. 7).~~and also low AoA. This seasonal variation in chemical abundance for stratospheric air masses is discussed further in the next section. In contrast to CH_4 and N_2O, CO mixing ratios show smaller seasonal variations in the upper ExUTLS than in the lower ExUTLS~~.~~, with the exception of the high mixing ratio in the upper ExUTLS in August. This can be explained by the transport of mid-latitude LT air masses, which have higher CO mixing ratios than the other air masses, to the lower ExUTLS during summer. In addition, a large fraction of air masses reach the upper ExUTLS only during August. The seasonal characteristics of SF_6 mixing ratios are similar to those of CH_4 and N_2O. ~~In particular, the~~The phase of seasonal variations in the upper ExUTLS is nearly synchronized with, but slightly precedes, those of CH_4 and N_2O, ~~whereas~~and more closely resembles the ~~relative amplitude~~upside-down pattern of

~~seasonal~~AoA variations ~~in the lower ExUTLS is somewhat smaller. The difference of amplitudes in the upper ExUTLS among SF_6, CH_4, and N_2O is likely caused by the presence or absence of sinks for these species in the stratosphere, as discussed further in the next section.~~(Fig. 20f). The phase of seasonal variations of CO_2 mixing ratios in the lower ExUTLS is nearly synchronized between the ~~mid-~~ML and ~~high latitudes~~HL ExUTLS, with the largest amplitude being evident in the ~~mid-latitude~~ML ExUTLS. The phase of CO_2 variations in the upper ExUTLS is quite different from that in the lower ExUTLS, with maxima during summer/autumn. This seasonal variation in the upper ExUTLS is consistent with observational estimates by Hoor et al. (2004) and Strahan et al. (2007).

Seasonal variations in AoA evaluated at the four locations are shown in Fig. ~~14~~20f. The phase of seasonal variations for the four locations is roughly synchronized, whereas the absolute values are clearly different. For example, AoA in the ~~high-latitude upper~~HU ExUTLS has a maximum of ~~more than~~ >2.5 years during spring and a minimum of ~1~~-year~~.3 years during the end of summer, whereas in the ~~mid-latitude lower~~ML ExUTLS the maximum is only ~0.45 years and occurs during the period from winter to spring. The amplitude of AoA variations in the ExUTLS is likely related to air-mass mixing from the ~~high-latitude~~ stratosphere, ~~especially~~particularly when this involves air masses that have been transported via the deep branch of the BDC. This point is discussed further in the next section, in relation to seasonal variations in chemical composition.

4.2 Original compositions and mixing effects

As discussed in the previous section, the distributions of CO and CO_2 in the ExUTLS are strongly affected by tropospheric air masses because CO has a short chemical lifetime and CO_2 shows large seasonal variations in the high- and mid-latitude LT. For CH_4, N_2O, and SF_6, however, seasonal variations in ~~mixing~~origin fractions of the stratospheric air masses and in the compositions of the original air masses are considered to be essential factors in their spatiotemporal distributions in the ExUTLS. Here, we discuss seasonal variations in the composition of stratospheric air masses and how this affects chemical distributions via mixing with tropospheric air masses in the ExUTLS. Figure ~~15~~21 shows the relationships between chemical abundances from CONTRAIL measurements and the AoA estimated from the trajectories and interpolated to each CONTRAIL measurement location~~, (i.e., $\phi_{eqC(t)}$, $\theta_{C(t)}$, and $\mathcal{M}_{C(t)}$ in Sect. 2.2),~~ along with these relationships for each original air mass. The AoA for stratospheric air masses are the same as those shown in Fig. ~~7~~14f, whereas the AoA for the tropical, mid- and high-latitude troposphere are set to zero. Thus, the denotations for the tropospheric air masses only move vertically in the cross-sections according to their seasonal variations. Overall, the CONTRAIL measurements are roughly distributed on lines connecting the tropospheric and stratospheric air masses for all seasons and chemical compositions. This linear distribution suggests that dynamical mixing of tropospheric with stratospheric air masses shapes the chemical distributions of the ExUTLS. Such linear "mixing lines" also suggest that the mixing took place rapidly (i.e., at a time-scale shorter than their chemical lifetimes) along an isentropic surface (Plumb, 2007 and references therein). A comparison of the distribution of CONTRAIL measurements with trends in the troposphere for SF_6 ~~and CO_2~~ shows that the CONTRAIL measurements are distributed along the lines of the sign-reversed ~~trends, whereas~~trend. According to Engel et al. (2002) and Bönisch et al. (2009), the mixing ratios of CO_2 and AoA do not correlate below a level of ~3 years AoA because the propagated signal of the tropospheric

seasonal cycle into the stratosphere is still detectable. In agreement with their results, the CONTRAIL CO_2 measurements also converge to the sign-reversed trend with increasing AoA. However, for CH_4 and N_2O, measurements depart from ~~the lines of~~ the sign-reversed trends toward lower mixing ratios with increasing AoA. This deflection can be interpreted as being due to their stratospheric sinks; i.e., ~~the photo-~~chemical destruction of CH_4 and N_2O in the stratosphere, with no such destruction of SF_6 and CO_2.

Both the AoA and chemical abundance of the original air masses from the ~~high-latitude~~ stratosphere show seasonal variations that might be caused by seasonal variations in mass fluxes from the deep and shallow branches of the BDC. Figure ~~15f~~21f shows seasonal variations in AoA and ~~integrated~~ the value that is calculated by integration of "age spectrum" (PDF) from 0 to ~~10 years~~*tf* for air masses originating in the ~~high-latitude~~ stratosphere as well as those separately evaluated for air masses that have travelled via the deep and shallow branches of the BDC. As the PDF is calculated with a weighting factor according to area and density, as in Eq. (1), their integrations reveal relative masses. Air masses originating in both the shallow ~~branch have a minimum in July~~ and ~~maximum in December, whereas the~~ deep ~~branch has a minimum~~branches have minima in September and ~~maximum~~maxima in March. These in-phase ~~lagged~~ seasonal variations ~~cause~~enhance both the seasonal variations ~~in~~of the total ~~mixing~~origin fractions of the ~~high-latitude~~ stratosphere and its ~~averaged~~average AoA~~, as well as the minima of~~.

Interesting cyclic structures appear in CH_4~~, N_2O,~~ and ~~SF_6~~N_2O mixing ratios ~~in spring. For example, we estimate 315 ppb N_2O and 1.4 years AoA in autumn, and 280 ppb and 2.3 years, respectively, in spring. This relationship between the decrease in N_2O from its tropospheric value and the AoA is consistent with those presented by Volk et al. (1997) and Andrews et al. (2001). If we assume that the N_2O destruction rate along its path through the shallow branch is negligibly small compared with that through the deep branch, the differences between the sign-reversed trend (dashed line in Fig. 15b) and the observed N_2O mixing ratios (small filled circles in Fig. 15b) or those estimated for the original high-latitude~~ and their AoAs in stratospheric air masses ~~(open circles in Fig. 15b) reflect the contribution~~. For example, the CH_4 mixing ratio is ~1750 ppb (AoA of ~~mixing with~~~2.3 years) in winter, ~1700 ppb (AoA of ~2.6 years) in spring, ~1650 ppb (AoA of ~2.3 years) in summer, and again ~1700 ppb (AoA of ~2.0 years) in autumn. Thus, clockwise rotations are the result of this pattern. The same is true for stratospheric N_2O and AoA. These rotations are formed by seasonal variations in AoA that are at a maximum in spring and a minimum in autumn, in combination with seasonal variations in the relative chemical loss rate along the AP (defined as γ_{Loss}^{S} and discussed in Sect. 2.2.2) that is at a maximum in winter and a minimum in summer. These $\pi/2$ phase-lagged seasonal variations result in rolling variations in the relationship between CH_4 and N_2O mixing ratios and AoA in stratospheric air masses ~~coming from~~. The seasonal variation in AoA is determined by the mixing of stratospheric air masses via the deep branch of the BDC~~.~~ (Fig. 21f). Although the mechanism driving the seasonality of the chemical loss rate along AP is unknown, it is likely involved that the seasonal change of the relationship between AP and AoA as a possible mechanism from dynamical viewpoint. Other candidate mechanisms from a chemical viewpoint are seasonal changes in the abundance of disrupting substance along the AP, or seasonal changes in the solar radiation intensity and sunlit time.

The abundance of N_2O and CH_4 in stratospheric air mass may be related to the fraction of air masses travelling via the deep and shallow branches. The relationship between the chemical abundance and mass fraction of the two branches is now

considered. The current study estimates approximately ~~25~~24 % and ~~10~~14 % of air masses following the deep branch are of stratospheric origin in spring and autumn, respectively, and the AoA is estimated to be ~~5.5~~6.4 years (Fig. ~~15f~~21f). Andrews et al. (2001) estimated the N_2O mixing ratio ~~to be ~80 ppb~~ in the mid-latitude deep stratosphere to be ~80 ppb and <40 ppb where the AoA is estimated ~~to be 5.5 years~~ from ~~the~~ CO2 mixing ratio to be 5.5 years and 6.0 years, respectively. As their estimates are normalized to 1997 tropospheric values, the quantitative difference in the baseline N_2O mixing ratios may differ by ~20 ppb from the present values. If we assume the N_2O mixing ratio of air masses originating in the deep branch of the BDC is ~~100~~60 ppb, and that air masses are mixed at ratios of ~~25~~24 % and ~~10~~14 % with air masses whose N_2O mixing ratio is 330 ppb, such mixing leads to ~~270~~265 ppb and ~~310~~290 ppb N_2O mixing ratios, respectively. These values ~~generally agree with~~ are up to ~20 ppb lower than the N_2O mixing ratios of ~280 ppb in ~~April~~May and ~~315~~310 ppb in ~~October~~November estimated for the original stratospheric air masses shown in Figs 14b and 21b. The same arguments are valid for CH_4 with respect to the relationship between stratospheric CH_4 mixing ratios and AoA; i.e., ~~Fig. 7b~~CH_4 mixing ratios are <600 ppb in regions where the AoA is >5.5 years, as estimated by Röckmann et al. (2011). These overestimations of N_2O and CH_4 mixing ratios for the original stratospheric air masses might be due to overestimation of the AoA and/or overestimation of the origin fraction of air masses originating in the deep branch of the BDC. These possibilities are discussed further in the next section.

~~The same arguments are valid for CH_4 with respect to the relationship between stratospheric CH_4 mixing ratios and AoA; i.e., ~600 ppb in regions where the AoA is 5.5 years, as estimated by Röckmann et al. (2011). Thus, the relationship between AoA and mixing ratios of N_2O and CH_4 in the ExUTLS, which changes with the season, is driven by seasonal variations in air masses transported via the shallow and deep branches of the BDC and by the mixing of such stratospheric air masses with tropospheric air masses in the ExUTLS.~~

4.3 Limitations of the current study

This study provides a detailed explanation of seasonal variations in chemical distributions and transport in the ExUTLS from a dynamical standpoint using trajectory analysis in combination with aircraft measurements. Results suggest that the spatiotemporal distributions of CH_4, N_2O, SF_6, and AoA in the ExUTLS are controlled primarily by air-mass transport via the deep and shallow branches of the BDC and by their mixing with tropospheric air masses in the ExUTLS, whereas those of CO and CO_2 are controlled largely by ~~the~~ tropospheric air masses, because CO has a short chemical lifetime and CO_2 shows large seasonal variations in the mid-latitude LT. However, some assumptions and limitations of the current study should be mentioned.

First, some uncertainty results from the use of ERA-Interim data in trajectory analyses. Trajectory results generally depend on the resolution of the input data. We performed sensitivity analyses to clarify this dependency in our ~~mixing~~origin fraction estimates (Appendix A). Results confirm that our estimates are independent of the resolution of the ERA-Interim data, at least as they relate to statistical characteristics. Furthermore, it is known that AoA calculated from trajectory analyses using ERA-Interim data are somewhat young-biased. For example, these estimated AoA values are ~30 % younger than those estimated from balloon-borne observations in the middle stratosphere, as demonstrated by Inai (2018). To address this issue, trajectory-

based AoA values are uniformly corrected by a correction factor of 1.43 5 (determined with reference to the AoA obtained from SF_6 mixing ratios) in this study. There is, however, a possibility that the bias differs with the meteorological region, because different mechanisms drive the shallow and deep branches of the BDC (e.g., Birner and Bönisch, 2011). In addition, to estimate mean AoA from an age spectrum with finite time lengths (e.g., the 10 years used in this study), a tail correction is required. Though this study does not employ a tail correction, the required correction is estimated to be less than 5 % by Inai (2018) and approximately 10 % by Ploeger and Birner (2016). Thus, it is smaller than the correction factor used here. Most importantly, AoA estimates used in this study agree well with those expected from observed SF_6 mixing ratios This is a possible cause of the inconsistent relationship between the abundance of N_2O and CH_4 in stratospheric air mass and the mass fraction of the air masses travelling via the deep and shallow branches of the BDC. If the AoA of air masses travelling via the deep branch is assumed to be ~5 years, the relationship approaches those of Andrews et al. (2001) and Röckmann et al. (2011). Trajectory results also generally depend on the vertical condition, i.e., kinematic (employed by the current study) or diabatic (employed by, for example, Diallo et al., 2017). Previous studies suggest that using kinematic trajectories leads to a stronger dispersion and somewhat young bias in AoA estimates compared with using diabatic trajectories (e.g., Schoeberl et al., 2003; Diallo et al., 2012). Therefore, using diabatic trajectories in this analysis might result in a correction factor (γTT) of <1.5.

The second limitation is related to the criteria for the determination of air- mass origin. These criteria might may strongly affect mixing origin fraction estimates and are thus expected to contribute to the uncertainty of this analysis, to some degree. A comprehensive sensitivity test to address this issue, focusing on in-mixing in the TTL, has been reported by Inai (2018), who found that the mixing fraction can vary by 40 % to 180 %, depending on the choice of criteria. Though the same test could be applied to the current study, the estimated mixing origin fraction distributions are comparable to those estimated by based on trace gas observations by the In-service Aircraft for a Global Observing System-Civil Aircraft for the Regular Investigation of the atmosphere Based on an Instrument Container (IAGOS-CARIBIC; Umezawa et al. (, 2015). Moreover, these estimates are indirectly validated by the CONTRAIL observations, through the reconstruction of the chemical distributions (as evident in Figs 5d and e, and 8–11). This agreement supports our criteria selection and suggests that our estimated mixing origin fractions are not, at least, grossly wrong. However, the breakdown of stratospheric air masses is subject to the limitations described in the last part of Sect. 4.2. If the relative fraction of air masses travelling via the deep branch is 7 % smaller than the estimated values (i.e., if they were 17 % and 7 % in spring and autumn), the relationship between the abundance of N_2O and CH_4 in stratospheric air mass and the mass fraction of the air masses travelling via the deep and shallow branches also approaches that of Andrews et al. (2001) and Röckmann et al. (2011).

Another limitation may arise from the analysis methodology. The observed mixing ratios of CH_4, N_2O, CO, SF_6, and CO_2 are used after removing linear trends for each time-series, and are considered to be a function of month- and treated separately from the long-term trend. This treatment decreases the precision of observations if the observed values have non-liner linear interannual variations-, which is mainly concerned for CO_2. Furthermore, the CONTRAIL measurements were conducted once a month. Thus, one observed value represents atmospheric conditions at a specific spatiotemporal point, whereas the analysis field has a coarser spatiotemporal resolution, corresponding to, at minimum, that of the grid scale in of the ERA-Interim dataset.

Such a mismatch in spatiotemporal resolution may contribute to the lack of agreement between the reconstructions and CONTRAIL measurements during summer, particularly for CO_2 (Fig. ~~10e~~5e). However, uncertainties arising from these issues are minimized by the use of equivalent latitude and potential temperature, which are dynamically conserved quantities~~.~~ in the stratosphere. In the troposphere, which is more unstable, potential temperature and potential vorticity are not conserved, or are conserved only on much short timescales, because of diabatic motion. It should be noted that tracer uplift from the LT into the UT during summer (particularly for CO_2, as discussed above) cannot be reduced with the coordinate system employed here. Though the current study covers only the ExUTLS over a longitudinal range from 0° E to 140° E for comparison with the CONTRAIL measurements, the ~~mixing~~origin fractions and reconstructions are trial-evaluated over ~~Europe and~~ North America (Appendix A). Results confirm that the ~~mixing~~origin fractions are consistent between the two regions, and thus support the robustness of the current study. In this study, linear trends for CH_4, N_2O, SF_6, and CO_2 are assumed for the reconstruction. Although this is a simplified treatment, given the length of the analysis period, these trends are roughly constant over this time period with the exception of CH_4, and the CH_4 reconstructions are more strongly affected by chemical loss, as is evident in a comparison of Figs 5a and 8a. In the reconstruction procedure described in Sect. 2.2.1, it was necessary to assign the average of tropical aircraft and mid-latitude LT measurements to the original values for $k = 2$ to prevent underestimations. As discussed in Sect. 2.2.1, one cause of this underestimation might be subgrid-scale tropospheric upward transport that, although common, cannot be accounted for in the trajectory analysis.

5 Summary

To identify the origin of air masses in the ExUTLS, kinematic backward trajectories were calculated for ~~90 days~~10 years following the method of Inai (2018) using ECMWF ERA-Interim data as input. The analysis period extends from January 2012 to December 2016, and trajectories were categorized by origins in the ~~high latitude~~ stratosphere, tropical troposphere, mid-latitude LT, and high-latitude LT~~, and unclassified regions (UTLS)~~ based on meteorological parameters along each individual trajectory. The ~~mixing~~origin fractions of air masses originating in each region were estimated as a function of equivalent latitude, potential temperature, and month. Furthermore, using ~~a 10-year~~the same trajectory, the mixing fractions of air masses originating via the shallow and deep branches of the BDC were separately estimated along with the AoA.

The ~~mixing~~origin fractions show obvious seasonal variations. In the mid-equivalent latitude upper ExUTLS, ~~mixing~~origin fractions of the tropical troposphere exceed ~~40~~50 % during boreal summer and autumn ~~in association with the Asian summer monsoon~~, whereas ~~mixing~~origin fractions of the ~~high latitude~~ stratosphere via the shallow branch of the BDC are dominant during winter and spring. In the high-equivalent latitude upper ExUTLS, ~~mixing~~origin fractions of the ~~high latitude~~ stratosphere exceed 60 % throughout the year. In the mid- and high-equivalent latitude lower ExUTLS, ~~mixing~~origin fractions of the mid- and high-latitude troposphere are large during summer, ~~while~~whereas during winter, ~~mixing~~origin fractions of the tropical troposphere ~~and UTLS~~ are dominant ~~in the mid- and high-latitude lower ExUTLS, respectively~~.

By incorporating the time-series of mixing ratios for several chemical species obtained from ground-based and air-borne observations into the estimated ~~mixing fractions~~trajectories, the spatiotemporal distributions of the chemical species CH_4, N_2O, CO, SF_6, and CO_2 in the ExUTLS were reconstructed, along with estimations of the original composition of the stratospheric ~~and UTLS~~ air masses. The reconstructions are calculated to agree ~~well~~ with CONTRAIL measurements in the ExUTLS. Furthermore, uniform spatiotemporal species distributions are obtained for the ExUTLS from non-uniform observations. The ~~mixing~~origin fractions and AoA of each reconstruction are discussed. Distributions of CO and CO_2 are strongly affected by tropospheric air masses because of the short chemical lifetime of the former and large seasonal variations in the troposphere of the latter. In contrast, CH_4, N_2O, and SF_6 distributions are controlled primarily by seasonal variations in air masses transported from the stratosphere~~, and in particular those transported via the deep branch of the BDC for CH_4 and N_2O.~~ and subsequent mixing with tropospheric air masses. This interpretation is qualitatively and quantitatively consistent with the spatiotemporal AoA distributions.

This study developed and demonstrated a unique and effective method to exploit the advantages of observational data in combination with trajectory analysis. This method provides a means to understand both ~~dynamical~~air-mass transport and chemical ~~distribution~~decay from a new perspective. Furthermore, this technique can be applied to other data (e.g., species isotope ratios) or analyses of regions where trajectory calculations ~~keep their effectiveness.~~ are effective.

Appendix A. Sensitivity analyses

It is well known that results from trajectory analyses are affected by the resolution of input meteorological data. For example, Inai (2018) suggests that the ~~mixing~~origin fraction of stratospheric air masses in the upper TTL can vary by ~50 % in magnitude. Here, the sensitivity of our results to data resolution is tested. Figure A1 shows the dependence of ~~mixing~~origin fractions on the resolution of meteorological data for trajectories launched each month. ~~Mixing~~Note that here, the trajectory calculation length is limited to 90 days due to limited computing resources. Origin fractions calculated from ERA-Interim data and used in this study (1.5° × 1.5° horizontal resolution, 37 vertical levels) are compared with those using a finer resolution (0.75° × 0.75° horizontal resolution, 60 vertical levels~~) are compared with those using a coarser resolution (1.5° × 1.5° horizontal resolution, 37 vertical levels~~). ~~Mixing~~Origin fractions were evaluated for each bin set in an equivalent latitude–potential temperature cross-section (crosses). Results confirm that these points are distributed in a linear fashion with slopes of around 1.0 regardless of season. This suggests that the ~~mixing~~origin fractions are not quantitatively or qualitatively dependent on the resolution of the input data. This independence differs from the findings of Inai (2018), possibly because transport mechanisms in the ExUTLS are related to synoptic-scale mechanisms rather than convective activity, which dominates the tropical region. In the current study, ~~mixing~~origin fractions were estimated only for the longitudinal region between 0° E and 140° E, selected for comparison with CONTRAIL measurements over Siberia. Previous studies have investigated mixing processes between tropospheric and stratospheric air masses over different longitudinal regions; e.g., over North America (Pan et al., 2010). To

compare our results with these studies, the dependence of ~~mixing~~origin fraction on longitudinal region was tested. Figure A2 compares ~~mixing~~origin fractions evaluated over Siberia and North America. Results confirm that the data points in Fig. A2 (crosses) are distributed in a linear fashion with slopes of around 1.0 regardless of season. This suggests that the ~~mixing~~origin fractions are not quantitatively and qualitatively dependent on longitudinal region. This independence may arise from the employment of equivalent latitude and potential temperature, which are dynamically conserved parameters, in this analysis.

Appendix B. Large-scale perspective of origin fractions and reconstructions

Detailed analyses of origin fractions and reconstructions for specific months are informative, but taking a larger perspective might provide insight into seasonal transport processes and tracer distributions in the ExUTLS. Here, we present a larger-scale perspectives of origin fractions and reconstructions for the ExUTLS. Figure B1 shows monthly origin fractions as a function of time of year. The axes of each panel are as in Figs 10–13. Thus, the seasonal behavior of air-mass transport into the ExUTLS from surrounding areas is visualized. Origin fractions of the stratosphere via both branches of the BDC increase from winter to spring. Subsequently, those via the deep branch become small during summer and autumn. In contrast, origin fractions of the tropical troposphere are prominent during summer and autumn, with the exception of regions of lower potential temperature. The lower ExUTLS is dominated by air masses originating in the mid-latitude LT throughout the year, but those originating in the high-latitude LT contribute to this lowermost region during summer. The seasonal behavior of reconstructed chemical species is shown in Fig. B2. The patterns of chemically passive tracers, particularly SF_6, follow that of AoA. However, CO_2 in the lower ExUTLS undergoes different seasonal variations. (Note that the CO_2 mixing ratio is likely not well-reconstructed during summer in the lower ExUTLS.) The patterns of CH_4 and N_2O are similar in that the mixing ratios in the deep ExUTLS become small during spring and summer. However, their seasonal transitions slightly differ from each other, which that of CH_4 varies more gradually than another. The mixing ratios of CO in the deep ExUTLS are small throughout the year, but increase slightly during autumn.

Author contribution

Yoichi Inai designed ~~the study~~ and carried ~~it~~ out the study. Toshinobu Machida, Hidekazu Matsueda, Yousuke Sawa, Kazuhiro Tsuboi, and Keiichi Katsumata obtained the measurement data, and Shinji Morimoto, Shuji Aoki, and Takakiyo Nakazawa developed the measurement system. Yoichi Inai and Ryo Fujita prepared the manuscript with contributions from all co-authors.

Acknowledgements

The authors would like to acknowledge the support of many engineers from Japan Airlines and JAMCO Tokyo. All trace- gas mixing- ratio data at ground-based sites were provided by NOAA/ESRL (National Oceanic and Atmospheric

Administration/Earth System Research Laboratory) and were downloaded from the WMO/WDCGG website (https://gaw.kishou.go.jp/). This work was supported by Grants-in-Aid for Scientific Research (18K03738 and 26220101) from the Japan Society for the Promotion of Science and the Arctic Challenge for Sustainability (ArCS) Project by the Ministry of Education, Culture, Sports, Science and Technology, Japan. We thank Masashi Kohma for valuable ~~discussion~~discussions. We also thank ECMWF for providing the ERA-Interim data. All figures were produced using the GFD-DENNOU Library. The authors sincerely appreciate the constructive comments of two reviewers that greatly improved the manuscript.

References

Andersson, S., Martinsson, B., Vernier, J.-P., Friberg, J., Brenninkmeijer, C., Hermann, M., Velthoven, M., and Zahn, A.: Significant radiative impact of volcanic aerosol in the lowermost stratosphere, Nat. Commun., 6, 7692, doi:10.1038/ncomms8692, 2015.

Andrews, A. E., Boering, K. A., Daube, B. C., Wofsy, S. C., ~~Hintsha, E. J., Weinstock, E. M., and Bui, T. P.: Empirical age spectra for the lower tropical stratosphere from in sitiu observations of CO_2: implications for stratospheric transport, J. Geophys. Res., 104, 26581–26596, 1999.~~

~~Andrews, A. E., Boering, K. A., Daube, B. C., Wofsy, S. C.,~~ Loewenstein, M., Jost, H., Podolske, J. R., Webster, C. R., Herman, R. L., Scott, D. C., Flesch, G. J., Moyer, E. J., Elkins, J. W., Dutton, G. S., Hurst, D. F., Moore, F. L., Ray, E. A., Romashkin, P. A., and Strahan, S. E.: Mean ages of stratospheric air derived from in situ observations of CO_2, CH_4, and N_2O, J. Geophys. Res., 106, 32295–32314, doi:10.1029/2001JD000465, 2001.

Appenzeller, C., Holton, J. R., and Rosenlof, K. H.: Seasonal variation of mass transport across the tropopause. J. Geophys. Res. 101, 15071–15078, 1996.

Birner, T., and Bönisch, H.: Residual circulation trajectories and transit times into the extratropical lowermost stratosphere, Atmos. Chem. Phys., 11, 817–827, doi:10.5194/acp-11-817-2011, 2011.

Bönisch, H., Engel, A., Curtius, J., Birner, Th., and Hoor, P.: Quantifying transport into the lowermost stratosphere using simultaneous in-situ measurements of SF_6 and CO_2, Atmos. Chem. Phys., 9, 5905-5919, https://doi.org/10.5194/acp-9-5905-2009, 2009.

Boothe, A. C. and Homeyer C. R.: Global large-scale stratosphere-troposphere exchange in modern reanalyses, Atmos. Chem. Phys., 17, 5537-5559, doi:10.5194/acp-17-5537-2017, 2017.

Brewer, A. W.: Evidence for a world circulation provided by the measurements of helium and water vapour distribution in the stratosphere, Q. J. Roy. Meteor. Soc., 75, 351–363, doi:10.1002/qj.49707532603, 1949.

Dee, D. P., Uppala, S. M., Simmons, A. J., Berrisford, P., Poli, P., Kobayashi, S., et al.: The ERA-Interim reanalysis: Configuration and performance of the data assimilation system. Quarterly Journal of the Royal Meteorological Society, 137(656), 553–597. https://doi.org/10.1002/qj.828, 2011.

Diallo, M., Legras, B., and Chédin, A.: Age of stratospheric air in the ERA-Interim, Atmos. Chem. Phys., 12, 12133-12154, https://doi.org/10.5194/acp-12-12133-2012, 2012.

Diallo, M., Legras, B., Ray, E., Engel, A. and Añel, J. A.: Global distribution of CO2 in the upper troposphere and stratosphere, Atmos. Chem. Phys., 17(6), 3861-3878, doi:10.5194/acp-17-3861-2017, 2017.

Dlugokencky, E. J., Crotwell, A. M., Lang, P. M., Mund, J. W., and, Rhodes, M. E.: Atmospheric Methane Dry Air Mole Fractions from quasi-continuous measurements at Barrow, Alaska and Mauna Loa, Hawaii, 1986-2017, Version: 2018-03-19, Path: ftp://aftp.cmdl.noaa.gov/data/trace_gases/ch4/in-situ/surface/, 2018a.

Dlugokencky, E. J., Lang, P. M., Crotwell, A. M., Mund, J. W., Crotwell, M. J., and Thoning, K. W.: Atmospheric Methane Dry Air Mole Fractions from the NOAA ESRL Carbon Cycle Cooperative Global Air Sampling Network, 1983-2017, Version: 2018-08-01, Path: ftp://aftp.cmdl.noaa.gov/data/trace_gases/ch4/flask/surface/, 2018b.

Dlugokencky, E. J., Lang, P. M., Mund, J. W., Crotwell, A. M., Crotwell, M. J., and Thoning, K. W.: Atmospheric Carbon Dioxide Dry Air Mole Fractions from the NOAA ESRL Carbon Cycle Cooperative Global Air Sampling Network, 1968-2017, Version: 2018-07-31, Path: ftp://aftp.cmdl.noaa.gov/data/trace_gases/co2/flask/surface/, 2018c.

Dobson, G. M. B.: Origin and Distribution of the Polyatomic Molecules in the Atmosphere, P. Roy. Soc. Lond. A. Mat., 236, 187–193, 1956.

Dutton, G., Elkins, J. II, Hall, B., and NOAA ESRL: Earth System Research Laboratory Halocarbons and Other Atmospheric Trace Gases Chromatograph for Atmospheric Trace Species (CATS) Measurements, Version 1. NOAA National Centers for Environmental Information. doi:10.7289/V5X0659V, 2017.

Engel, A., Strunk, M., Muller, M., Haase, H. P., Poss, C., Levin, I., and Schmidt, U.: Temporal development of total chlorine in the high-latitude stratosphere based on reference distributions of mean age derived from CO_2 and SF_6, J. Geophys. Res., 107(D12), doi:Artn 4136, Doi 10.1029/2001jd000584, 2002.

Gettelman, A., Hoor, P., Pan, L. L., Randel, W. J., Hegglin, M. I., and Birner, T.: The extratropical upper troposphere and lower stratosphere, Rev. Geophys., 49, RG3003, doi:10.1029/2011RG000355, 2011.

Hall, T. M., and Plumb, R. A.: Age as a Diagnostic of Stratospheric Transport, J. Geophys. Res., 99(D1), 1059-1070, 1994.

Holton, J. R. et al.: Stratosphere-troposphere exchange, Rev. Geophys., 33, 403-440, 1995.

Hoor, P., Gurk, C., Brunner, D., Hegglin, M. I., Wernli, H., and Fischer, H.: Seasonality and extent of extratropical TST derived from in-situ CO measurements during SPURT, Atmos. Chem. Phys., 4, 1427-1442, 2004.

Inai, Y.: Long-term variation in the mixing fraction of tropospheric and stratospheric air masses in the upper tropical tropopause layer. Journal of Geophysical Research: Atmospheres, 123, https://doi.org/10.1029/2018JD028300, 2018.

Ishijima, K., Nakazawa, T., Sugawara, S., Aoki, S., and Saeki, T.: Concentration variations of tropospheric nitrous oxide over Japan, Geophys. Res. Lett., 28, 171–174, doi:10.1029/2000GL011465, doi:10.1029/2000GL011465, 2001.

Krause, J., Hoor, P., Engel, A., Plöger, F., Grooß, J.-U., Bönisch, H., Keber, T., Sinnhuber, B.-M., Woiwode, W., and Oelhaf, H.: Mixing and ageing in the polar lower stratosphere in winter 2015–2016, Atmos. Chem. Phys., 18, 6057-6073, https://doi.org/10.5194/acp-18-6057-2018, 2018.

Lin, P., Ming, Y. and Ramaswamy, V.: Tropical climate change control of the lower stratospheric circulation, Geophys. Res. Lett., 42, 941–948, doi:10.1002/2014GL062823, 2015.

Manney, G. L., et al.: Jet characterization in the upper troposphere/lower stratosphere (UTLS): Applications to climatology and transport studies, Atmos. Chem. Phys., 11, 6115-6137, 2011.

Machida, T., Matsueda, H., Sawa, Y., Nakagawa, Y., Hirotani, K., Kondo, N., Goto, K., Nakazawa, T., Ishikawa, K., and Ogawa, T.: Worldwide measurements of atmospheric CO2 and other trace gas species using commercial airlines, J. Atmos. Oceanic Technol., 25(10), 1744–1754, doi:10.1175/2008JTECHA1082.1, 2008.

Matsueda, H., and Inoue, H. Y., Measurements of atmospheric CO2 and CH4 using a commercial airliner from 1993 to 1994, Atmos. Environ., 30, 1647–1655, 1996.

Matsueda, H., Inoue, H. Y., and Ishii, M.: Aircraft observation of carbon dioxide at 8–13 km altitude over the western Pacific from1993 to 1999, Tellus Ser. B, 54, 1–21, 2002.

Nakazawa, T., Morimoto, S., Aoki, S., and Tanaka, M.: Time and space variations of the carbon isotopic ratio of tropospheric carbon dioxide over Japan, Tellus B, 45, 258–274, 1993.

Pan, L. L., Bowman, K. P., Atlas, E. L., Wofsy, S. C., Zhang, F., Bresch, J. F., Ridley, B. A., Pittman, J. V., Homeyer, C. R., Romashkin, P. A., and Cooper, W. A.: The Stratosphere–Troposphere Analyses of Regional Transport 2008 Experiment, B. Am. Meteorol. Soc., 91, 327–342, https://doi.org/10.1175/2009BAMS2865.1, 2010.

Pan, L. L., Honomichl, S. B., Kinnison, D. E., Abalos, M., Randel, W. J., Bergman, J. W., and Bian, J.: Transport of chemical tracers from the boundary layer to stratosphere associated with the dynamics of the Asian summer monsoon, J. Geophys. Res., 121, 14159–14174, https://doi.org/10.1002/2016JD025616, 2016.

Petron, G., Crotwell, A.M., Lang, P. M., and Dlugokencky, E.: Atmospheric Carbon Monoxide Dry Air Mole Fractions from the NOAA ESRL Carbon Cycle Cooperative Global Air Sampling Network, 1988-2017, Version: 2018-10-17, Path: ftp://aftp.cmdl.noaa.gov/data/trace_gases/co/flask/surface/, 2018.

Ploeger, F., and Birner T.: Seasonal and inter-annual variability of lower stratospheric age of air spectra, Atmos. Chem. Phys., 16(15), 10195-10213, doi:10.5194/acp-16-10195-2016, 2016.

Ploeger, F., Konopka, P., Walker, K., and Riese, M.: Quantifying pollution transport from the Asian monsoon anticyclone into the lower stratosphere, Atmos. Chem. Phys., 17, 7055-7066, https://doi.org/10.5194/acp-17-7055-2017, 2017.

Plumb, R. A., Tracer interrelationships in the stratosphere, Rev. Geophys., 45(4), Artn Rg4005, doi:10.1029/2005rg000179, 2007.

Randel, W. J. and Park, M.: Deep convective influence on the Asian summer monsoon anticyclone and associated tracer variability observed with Atmospheric Infrared Sounder (AIRS), J. Geophys. Res., 111, D12314, doi:10.1029/2005JD006490, 2006.

Randel, W. J., Park, M., Emmons, L., Kinnison, D., Bernath, P., Walker, K. A., Boone, C., and Pumphrey, H.: Asian Monsoon Transport of Pollution to the Stratosphere, Science, 328, 611– 613, doi:10.1126/science.1182274, 2010.

Röckmann, T., Brass, M., Borchers, R., and Engel, A.: The isotopic composition of methane in the stratosphere: high-altitude balloon sample measurements, Atmos. Chem. Phys., 11, 13287-13304, https://doi.org/10.5194/acp-11-13287-2011, 2011.

Sawa, Y., Machida, T., Matsueda, H., Niwa, Y., Tsuboi, K., Murayama, S., Morimoto, S., and Aoki, S.: Seasonal changes of CO_2, CH_4, N_2O, and SF_6 in the upper troposphere/lower stratosphere over the Eurasian continent observed by commercial airliner, Geophys. Res. Lett., 42, 2001–2008, doi:10.1002/2014GL062734, 2015.

Schoeberl, M. R., Sparling, L. C., Jackman, C. H., and Fleming, E. L.: A Lagrangian view of stratospheric trace gas distributions, Journal of Geophysical Research: Atmospheres, 105(D1), 1537-1552, doi:10.1029/1999JD900787, 2000.

Schoeberl, M. R., Douglass, A. R., Zhu, Z., and Pawson, S.: A comparison of the lower stratospheric age spectra derived from a general circulation model and two data assimilation systems. Journal of Geophysical Research, 108(D3), 4113. https://doi.org/10.1029/2002JD002652, 2003.

Strahan, S. E., Duncan, B. N., and Hoor, P.: Observationally derived transport diagnostics for the lowermost stratosphere and their application to the GMI chemistry and transport model, Atmos. Chem. Phys., 7, 2435-2445, https://doi.org/10.5194/acp-7-2435-2007, 2007.

Thoning, K. W., Kitzis, D. R., and Crotwell, A.: Atmospheric carbon dioxide dry air mole fractions from quasi-continuous measurements at Barrow, Alaska, Version: 2018-10, Path: http://dx.doi.org/10.7289/V5RR1W6B, 2017.

Umezawa, T., Goto, D., Aoki, S., Ishijima, K., Patra, P. K., Sugawara, S., Morimoto, S., and Nakazawa, T.: Variations of tropospheric methane over Japan during 1988–2010, Tellus B, 66, 23837, doi:10.3402/tellusb.v66.23837, 2014.

Umezawa, T., Baker, A. K., Brenninkmeijer, C. A. M., Zahn, A., Oram, D. E., and van Velthoven, P. F. J.: Methyl chloride as a tracer of tropical tropospheric air in the lowermost stratosphere inferred from IAGOS-CARIBIC passenger aircraft measurements, J. Geophys. Res., 120, 12313–12326, doi:10.1002/2015JD023729, 2015.

Vogel, B., et al.: Long-range transport pathways of tropospheric source gases originating in Asia into the northern lower stratosphere during the Asian monsoon season 2012, Atmos. Chem. Phys., 16, 15301-15325, https://doi.org/10.5194/acp-16-15301-2016, 2016.

Volk, C. M., Elkins, J. W., Fahey, D. W., Dutton, G. S., Gilligan, J. M., Loewenstein, M., Podolske, J. R., Chan, K. R., and Gunson, M. R.: Evaluation of source gas lifetimes from Stratospheric observations, J. Geophys. Res., 102(D21), 25 543– 25 564, doi:10.1029/97JD02215, 1997.

Wernli, H., and Bourqui, M.: A Lagrangian ‘‘1-year climatology’’ of (deep) cross-tropopause exchange in the extratropical Northern Hemisphere, J. Geophys. Res., 107(D2), 4021, doi:10.1029/2001JD000812, 2002.

Table 1: Criteria for determining ~~the~~ air mass origin. Each trajectory is categorized once it continuously satisfies one set of criteria *k* = 1, 2, 3, or 4 during three continuous days along its path.

Category #	Origin	Criteria
k = 1d	Deep stratosphere	Pot. temperature >400 K; P <30 hPa within 4 years
k = ~~1~~1s	~~High latitude~~Shallow stratosphere	Pot. temperature >~~380~~400 K; ~~lat. >45° N; pot. vorticity >6 PVU~~not satisfied *k* = 1d
k = 2	Tropical troposphere	Pot. temperature <350 K; lat. <~~30~~20° N; pot. vorticity <~~2~~1 PVU
k = 3	Mid-latitude LT	Z <4 km; 20° N < lat. <~~-~~45° N
k = 4	High-latitude LT	Z <4 km; lat. >45° N
~~k = 5~~	~~Unclassified (UTLS)~~	~~None of the above~~

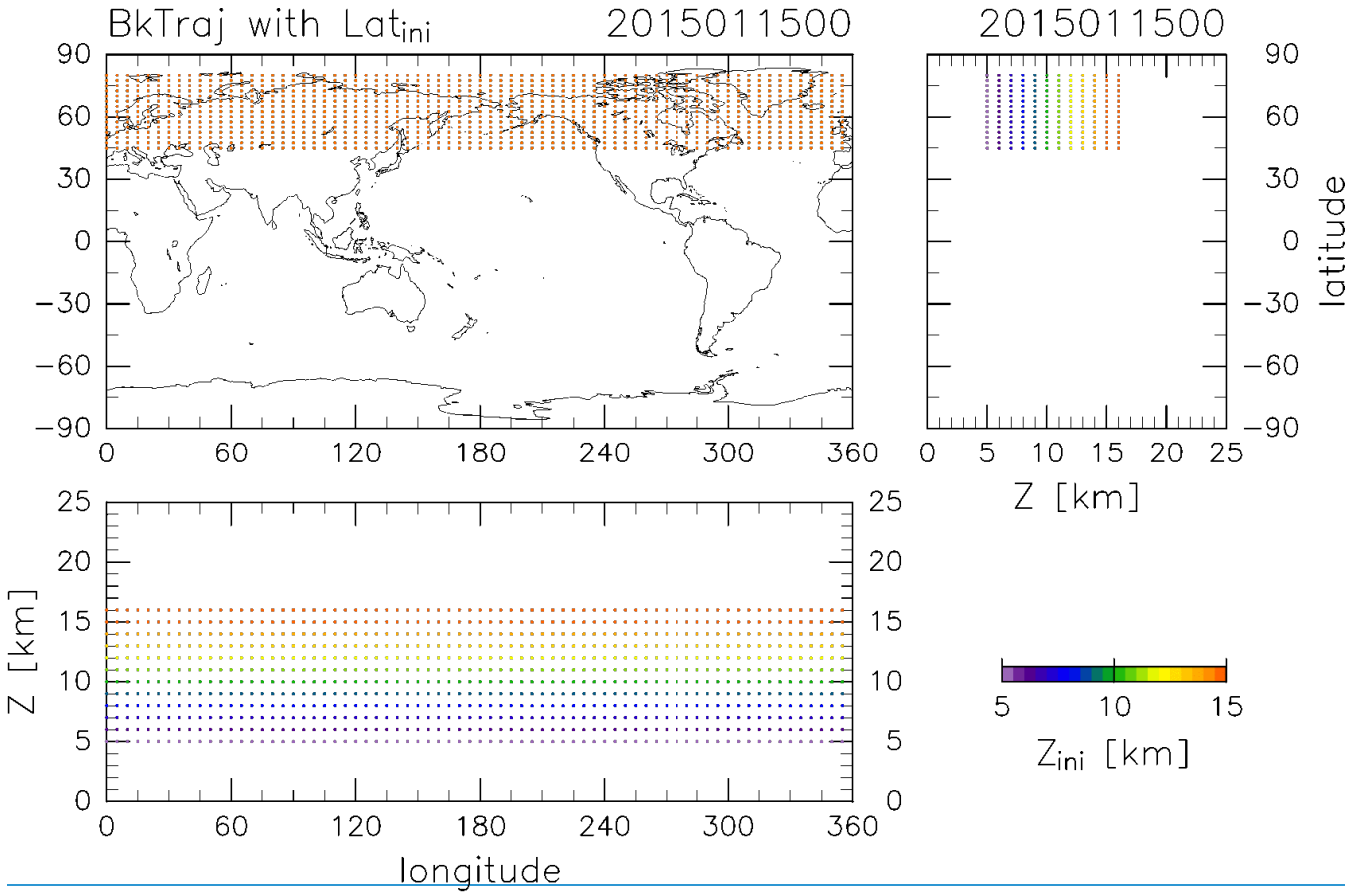
BkTraj with Lat$_{ini}$
2015011500
2015011500
90
60
30
0
−30
−60
−90
0
60
120
180
240
300
360
0
5
10
15
20
25
Z [km]
latitude
longitude
Z [km]
5
10
15
Z$_{ini}$ [km]

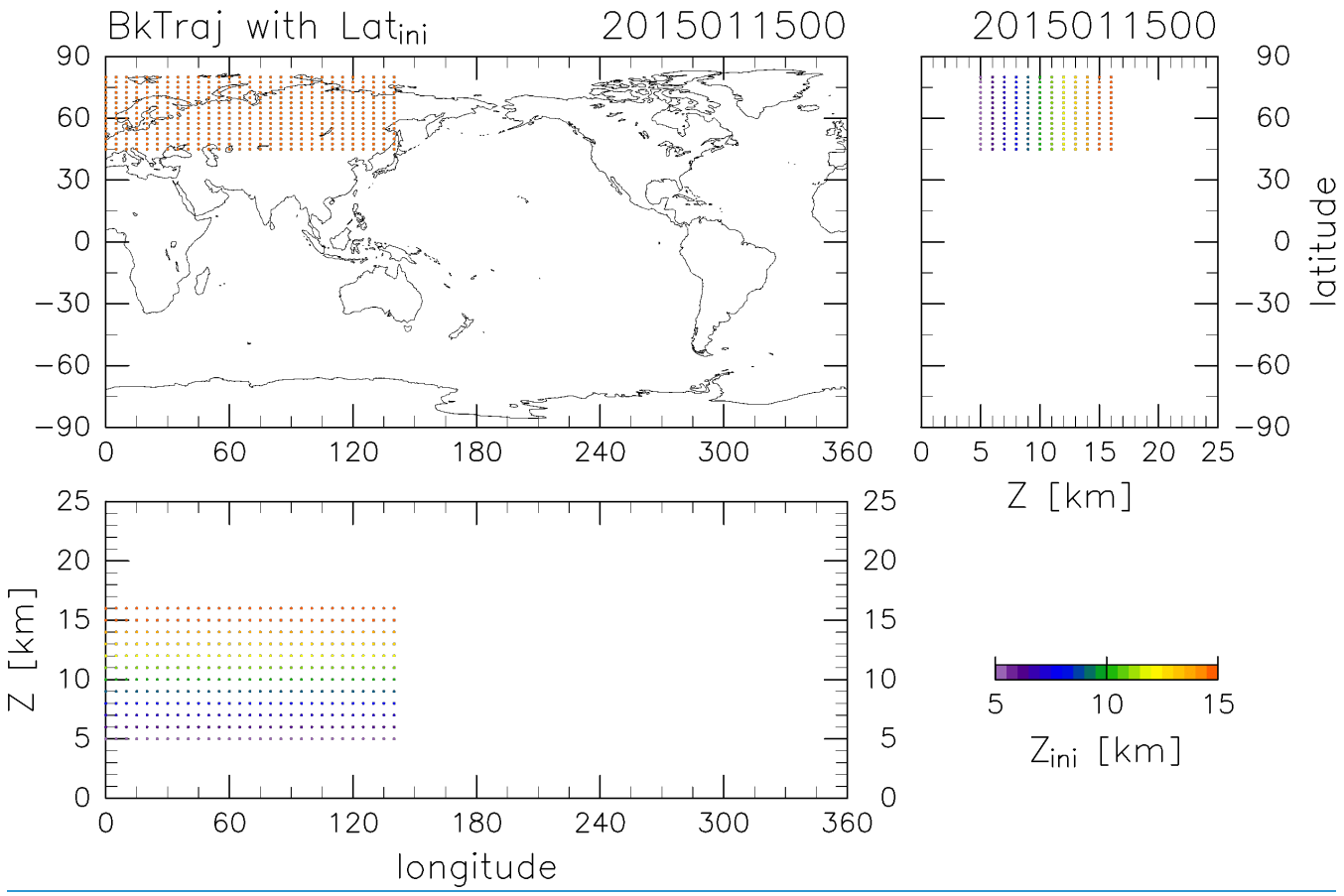

Figure 1: Initial trajectory positions projected in (top-left) longitude–latitude, (top-right) height–latitude, and (bottom) longitude–height sections. Colours indicate the initial height for each position.

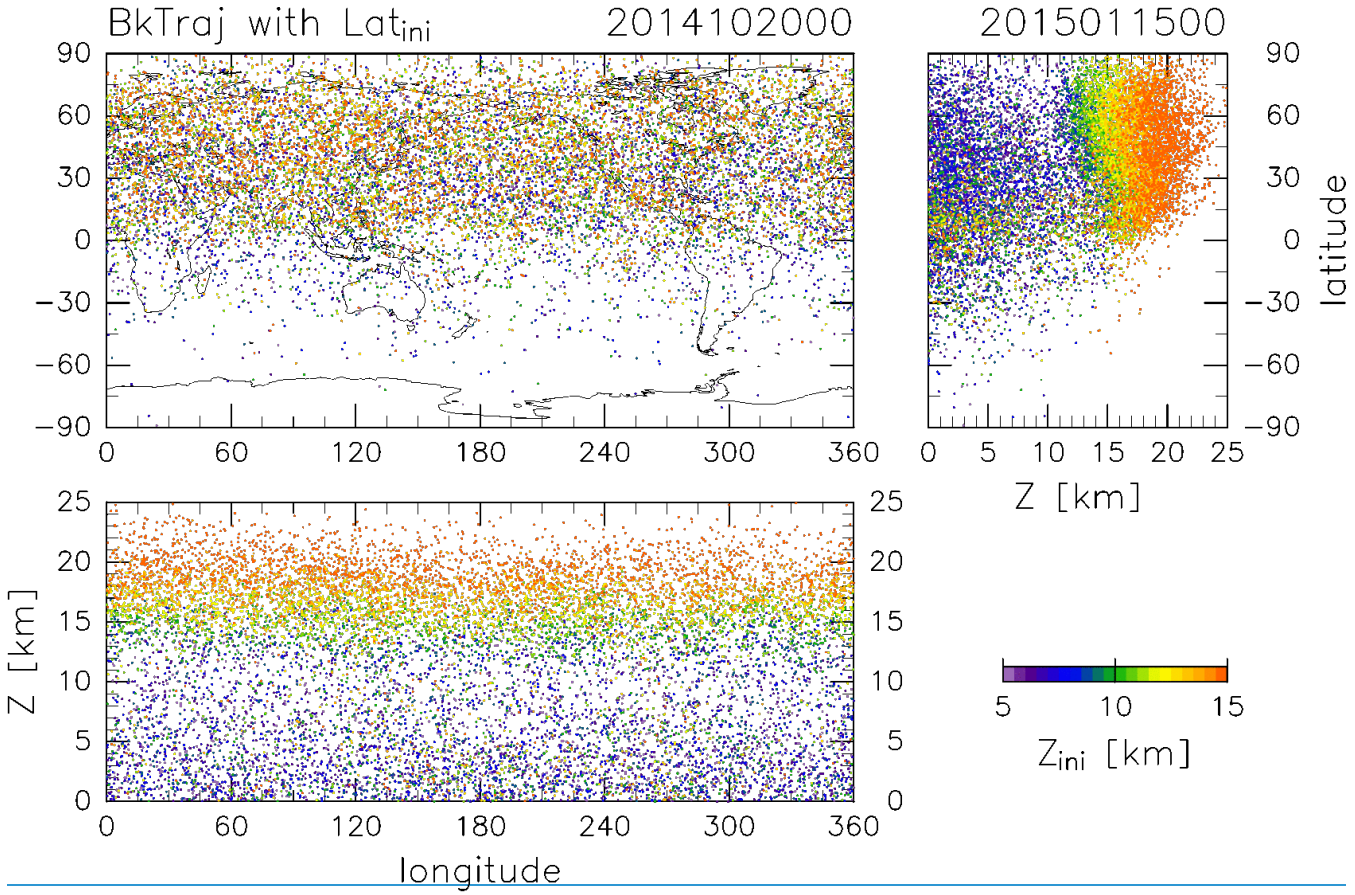
BkTraj with Lat$_{ini}$
2014102000
2015011500
90
60
30
0
−30
−60
−90
0
60
120
180
240
300
360
0
5
10
15
20
25
Z [km]
latitude
longitude
Z$_{ini}$ [km]

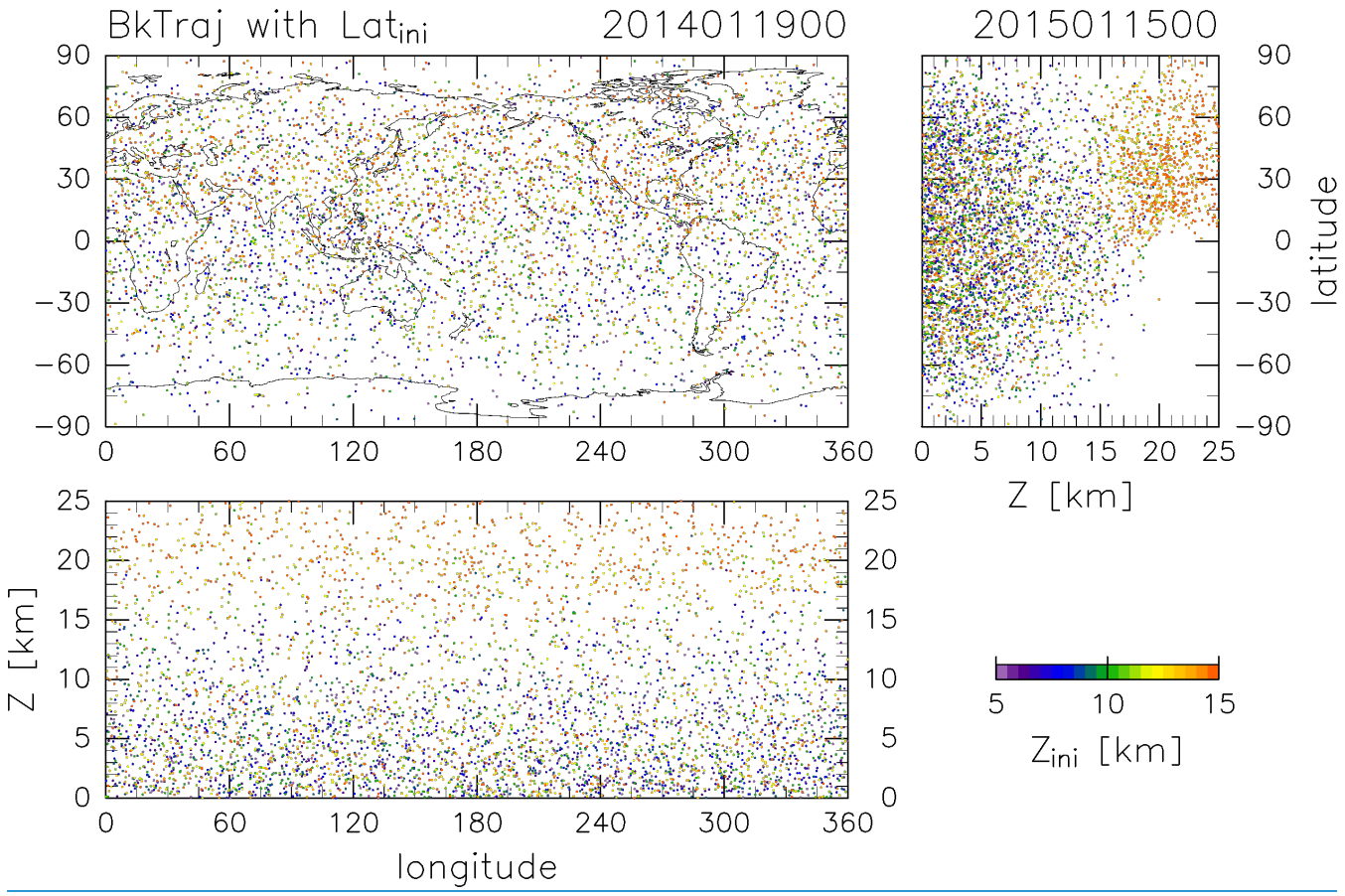

Figure 2: ~~Same as~~As in **Fig. 1, but for the terminal positions of trajectories after calculating backward for** ~~90~~361 **days.**

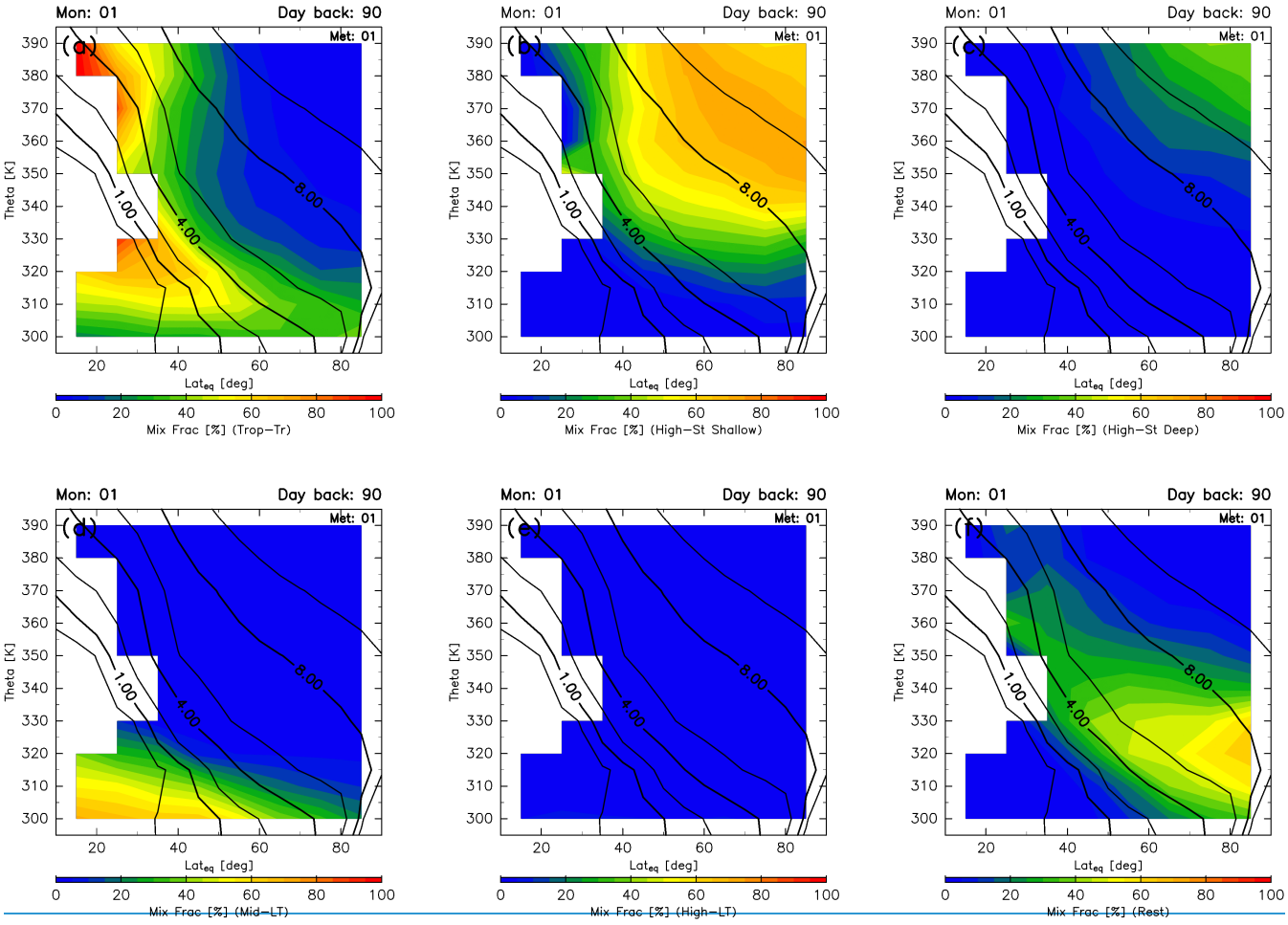
Mon: 01
Day back: 90
Met: 01
(a)
(b)
(c)
(d)
(e)
(f)
Theta [K]
Lat$_{eq}$ [deg]
1.00
4.00
8.00
Mix Frac [%] (Trop−Tr)
Mix Frac [%] (High−St Shallow)
Mix Frac [%] (High−St Deep)
Mix Frac [%] (Mid−LT)
Mix Frac [%] (High−LT)
Mix Frac [%] (Rest)

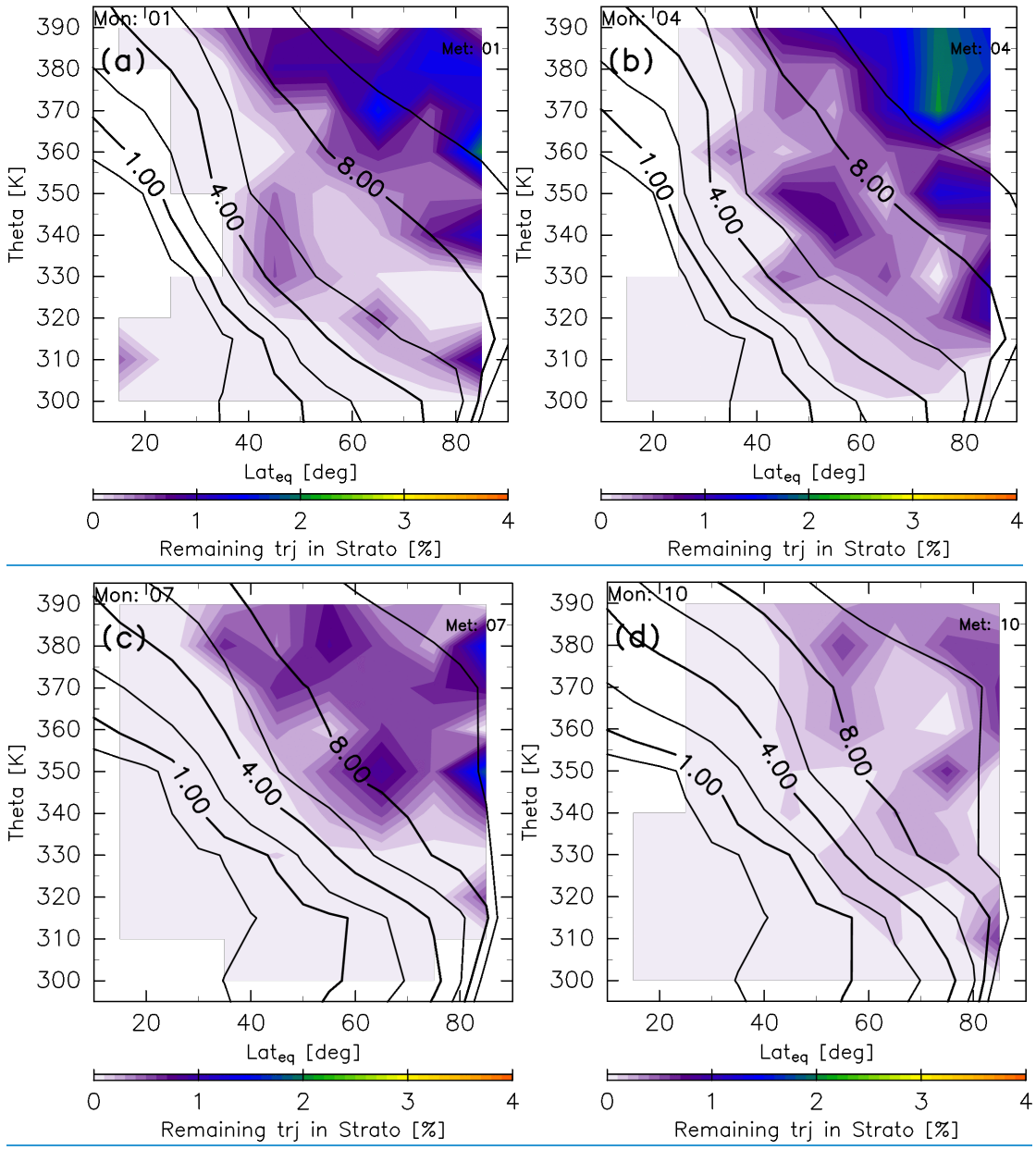

Figure 3: Meridional distributions of ~~mixing fractions~~percentage of trajectories that remain in the stratosphere after 10-year backward calculations for (a) ~~tropical tropospheric, (b) high latitude stratospheric (through the shallow branch of the BDC), (c) high latitude stratospheric (through the deep branch of the BDC), (d) mid-latitude LT, (e) high-latitude LT, and (f) the unclassified air masses estimated for~~ January~~.~~, (b) April, (c) July, and (d) October. Black contours indicate monthly ~~averaged~~average potential vorticity during ~~the period from~~ 2012 ~~to~~ 2016.

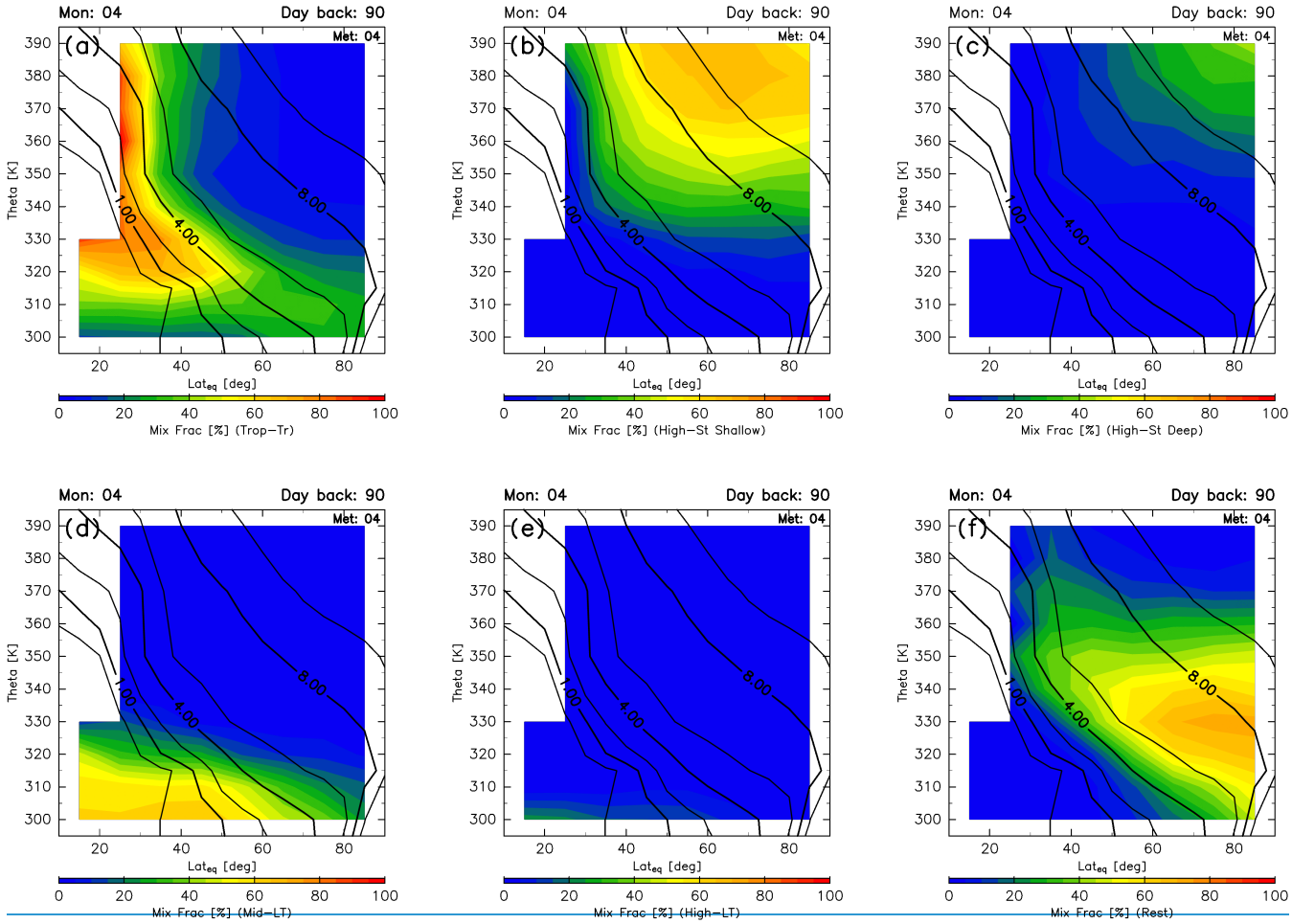

Figure 4: Same as Fig. 3, but for April.

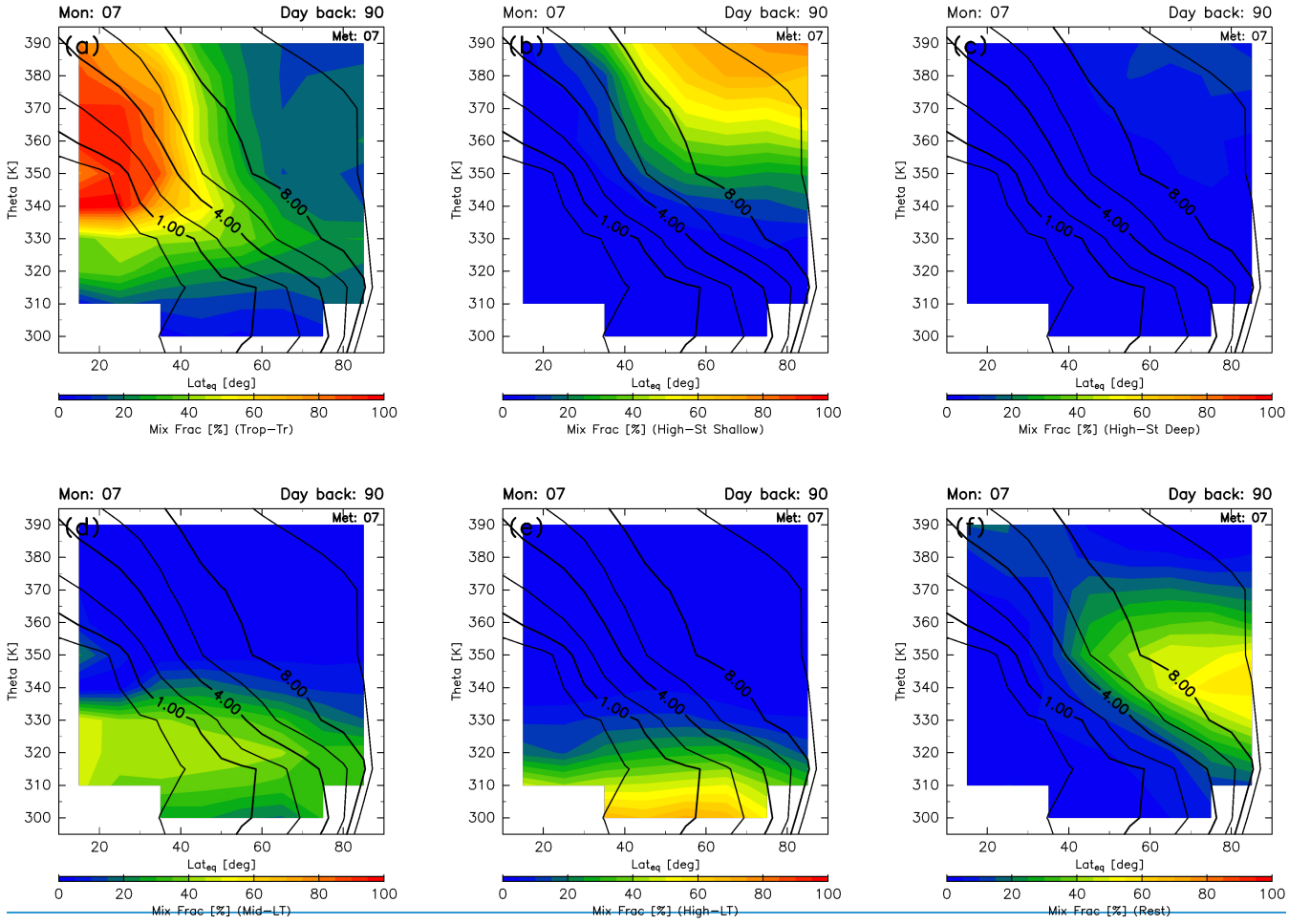

~~Figure 5: Same as Fig. 3, but for July.~~

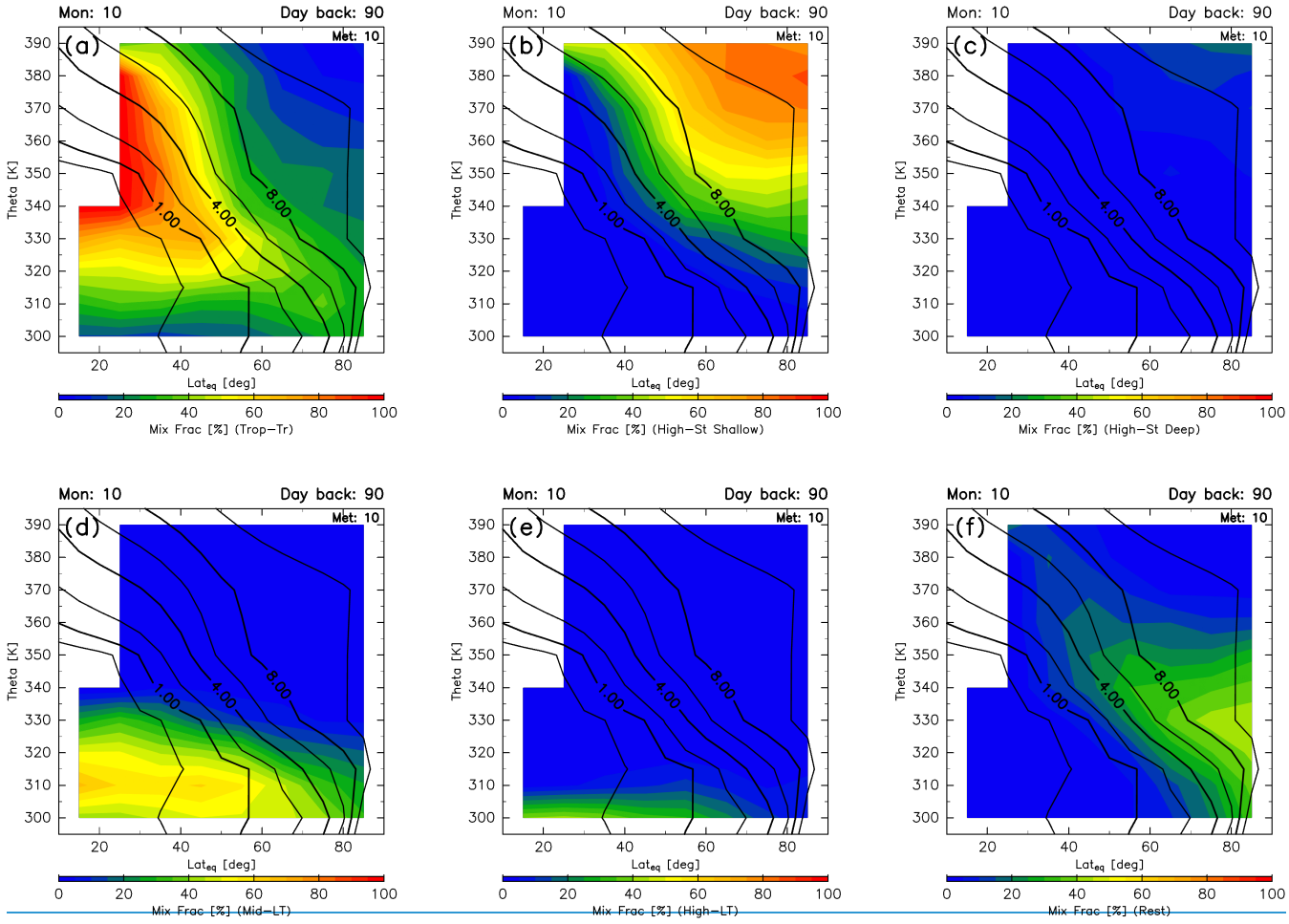

Figure 6: Same as Fig. 3, but for October.

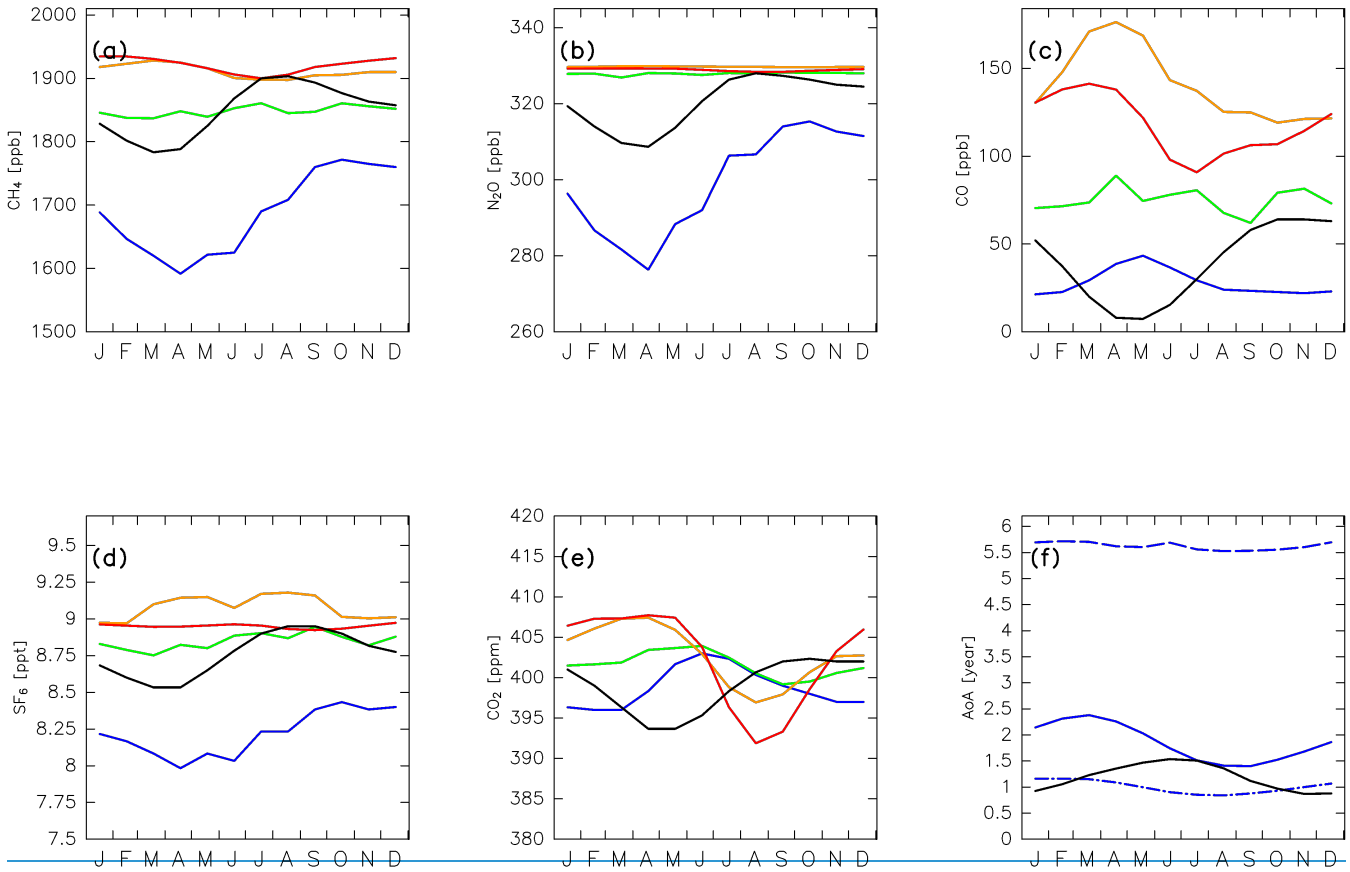

~~**Figure 7: Seasonal variations in (a) CH_4, (b) N_2O, (c) CO, (d) SF_6, and (e) CO_2 mixing ratios estimated for (green) tropical tropospheric, (blue) high latitude stratospheric, (orange) mid latitude LT, (red) high latitude LT, and (black) unclassified air masses. Seasonal variations in the age of air estimated for (blue solid) high latitude stratospheric and (black) unclassified air masses are shown in (f). The dashed, dotted and dashed lines in (f) show the age of air separately estimated for high latitude stratospheric air masses that travelled via the shallow and deep branches of the BDC, respectively.**~~

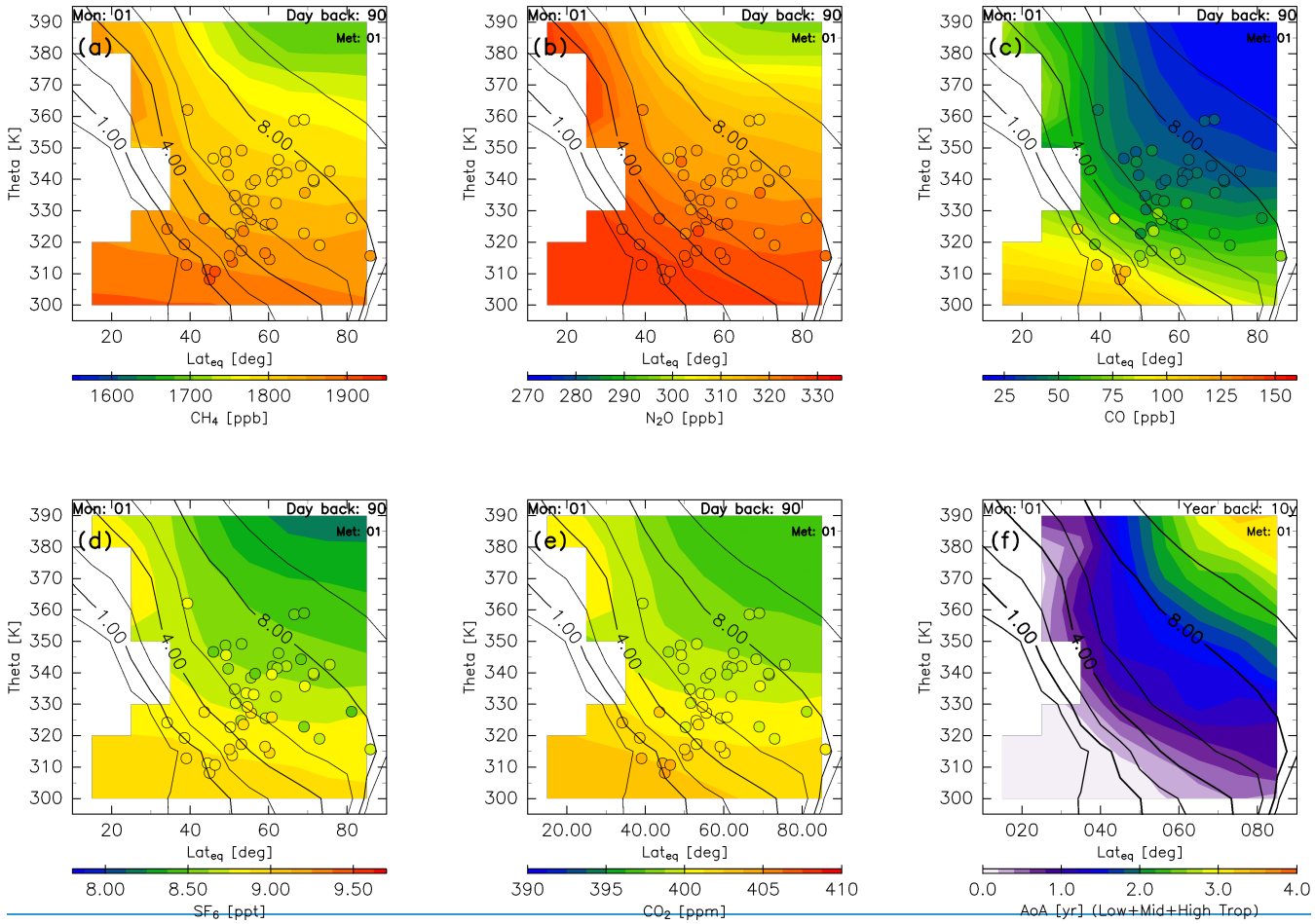

~~**Figure 8: Meridional distributions of reconstructions for (a) CH_4, (b) N_2O, (c) CO, (d) SF_6, and (e) CO_2 for January. Detrended CONTRAIL measurements in April are plotted as circles using the same colour scale. The distribution of the age of air estimated for January is shown in (f). Black contours indicate monthly averaged potential vorticity during the period from 2012 to 2016.**~~

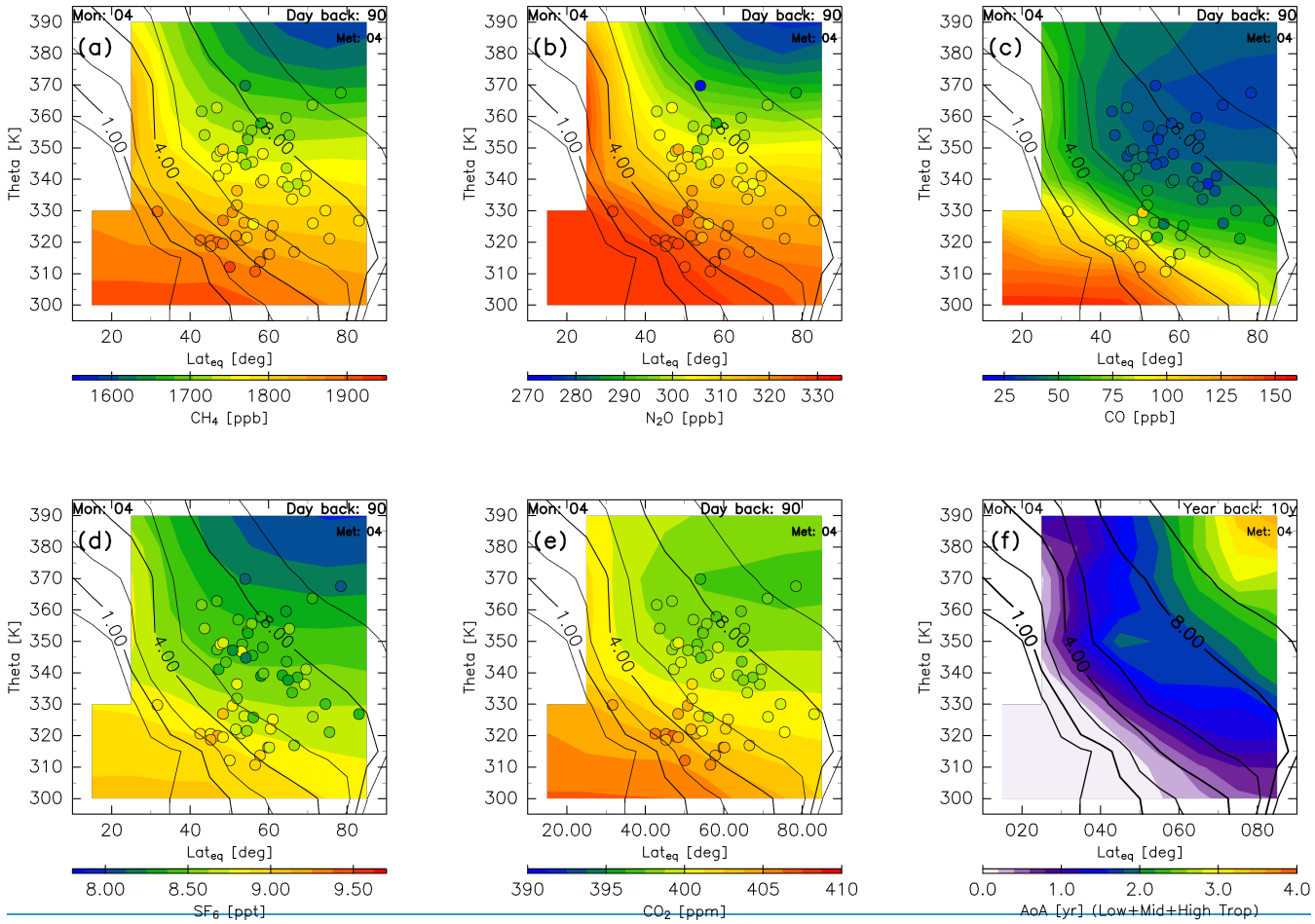
Mon: 04
Day back: 90
Met: 04
(a)
(b)
(c)
(d)
(e)
(f)
Year back: 10y
Theta [K]
Lateq [deg]
CH4 [ppb]
N2O [ppb]
CO [ppb]
SF6 [ppt]
CO2 [ppm]
AoA [yr] (Low+Mid+High Trop)
1.00
4.00
8.00

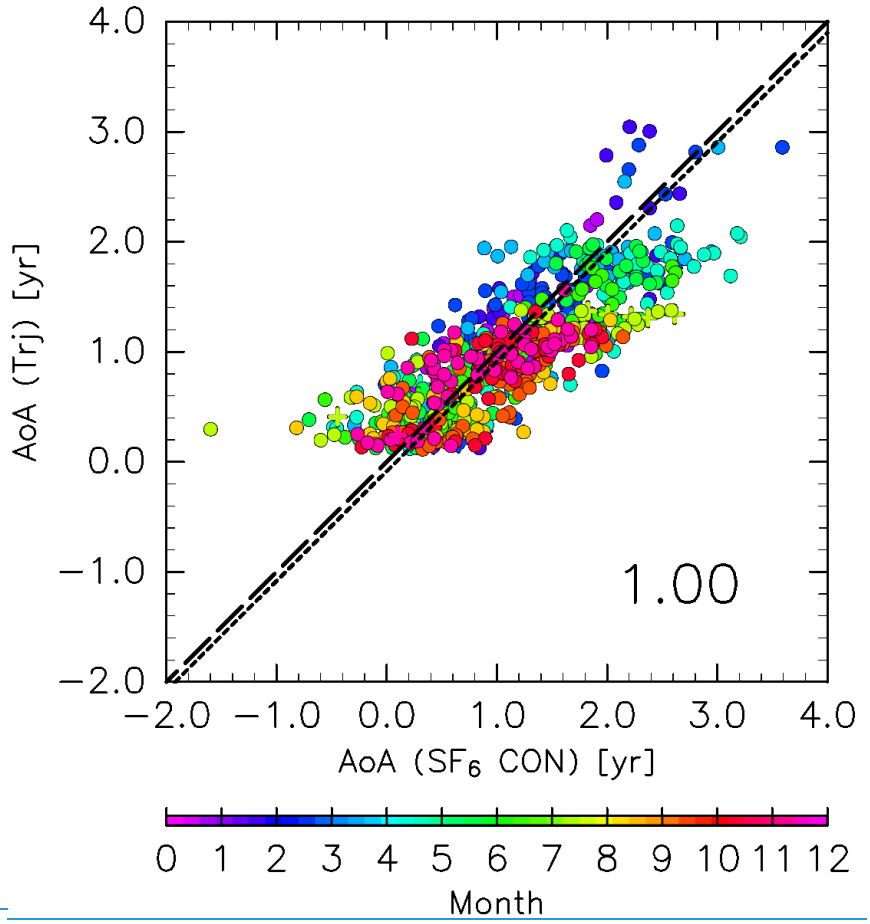

~~Figure 9: Same as Fig.~~

Figure 4: Scatter plot of the age of air (AoA) estimated from SF_6 mixing ratios obtained from CONTRAIL measurements versus those from trajectories with a correction factor of 1.5 (see text for details). Colours indicate the month, and the dashed and dotted lines indicate the 1:1 line and the regression line, respectively. The number in the lower-right of the panel indicates the slope of the regression line. CONTRAIL data with CO mixing ratios higher than 80 ppb in the region above 340 K and north of 60° N equivalent latitude are plotted in crosses.

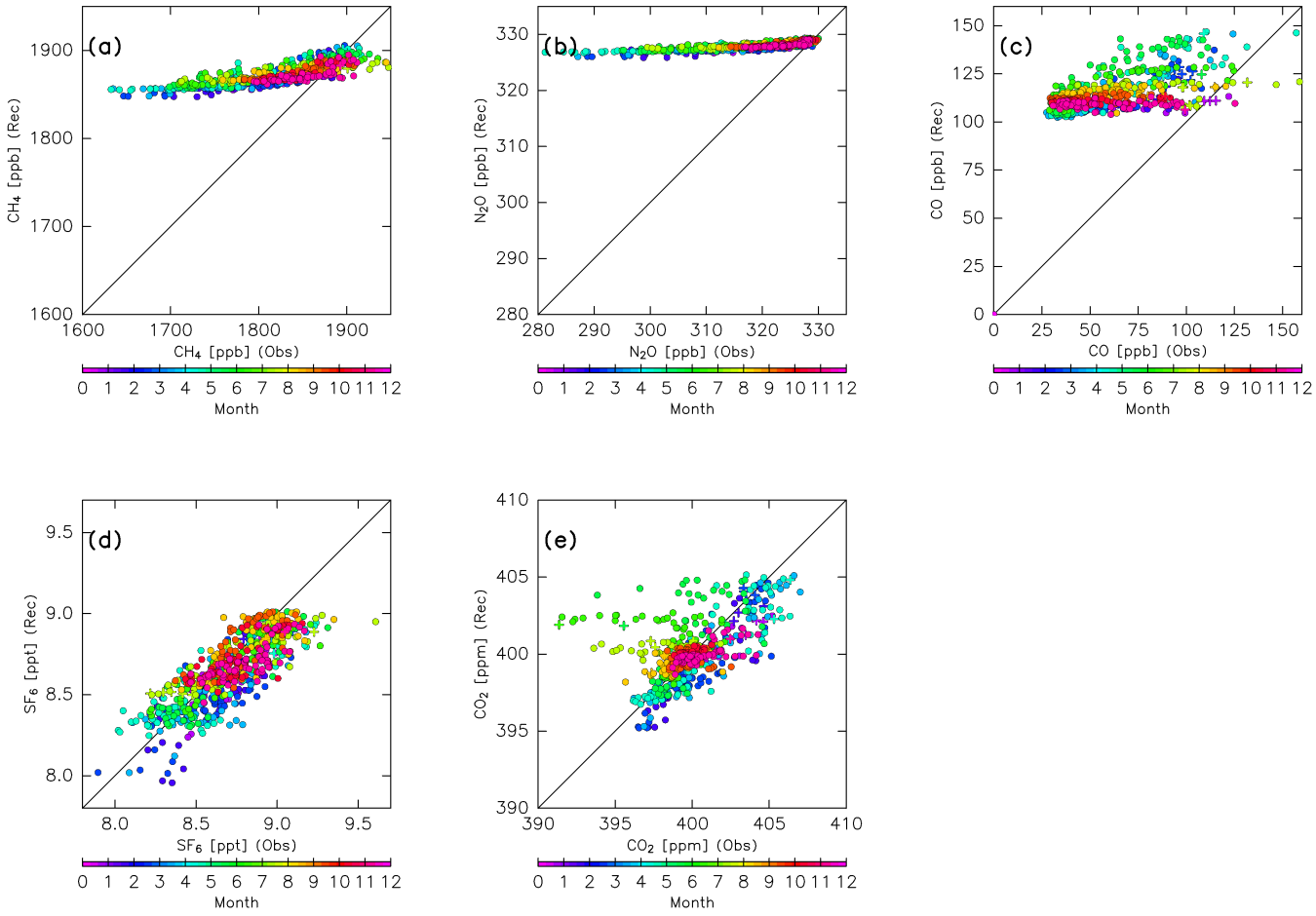

Figure 5~~8, but for April.~~

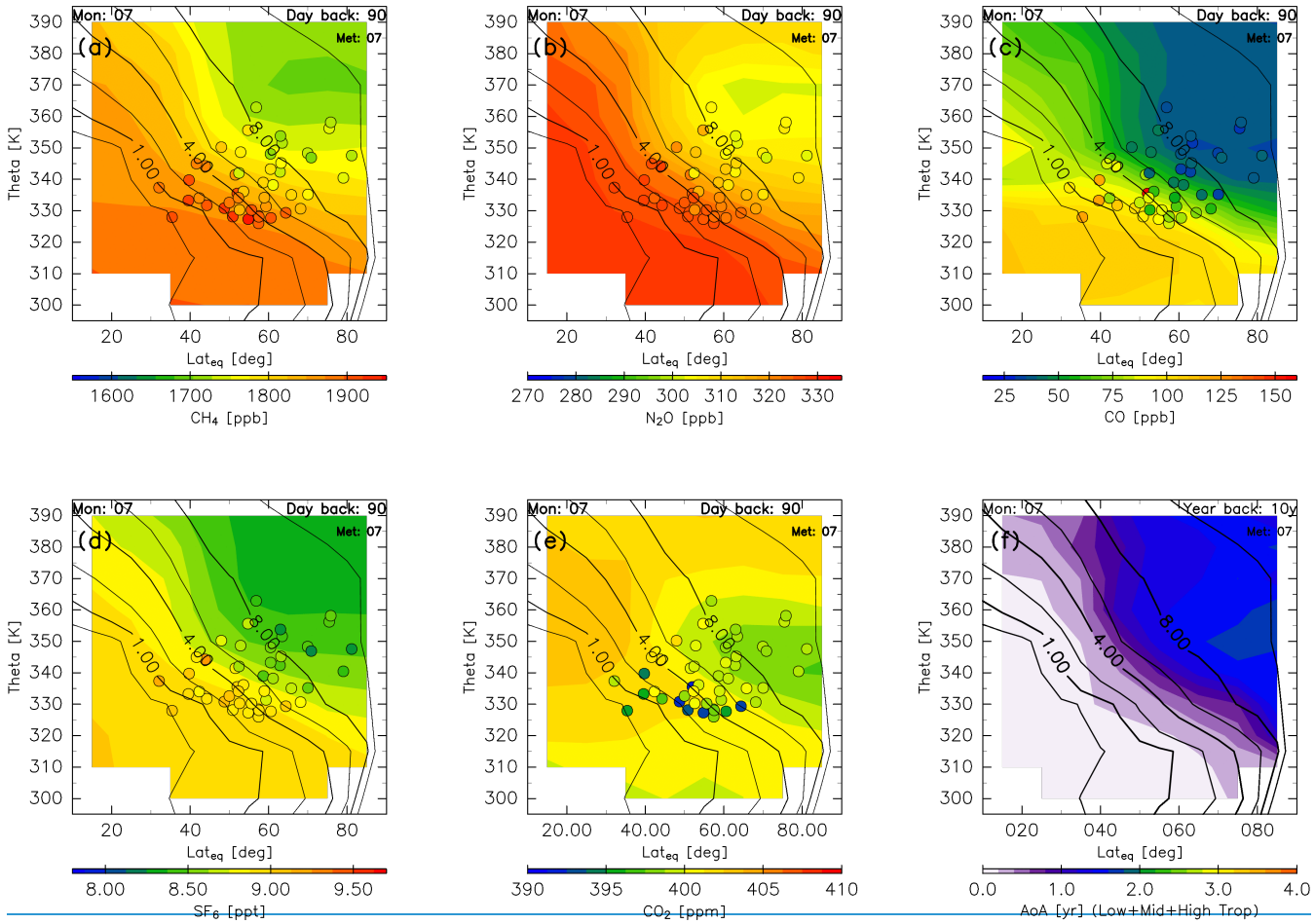

Figure 10: Same as Fig. 8, but for July.

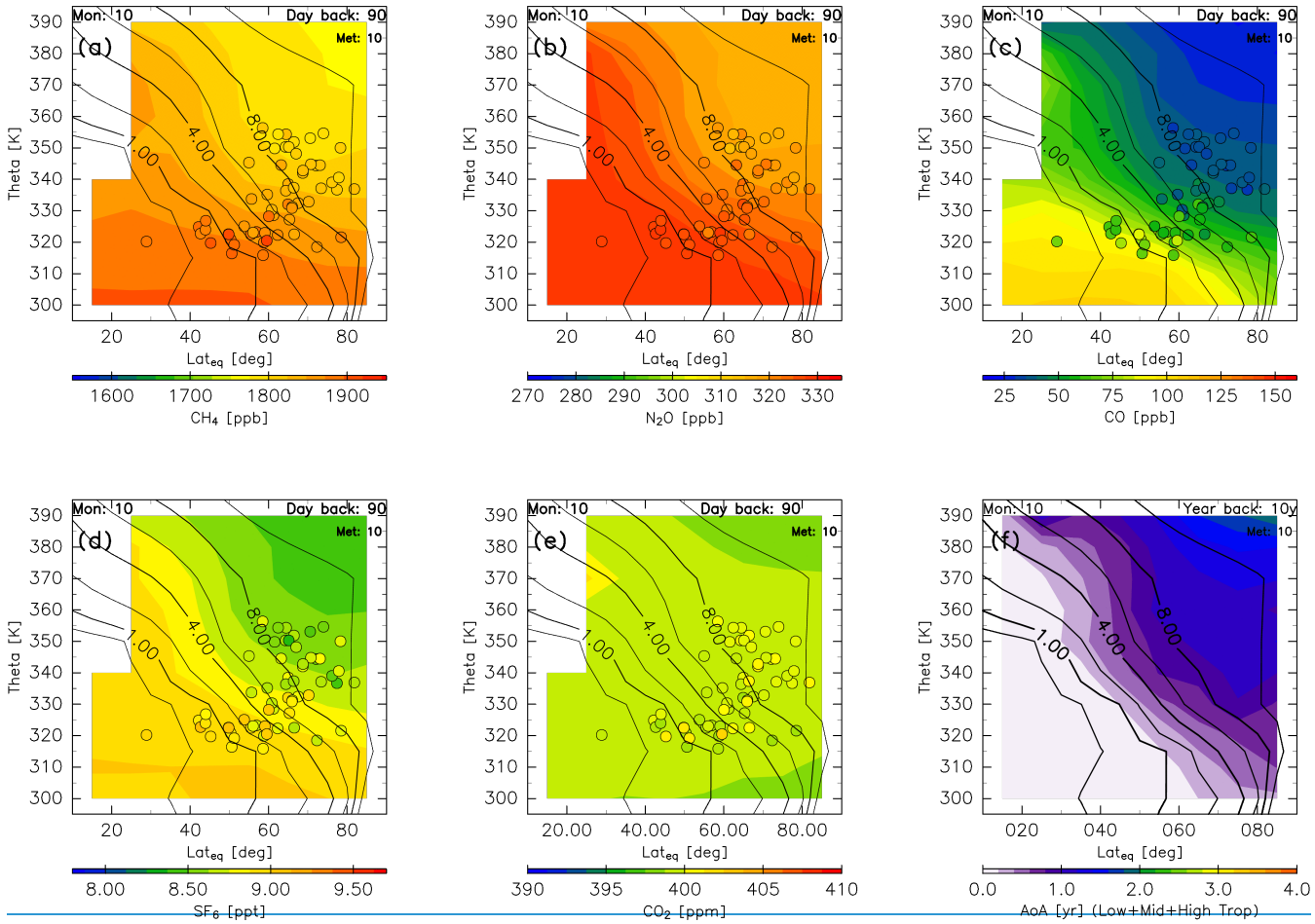

Figure 11: Same as Fig. 8, but for October.

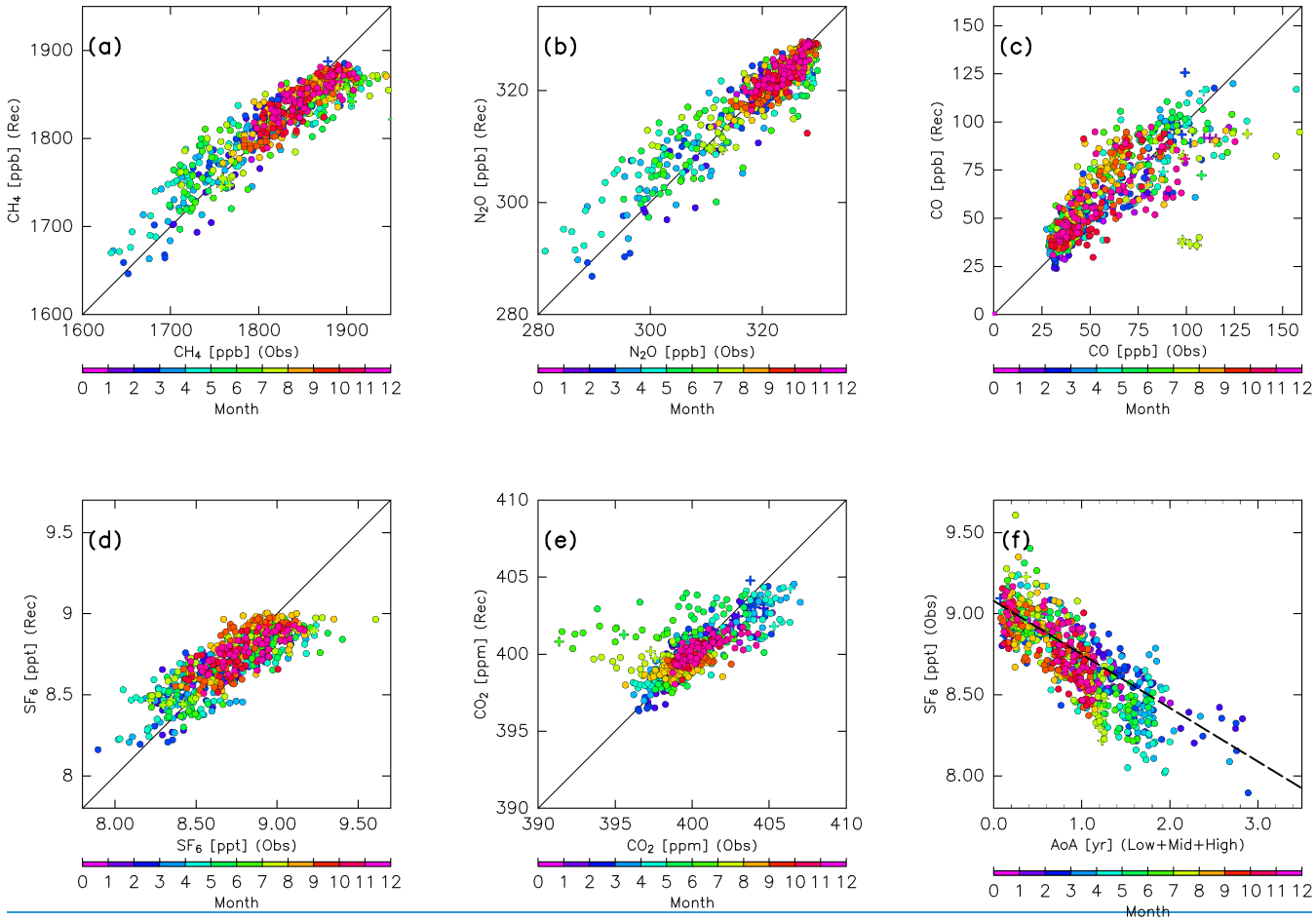

~~Figure 12~~: Scatter plots of CONTRAIL measurements versus reconstructions for (a) CH_4, (b) N_2O, (c) CO, (d) SF_6, and (e) CO_2~~~~, and (f) the age of air versus SF_6 measured by CONTRAIL. Colours indicate the month, and the dashed line in (f) shows the sign-reversed trend in tropospheric SF_6 (−0.33 ppt/year) with the intercept of the annual-averaged mixing ratio at mid-latitudes for 2016 (9.08 ppt).~~ without chemical loss. Colours indicate the month.

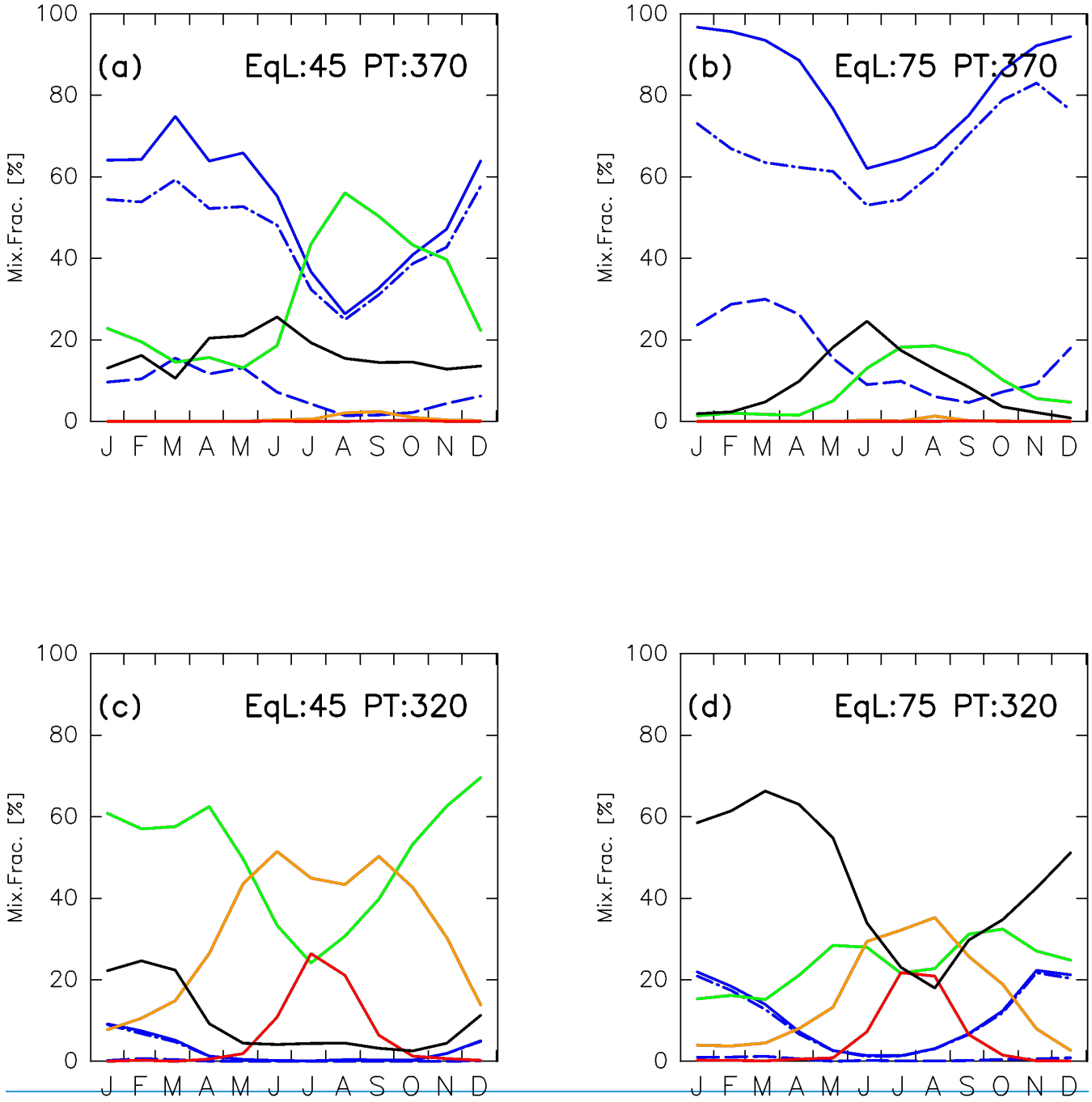
(a) EqL:45 PT:370
(b) EqL:75 PT:370
(c) EqL:45 PT:320
(d) EqL:75 PT:320
Mix.Frac. [%]
100
80
60
40
20
0
J F M A M J J A S O N D

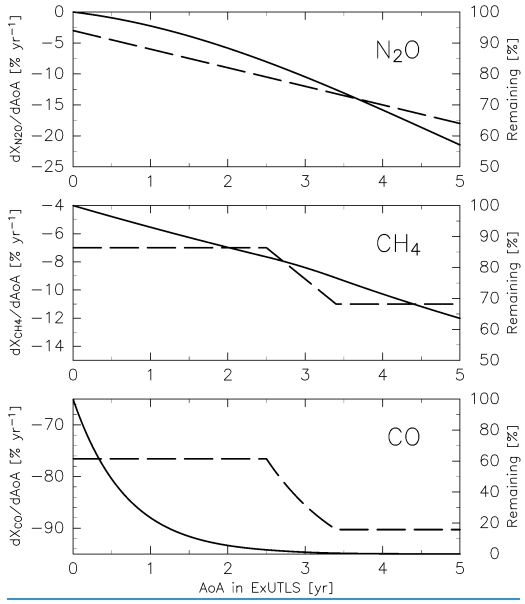

Figure 6: Relationships between the age of air (AoA) and the gradient of chemical loss rates (dashed lines; left axis) and relative abundance (solid lines; right axis), determined according to figure 6a of Volk et al. (1997). Note that CO is assumed to be 20-times the CH_4 value.

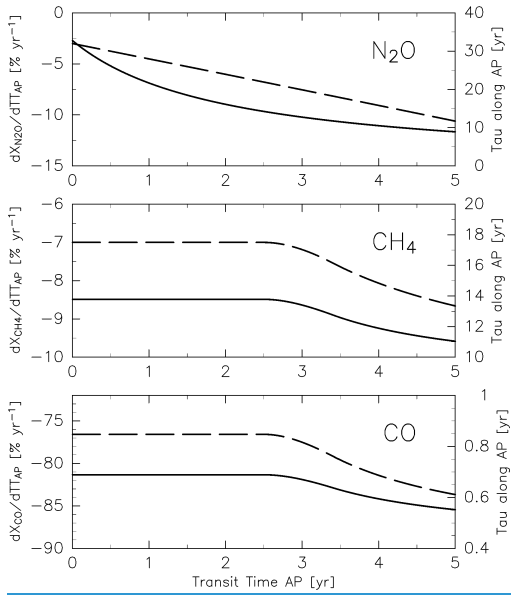

Figure 7: Relationships between transit time along the "average path" (AP) and the gradient of chemical loss rate with respect to transit time that produces the same relationship between age of air (AoA) and the gradient of chemical loss rate shown in Fig. 6 (dashed lines; left axis; see text for details), and e-folding times corresponding to chemical loss rates along an AP (solid lines; right axis).

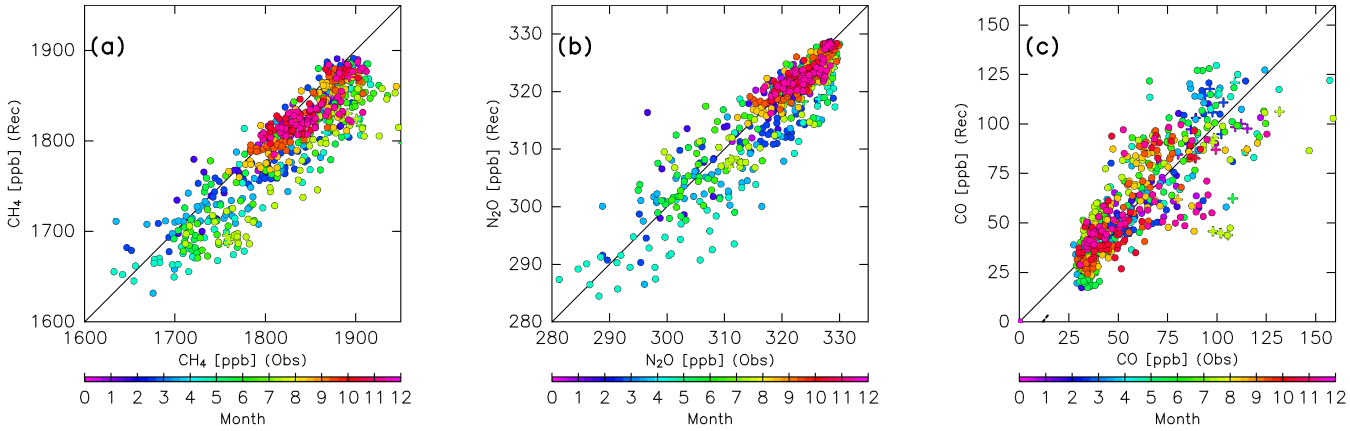

Figure 8: As in Fig. 6, but for reconstructions with chemical loss.

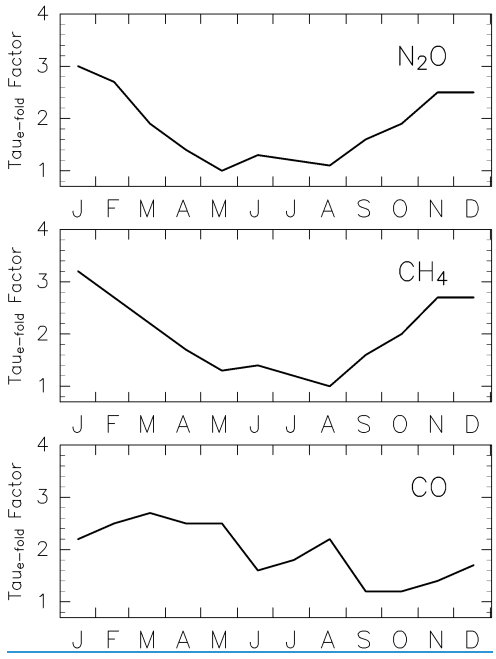

Figure 9: Estimated correction factor for e-folding times for three chemically active species.

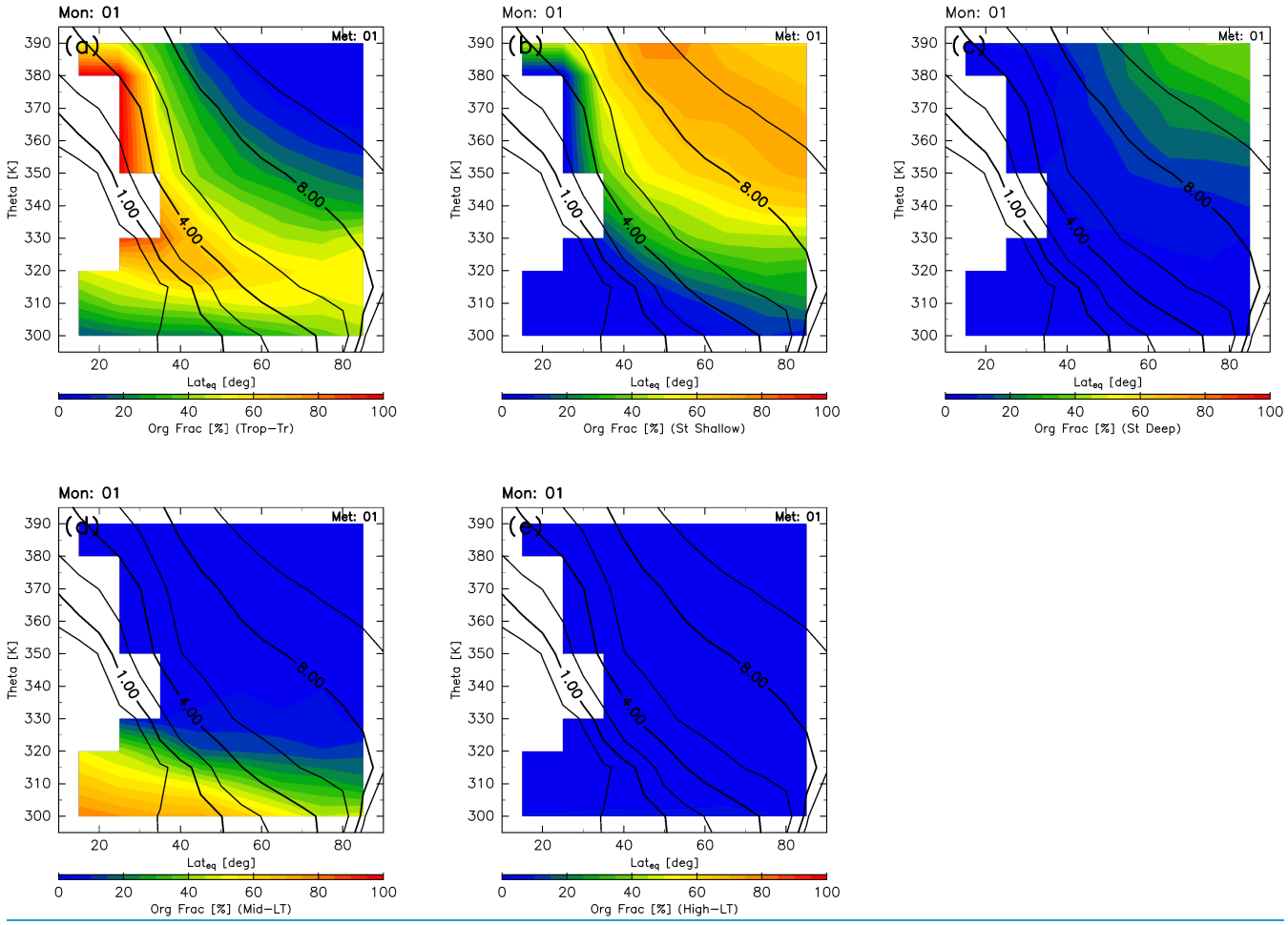

Figure 10: Meridional distributions of origin fractions for (a) tropical tropospheric, (b) stratospheric (through the shallow branch of the BDC), (c) stratospheric (through the deep branch of the BDC), (d) mid-latitude LT, and (e) high-latitude LT air masses estimated for January. Black contours indicate monthly averaged potential vorticity during the period from 2012 to 2016.

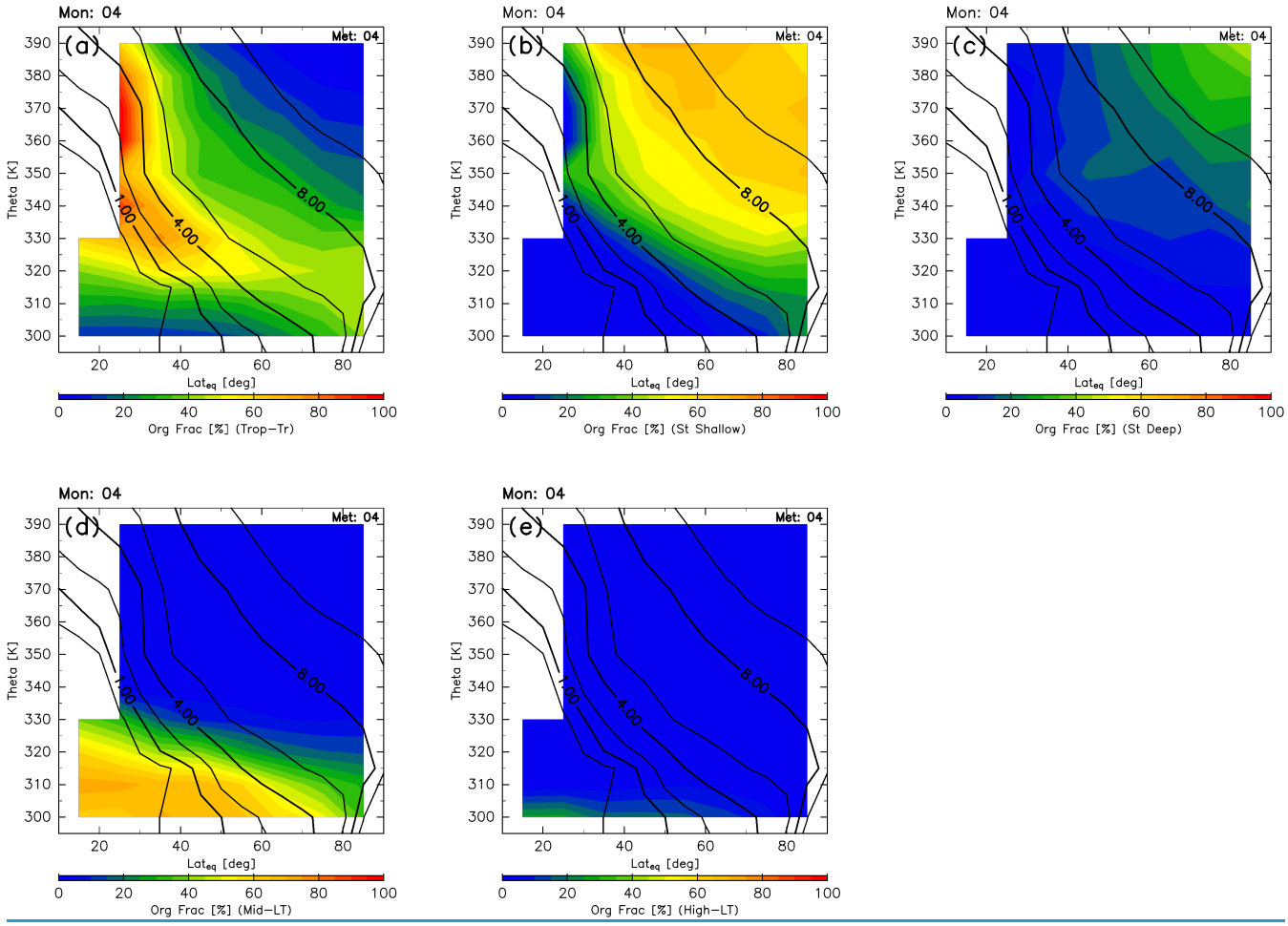

Figure 11: As in Fig. 10, but for April.

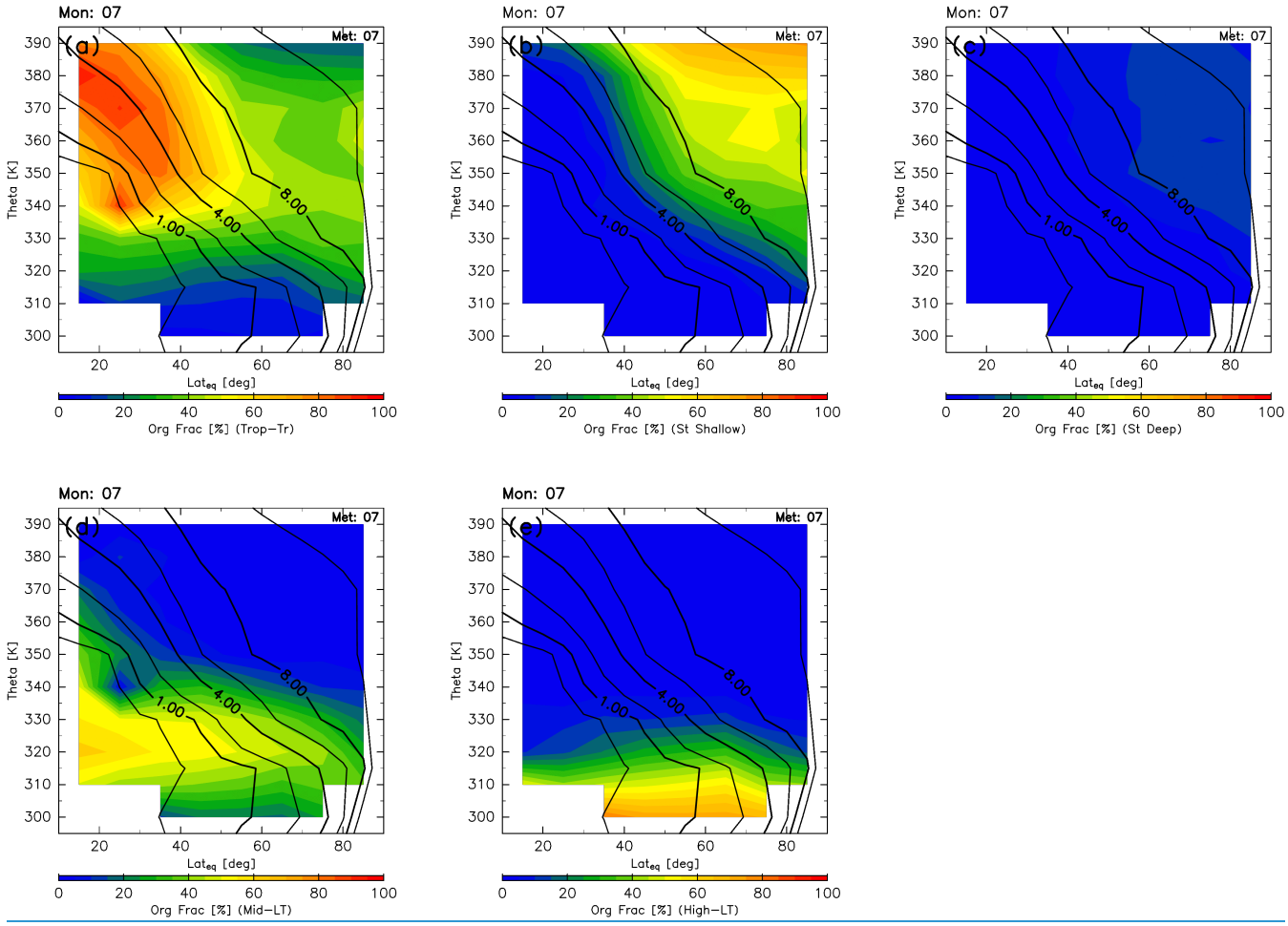

Figure 12: As in Fig. 10, but for July.

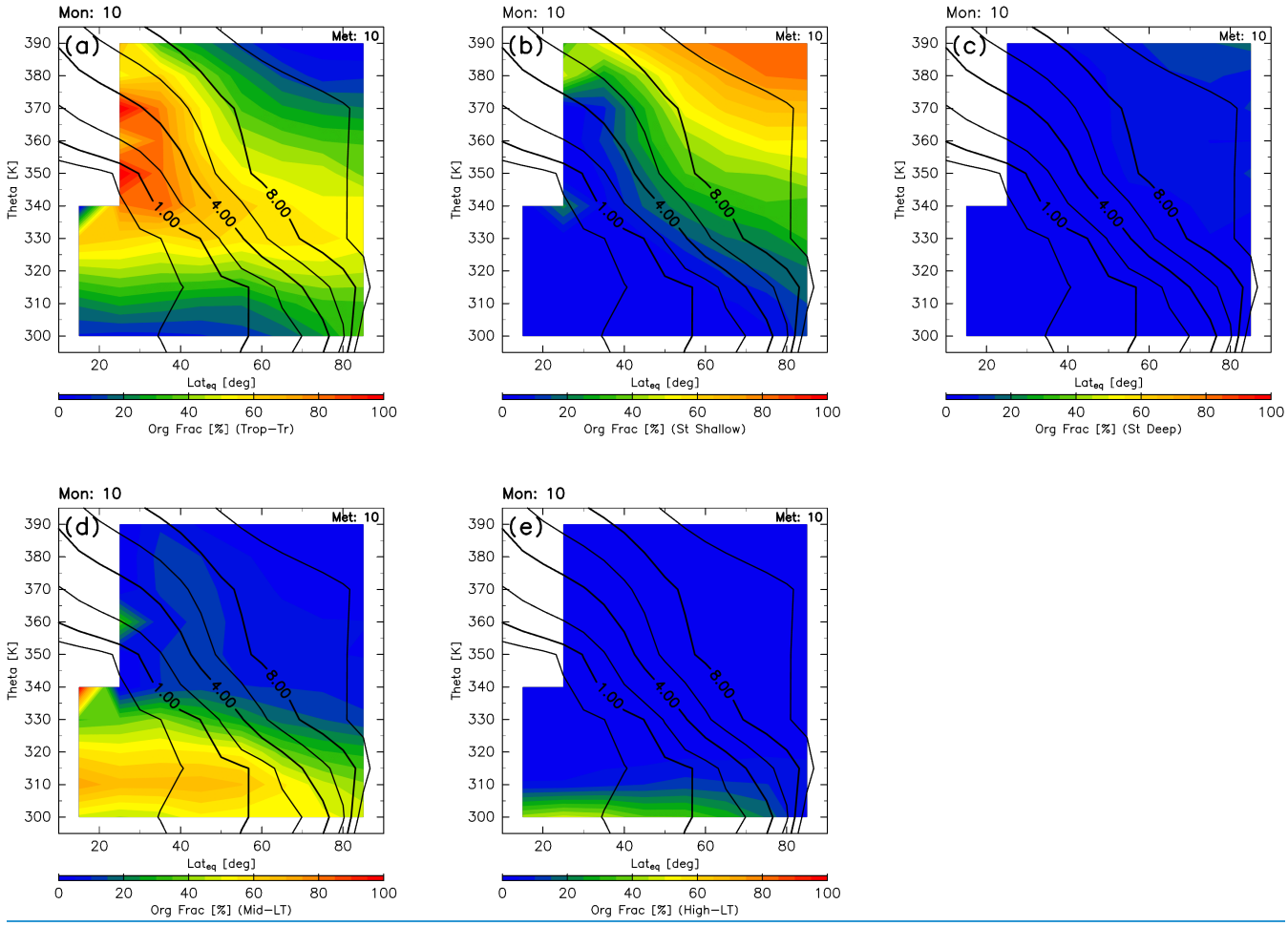

Figure 13: As in Fig. 10, but for October.

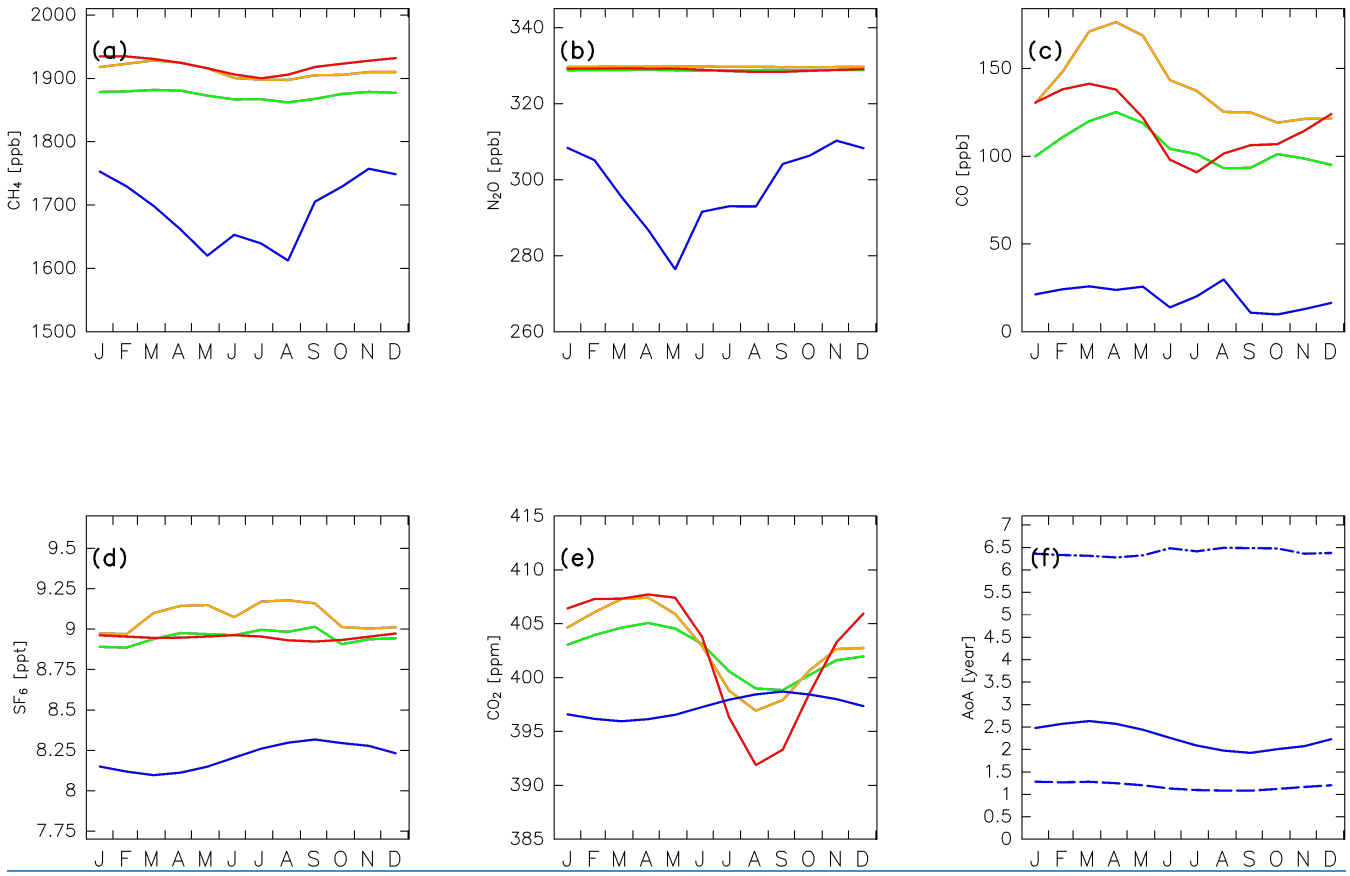

Figure 14: Seasonal variations in (a) CH_4, (b) N_2O, (c) CO, (d) SF_6, and (e) CO_2 mixing ratios assigned to (green) tropical tropospheric, (~~blue) high-latitude stratospheric,~~ (orange) mid-latitude LT, and (red) high-latitude LT air masses. Blue lines in (a–e) show the mixing ratios of each species estimated for stratospheric air masses (see text for details). Seasonal variations in the age of air (AoA) estimated for (blue solid lines) stratospheric air masses are shown in (f). Dashed–dotted and dashed lines in (f) indicate the AoA separately estimated for stratospheric air masses that travelled via the deep and shallow branches of the BDC, respectively.

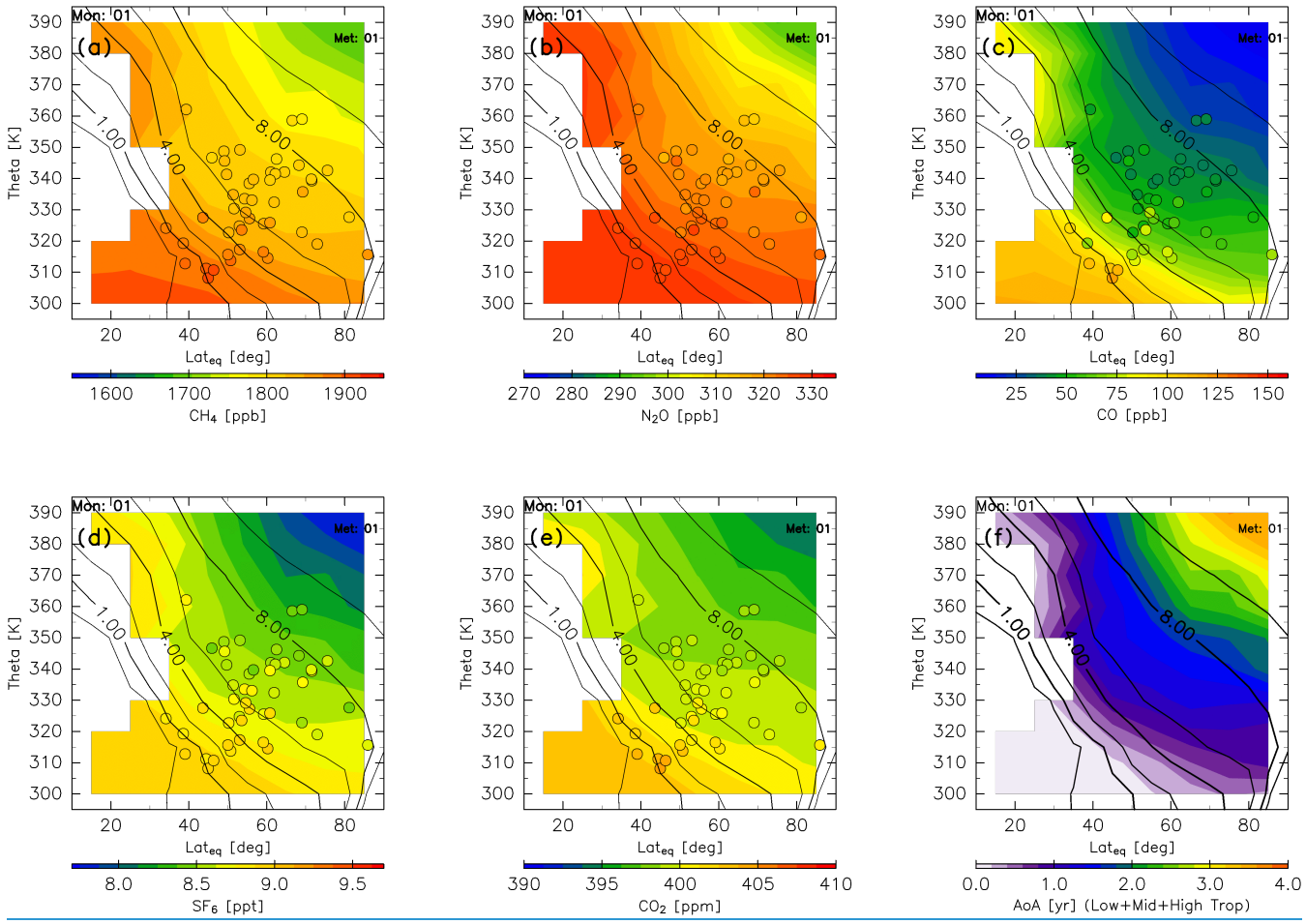

Figure 15: Meridional distributions of reconstructions for (a) CH_4, (b) N_2O, (c) CO, (d) SF_6, and (e) CO_2 for January. Detrended CONTRAIL measurements in January are plotted as circles using the same colour scale. The distribution of the age of air (AoA) estimated for January is shown in (f). Black contours indicate monthly average potential vorticity during the period from 2012 to 2016.

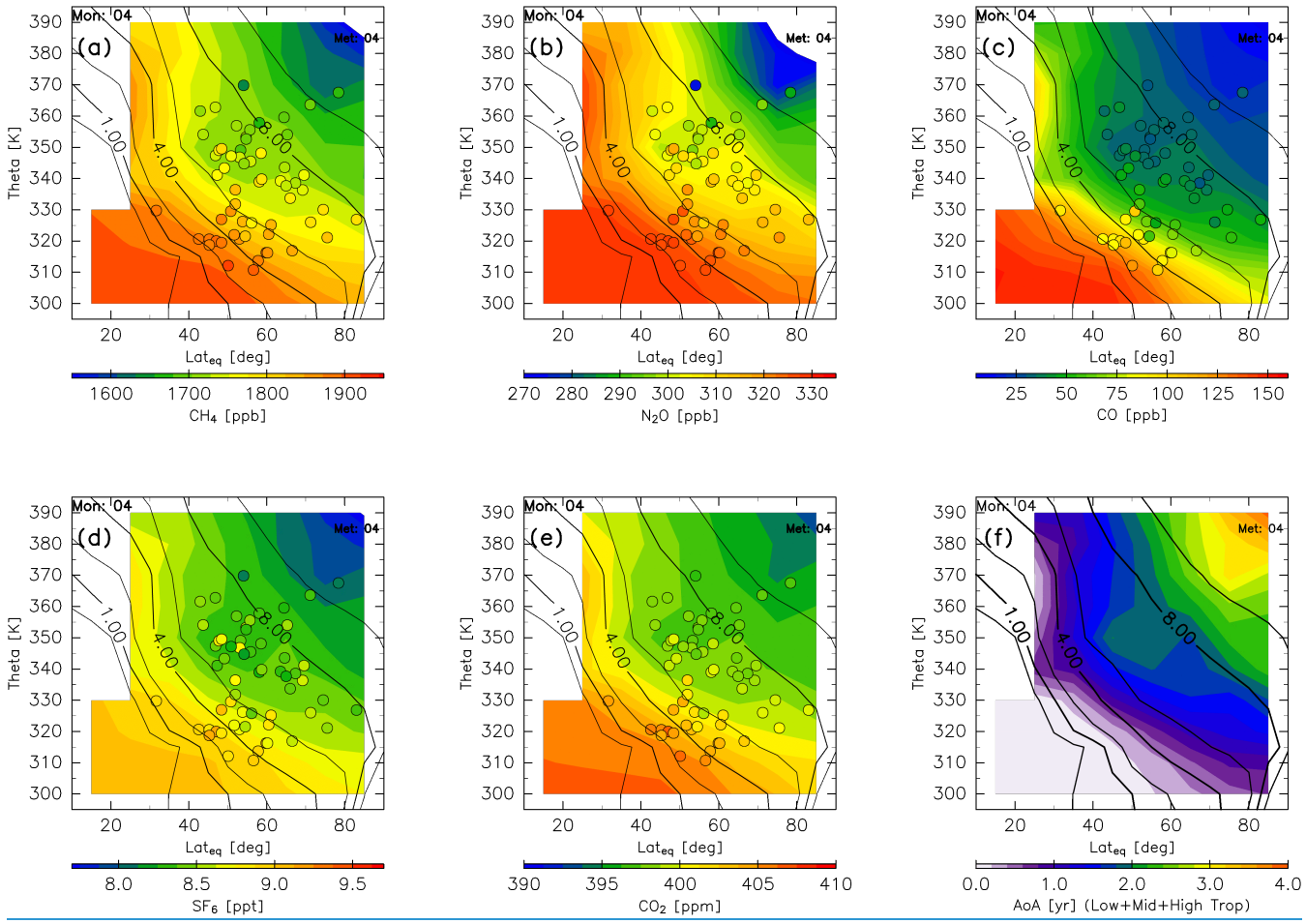

Figure 16: As in Fig. 8, but for April.

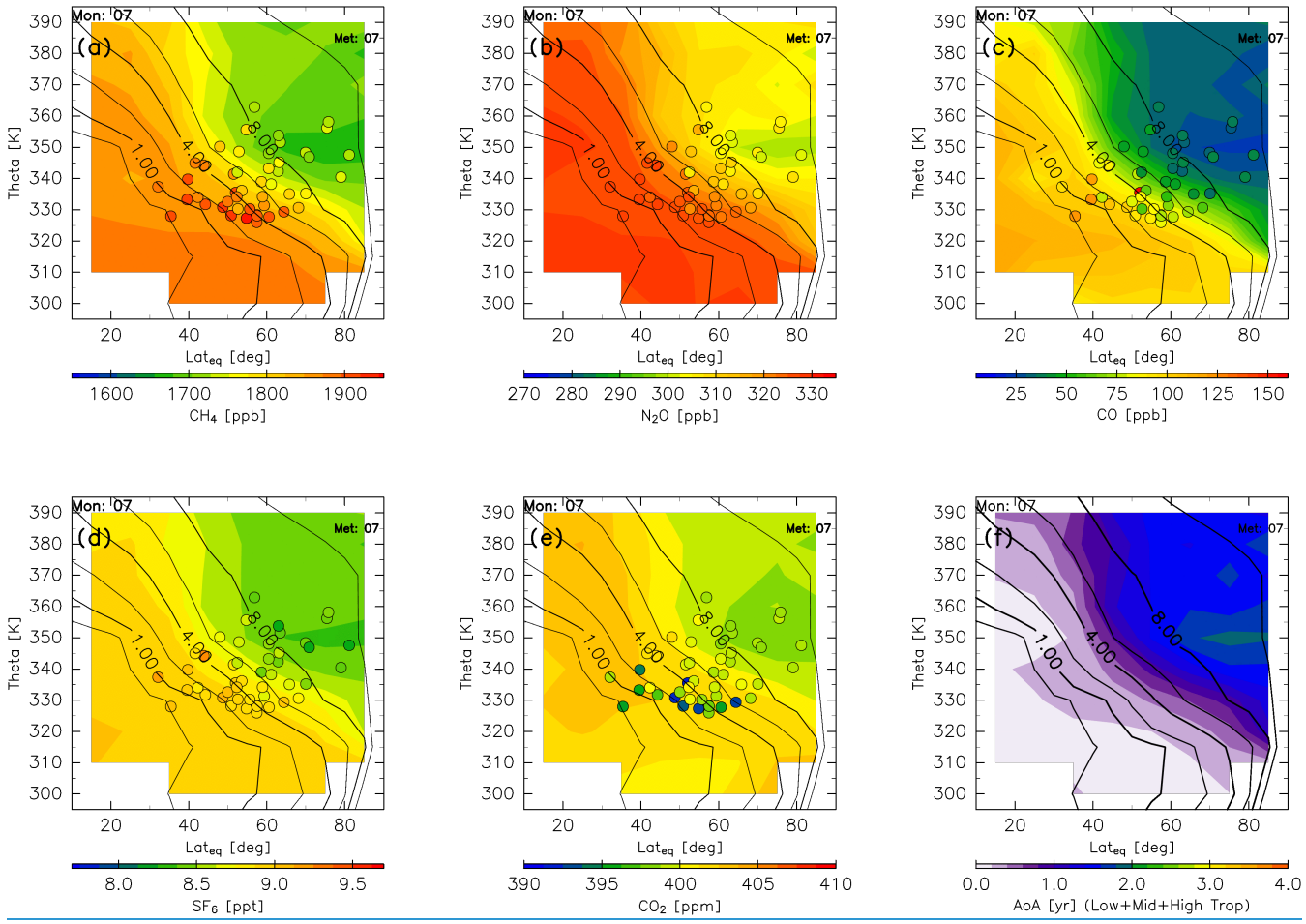

Figure 17: As in Fig. 8, but for July.

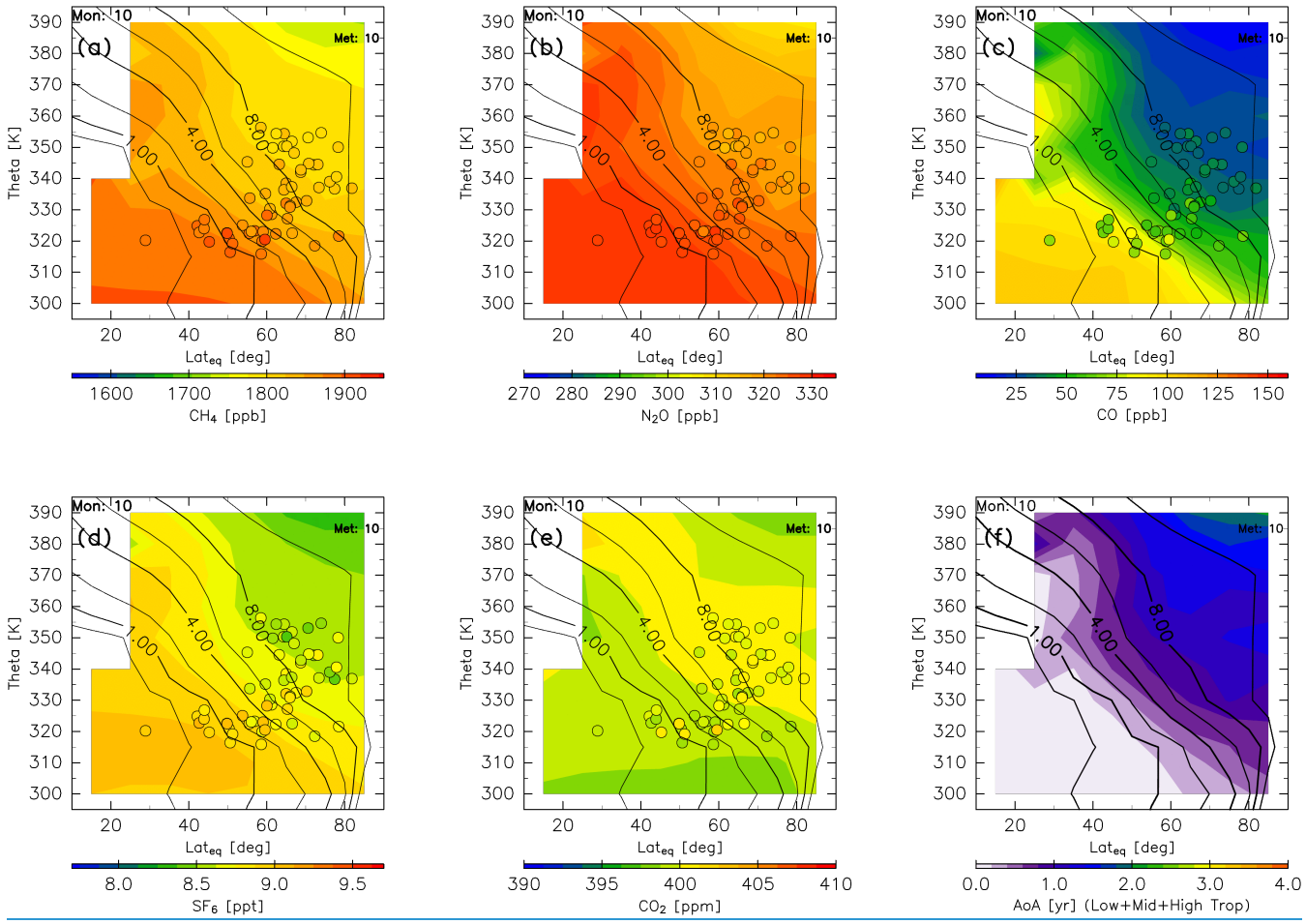

Figure 18: As in Fig. 8, but for October. ~~and (black) unclassified mixing~~

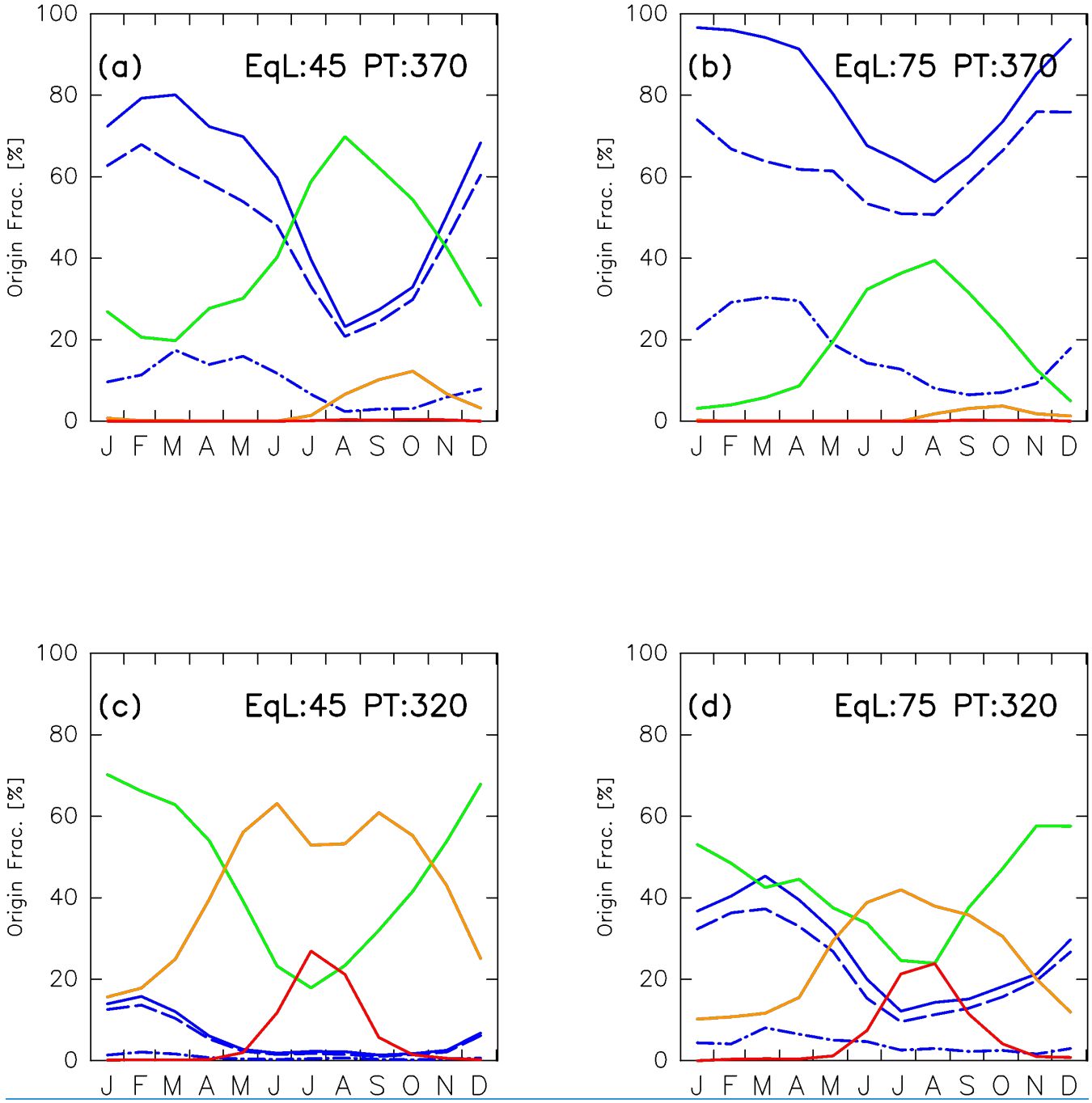

Figure 19: Seasonal variations in (green) tropical tropospheric, (blue) stratospheric, (orange) mid-latitude LT, and (red) high-latitude LT origin fractions estimated for the (a) mid-latitude upper ($\emptyset_{eq} = 45°N$; $\theta = 370$ K), (b) high-latitude upper ($\emptyset_{eq} = 75°N$; $\theta = 370$ K), (c) mid-latitude lower ($\emptyset_{eq} = 45°N$; $\theta = 320$ K), and (d) high-latitude lower ($\emptyset_{eq} = 75°N$; $\theta = 320$ K) ExUTLS. The blue dashed–dotted and dashed lines show the ~~mixing~~origin fractions of ~~high-latitude~~ stratospheric air masses that travelled through the deep and shallow ~~and deep~~ branches of the BDC, respectively.

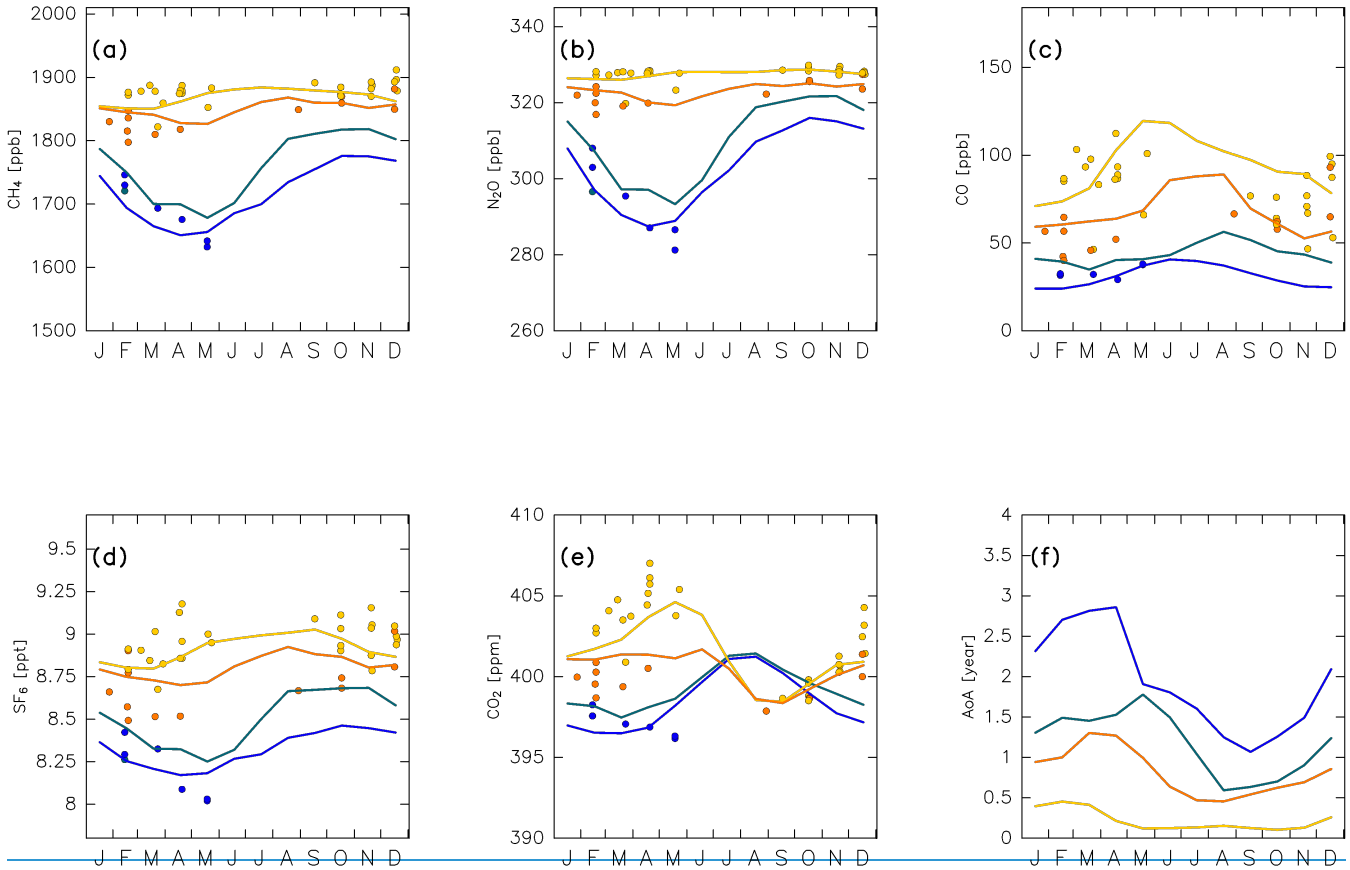
(a)
CH4 [ppb]
2000
1900
1800
1700
1600
1500
(b)
N2O [ppb]
340
320
300
280
260
(c)
CO [ppb]
150
100
50
0
(d)
SF6 [ppt]
9.5
9.25
9
8.75
8.5
8.25
8
(e)
CO2 [ppm]
410
405
400
395
390
(f)
AoA [year]
4
3.5
3
2.5
2
1.5
1
0.5
0
J F M A M J J A S O N D

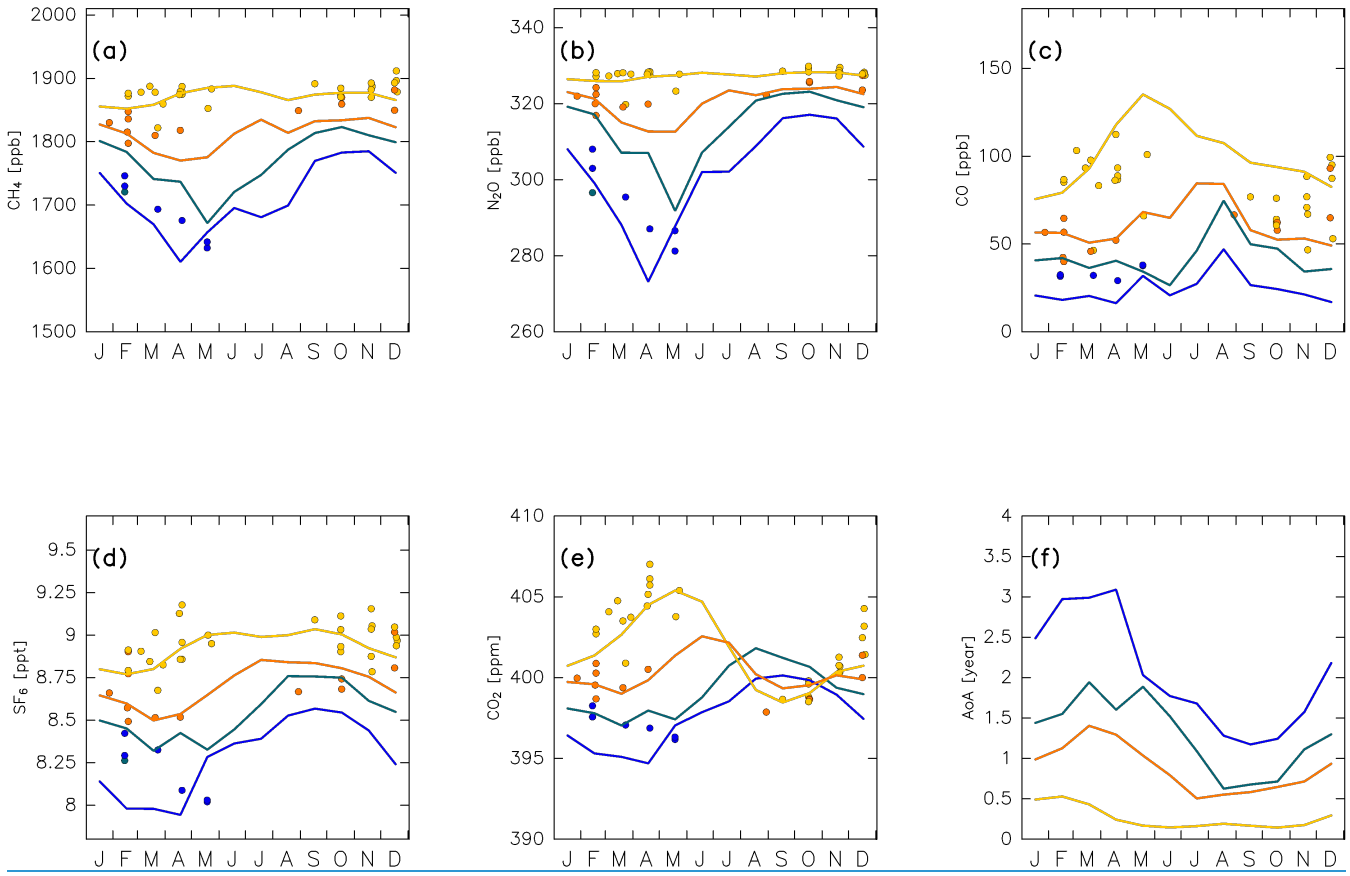

Figure ~~14~~20: Seasonal variations in (a) CH_4, (b) N_2O, (c) CO, (d) SF_6, and (e) CO_2 mixing ratios estimated for the (green) mid-latitude upper ($\emptyset_{eq} = 45°N$; $\theta = 370$ K), (blue) high-latitude upper ($\emptyset_{eq} = 75°N$; $\theta = 370$ K), (yellow) mid-latitude lower ($\emptyset_{eq} = 45°N$; $\theta = 320$ K), and (orange) high-latitude lower ($\emptyset_{eq} = 75°N$; $\theta = 320$ K) ExUTLS superimposed on ~~the~~ detrended CONTRAIL measurements, which are ~~color~~colour-coded according to measurements within ±5° in equivalent latitude and ±5 K in potential temperature of the reconstruction regions. Seasonal variations of the age of air (AoA) estimated for the same locations are shown in (f).

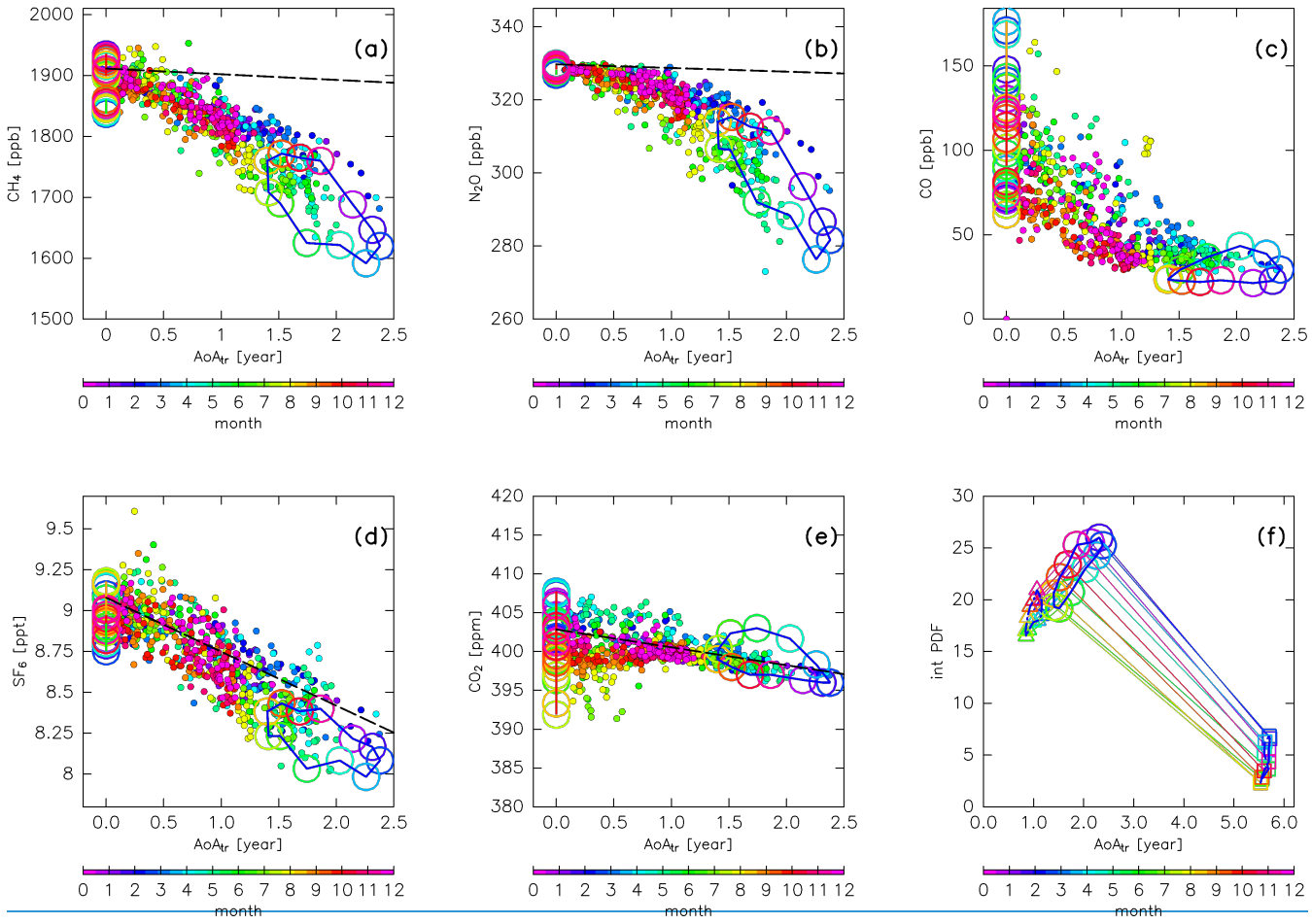
(a)
CH4 [ppb]
AoAtr [year]
month
(b)
N2O [ppb]
AoAtr [year]
month
(c)
CO [ppb]
AoAtr [year]
month
(d)
SF6 [ppt]
AoAtr [year]
month
(e)
CO2 [ppm]
AoAtr [year]
month
(f)
int PDF
AoAtr [year]
month

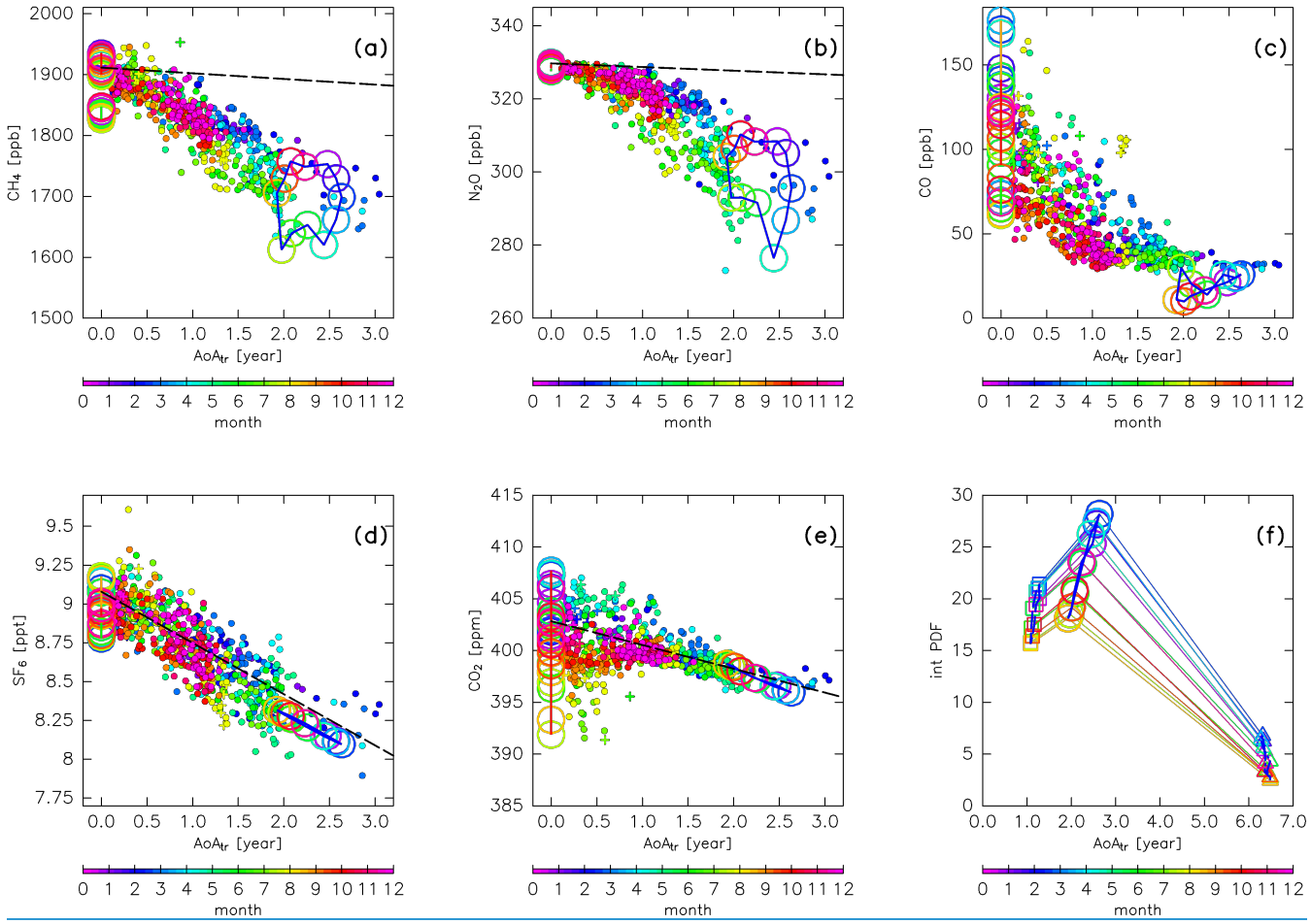

Figure ~~15~~21: Scatter plots of the mean age of air (AoA) versus (a) CH_4, (b) N_2O, (c) CO, (d) SF_6, and (e) CO_2 mixing ratios measured by CONTRAIL (filled circles; colours indicate the month). Lines with open circles, coloured according to month, show the original compositions for (green) tropical tropospheric, (blue) ~~high-latitude~~ stratospheric, (orange) mid-latitude LT, and (red) high-latitude LT air masses. Dashed lines in (a), (b), (d), and (e) show the sign-reversed trends of tropospheric CH_4 (−9.3 ppb/year), N_2O (−1.0 ppb/year), SF_6 (−0.33 ppt/year), and CO_2 (−2.3 ppm/year) with intercepts of the annual averaged mixing ratios at mid-latitudes for 2016 (1911 ppb, 330 ppb, 9.08 ppt, and 403 ppm), respectively. Mixing ratios estimated for stratospheric air masses in (a–e) are plotted after taking 3-month running averages to reduce fluctuations. Panel (f) shows the ~~mean age of air~~AoA estimated for air masses originating in the ~~high-latitude~~ stratosphere (open circles), along with those estimated only for air masses passing through the deep (~~squares~~triangles) and shallow branches (~~triangles~~squares) of the BDC. The ordinate is the integral of PDF of the "age spectrum" for each subset.

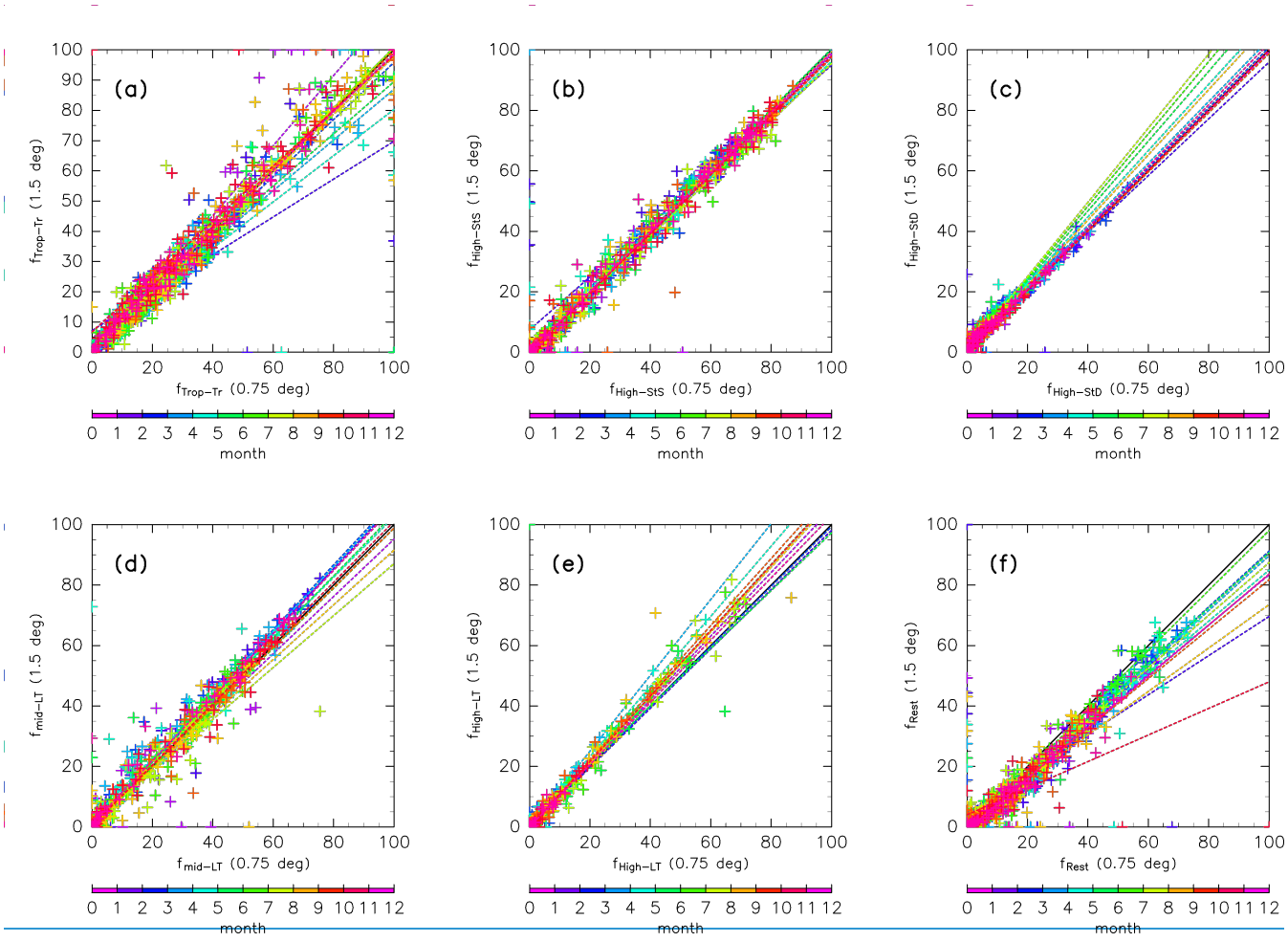
(a)
$f_{Trop-Tr}$ (1.5 deg)
$f_{Trop-Tr}$ (0.75 deg)
(b)
$f_{High-StS}$ (1.5 deg)
$f_{High-StS}$ (0.75 deg)
(c)
$f_{High-StD}$ (1.5 deg)
$f_{High-StD}$ (0.75 deg)
(d)
f_{mid-LT} (1.5 deg)
f_{mid-LT} (0.75 deg)
(e)
$f_{High-LT}$ (1.5 deg)
$f_{High-LT}$ (0.75 deg)
(f)
f_{Rest} (1.5 deg)
f_{Rest} (0.75 deg)
month

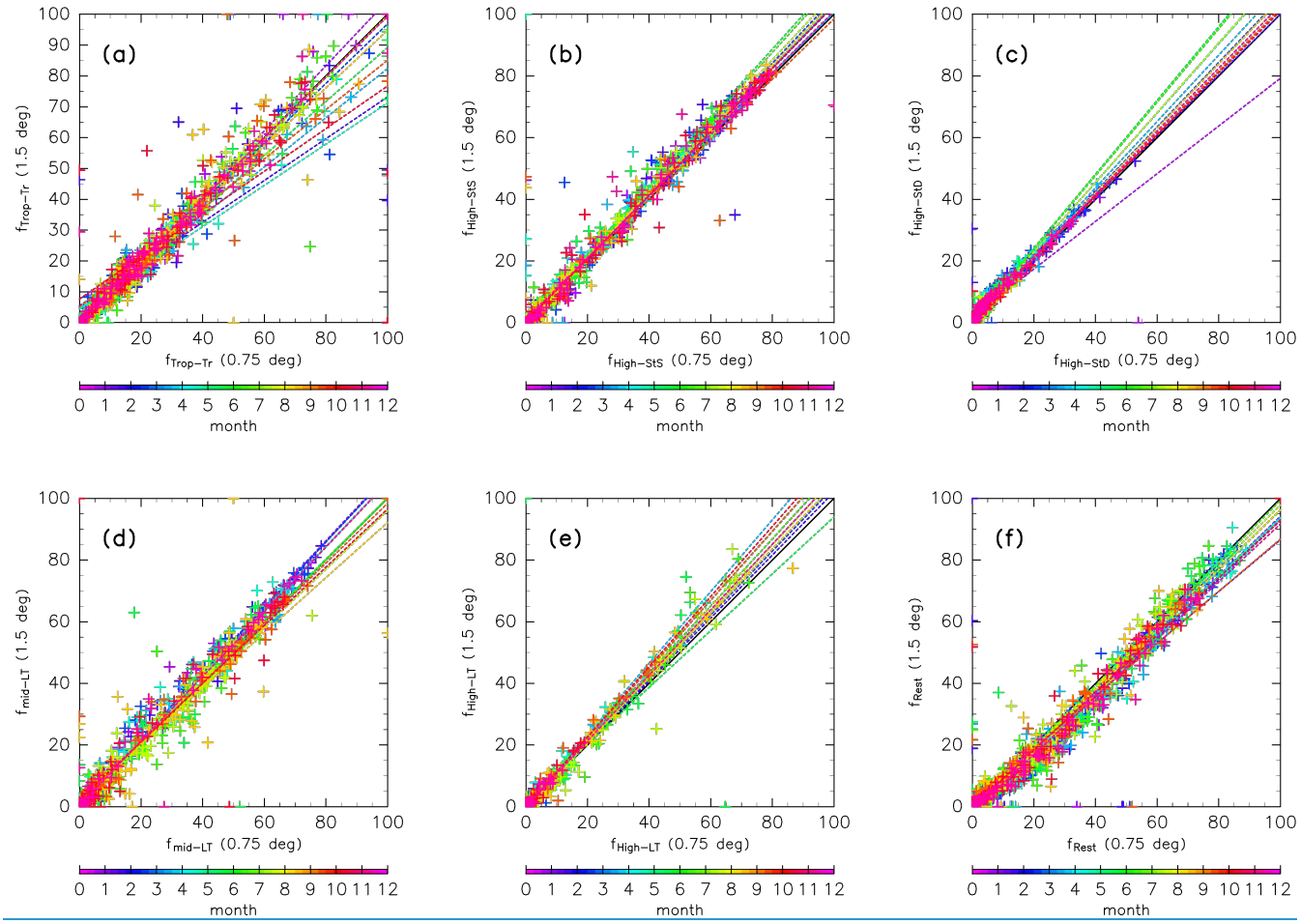

Figure A1: Scatter plots of ~~mixing~~origin fractions calculated using ERA-Interim data with a horizontal resolution of 0.75° and 60 model levels versus those with 1.5° horizontal resolution and 37 pressure levels. Both are estimated by 90-day trajectory calculations because of computing limitations. Crosses indicate mixing fractions evaluated for all bins in the $\emptyset_{eq}$–θ cross-sections shown in Figs ~~3–6~~10–13 for (a) tropical tropospheric, (b) ~~high-latitude~~ stratospheric (through the shallow branch of the BDC), (c) ~~high-latitude~~ stratospheric (through the deep branch of the BDC), (d) mid-latitude LT, (e) high-latitude LT, and (f) unclassified air masses~~.~~ from 90-day trajectories. Colours indicate the month and dotted lines indicate the regression line for each month.

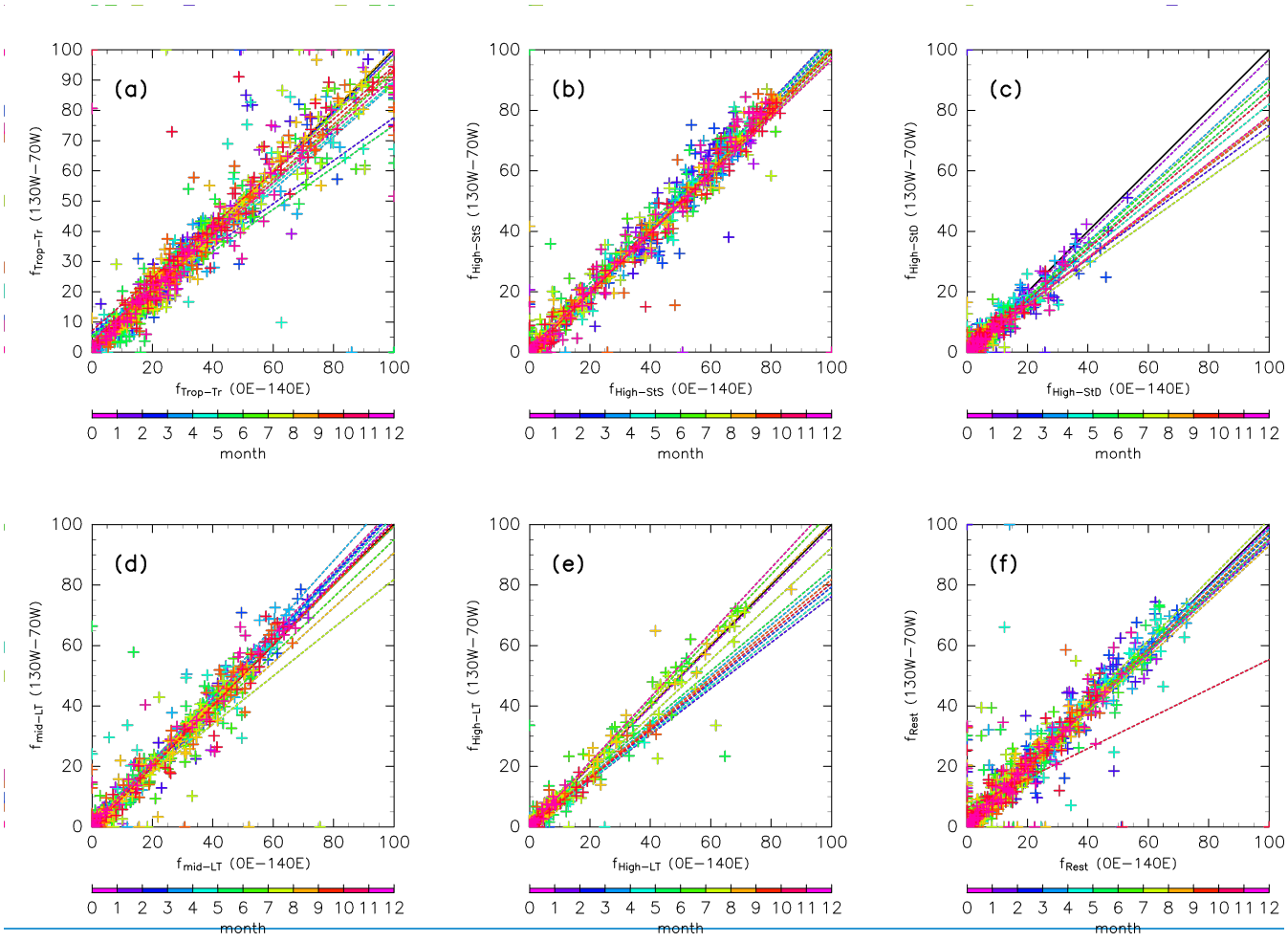
(a)
(b)
(c)
(d)
(e)
(f)
f_Trop−Tr (130W−70W)
f_Trop−Tr (0E−140E)
f_High−StS (130W−70W)
f_High−StS (0E−140E)
f_High−StD (130W−70W)
f_High−StD (0E−140E)
f_mid−LT (130W−70W)
f_mid−LT (0E−140E)
f_High−LT (130W−70W)
f_High−LT (0E−140E)
f_Rest (130W−70W)
f_Rest (0E−140E)
month

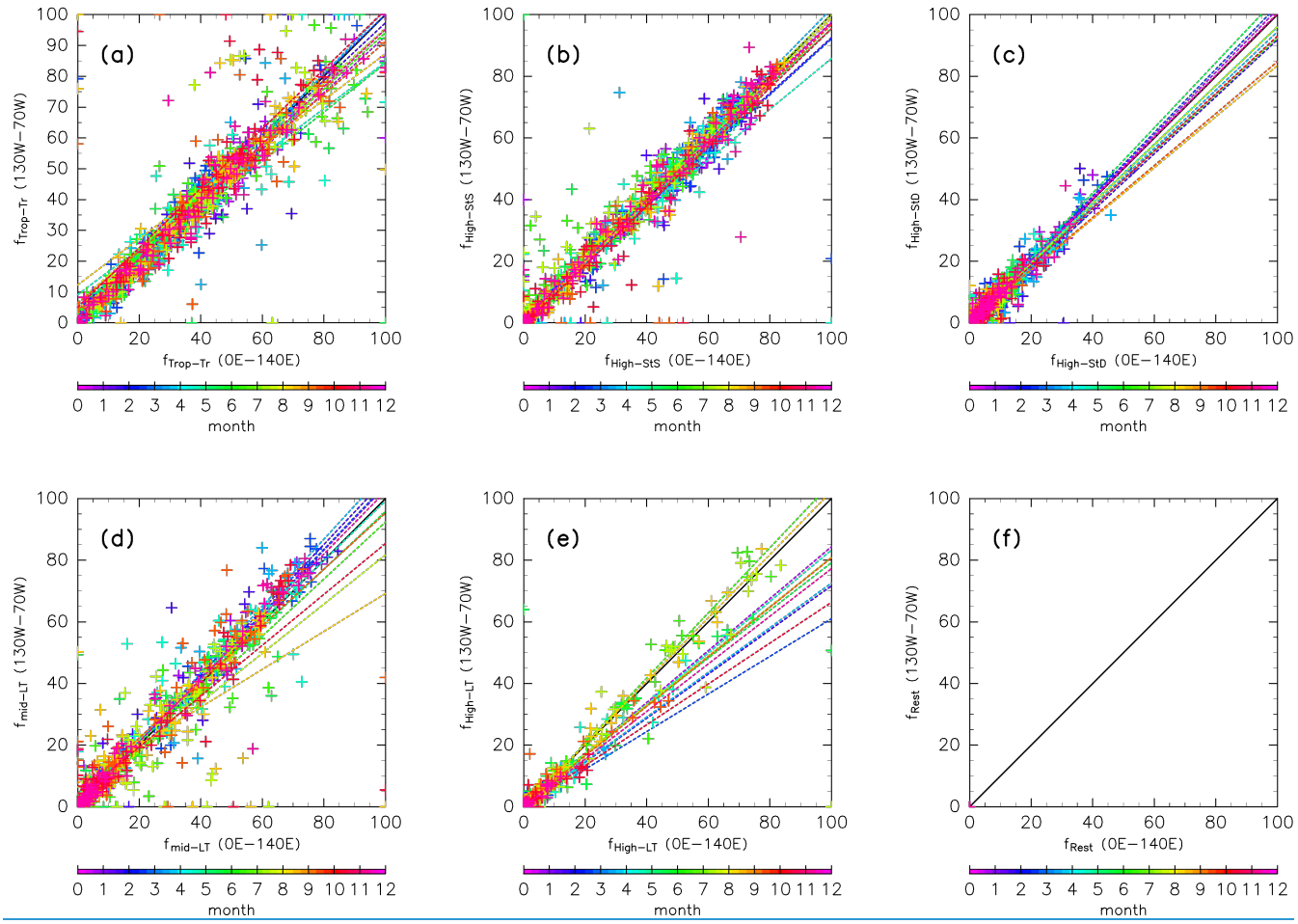

Figure A2: ~~Same as~~As in **Fig. A1, but for** ~~mixing~~origin **fractions** using 10-year trajectories **calculated for the longitudinal region within 0° E–140° E (default) versus those for the region within 130° W–70° W.**

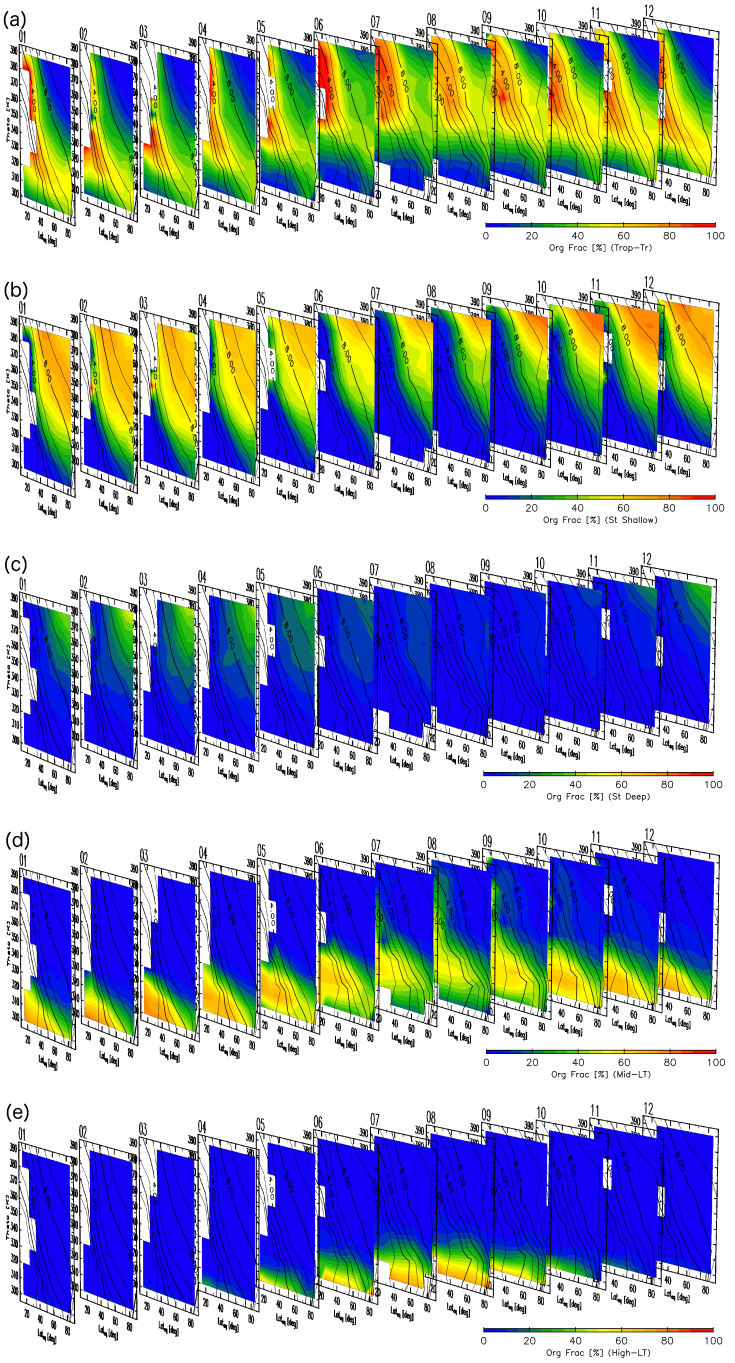

Figure B1: Origin fractions for (a) tropical tropospheric, (b) stratospheric (via the shallow branch of the BDC), (c) stratospheric (via the deep branch of the BDC), (d) mid-latitude LT, and (e) high-latitude LT air masses estimated for each month of the year with axes as in Figs 10–13. Black contours indicate monthly average potential vorticity during the period 2012–2016.

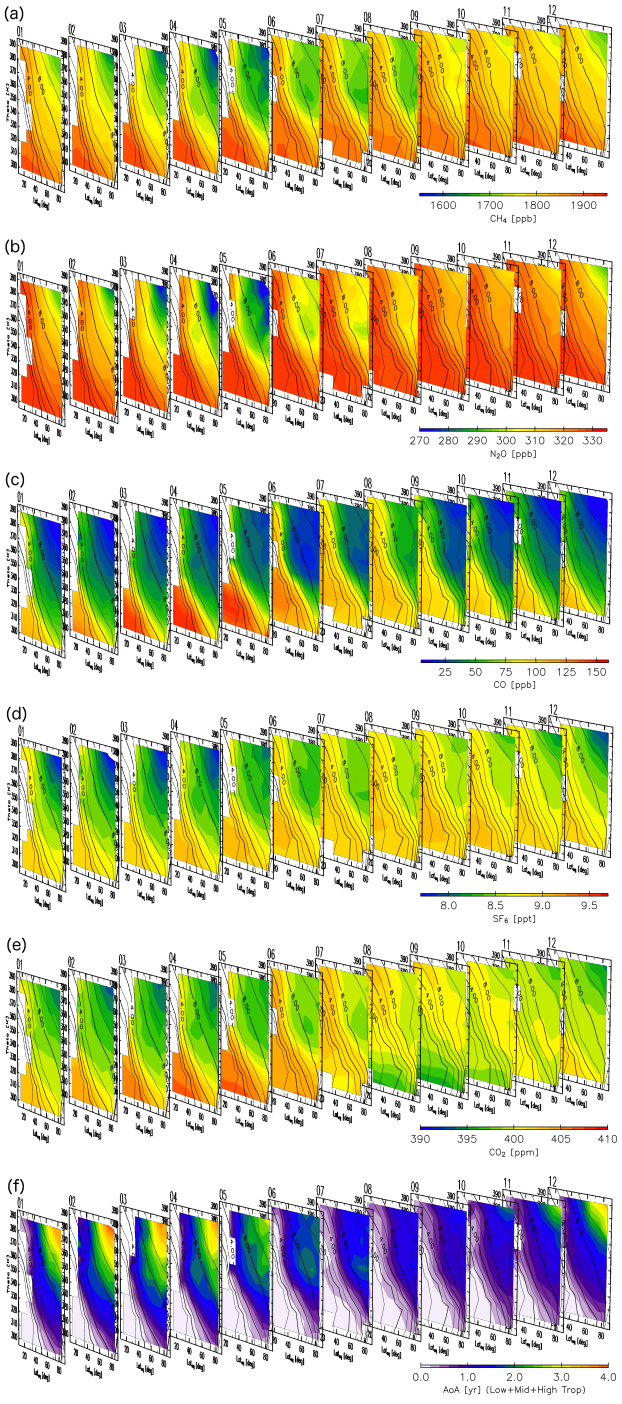

Figure B2: As in Fig. B1, but for reconstructions for (a) CH_4, (b) N_2O, (c) CO, (d) SF_6, and (e) CO_2, along with (f) the age of air (AoA) for each month.